

INVESTIGATION OF THE LIPID METABOLIC CHANGES INDUCED BY
NOVEL ALPHA TOCOPHEROL ANALOG (TC6OH) IN LUMINAL A TYPE
BREAST CANCER CELLS

A THESIS SUBMITTED TO
THE GRADUATE SCHOOL OF NATURAL AND APPLIED SCIENCES
OF
MIDDLE EAST TECHNICAL UNIVERSITY

BY

SEHER GÖK

IN PARTIAL FULFILLMENT OF THE REQUIREMENTS
FOR
THE DEGREE OF DOCTOR OF PHILOSOPHY
IN
BIOLOGY

JULY 2017

Approval of the thesis:

**INVESTIGATION OF THE LIPID METABOLIC CHANGES INDUCED BY
NOVEL ALPHA TOCOPHEROL ANALOG (TC6OH) IN LUMINAL A TYPE
BREAST CANCER CELLS**

submitted by **SEHER GÖK** in partial fulfillment of the requirements for the degree
of **Doctor of Philosophy in Biology Department, Middle East Technical
University** by,

Prof. Dr. Gülbin Dural Ünver
Dean, Graduate School of **Natural and Applied Sciences**

Prof. Dr. Orhan Adalı
Head of Department, **Biology**

Prof. Dr. Feride Severcan
Supervisor, **Biology Dept., METU**

Examining Committee Members:

Assoc. Prof. Dr. Çağdaş D. Son
Biology Dept., METU

Prof. Dr. Feride Severcan
Biology Dept., METU

Assoc. Prof. Dr. A. Elif Erson Bensan
Biology Dept., METU

Assist. Prof. Dr. Özgür Şahin
Molecular Biology & Genetics Dept., Bient University

Assist. Prof. Dr. Ayça Mollaoğlu
Physiology Dept. İstanbul Kemerburgaz University

Date: 11.07.2017

I hereby declare that all information in this document has been obtained and presented in accordance with academic rules and ethical conduct. I also declare that, as required by these rules and conduct, I have fully cited and referenced all material and results that are not original to this work.

Name, Last name: Seher GÖK

Signature:

ABSTRACT

INVESTIGATION OF THE LIPID METABOLIC CHANGES INDUCED BY NOVEL ALPHA TOCOPHEROL ANALOG (TC6OH) IN LUMINAL A TYPE BREAST CANCER CELLS

Gök, Seher

Ph.D., Department of Biology

Supervisor: Prof. Dr. Feride SEVERCAN

July 2017, 113 pages

Although the traditional chemotherapeutic agents able to suppress breast tumor progression, they are mostly unspecific in their mechanism of action and have toxic effects to normal tissues. Instead, it has been reported that tumor cells are more sensitive to some forms of Vitamin E (VE) and its synthetic derivatives than healthy cells. Studies of drug-cell interactions and understanding the mechanism underlying cytotoxic activity and biological effects at molecular level in cancer model cells are essential in the preclinical stage of drug discovery. TC6OH, a derivative of α -tocopherol with side chain modification has been shown to possess anti-cancer activity in preliminary studies. It was hypothesized that, as VE and VE analogs are fat soluble lipophilic molecules, they exert their function by modulating the lipid metabolism and related pathways. This study aimed to evaluate cellular impact of VE analog, using α -tocopherol as a reference compound through the experiments. Their effects on the cellular metabolism, biophysical properties of cellular lipids and functional characteristics of cells were monitored in human Estrogen Receptor (ER) positive breast cancer MCF7 cell line at 48 h drug exposure. Analog induces cell cycle arrest and differentiation, triggers apoptosis and inhibits migration while showing no cytotoxic effect on MCF10A breast epithelial cells at the same doses. In

addition, analog treatment increases cellular fatty acid and cholesterol levels, changes the membrane dynamics while decreasing the lipid peroxidation which are thought to be related in apoptotic processes. It has been documented that analog treatment induces tumor cell apoptosis by dissipating mitochondrial membrane potential, modulating the lipid synthesis, transportation and degradation as well as down-regulating the certain anti-apoptotic and growth factor related proteins in MCF7 cells. Due to resistance of ER positive cells to the established therapies, the findings of this study are of translational value.

Keywords: Vitamin E analog, tocopherol, lipid metabolism, breast cancer, spectroscopy

ÖZ

LUMİNAL A TİP MEME KANSERİ HÜCRELERİNDE YENİ BİR E VİTAMİNİ ANALOĞUNUN (TC6OH) TETİKLEDİĞİ LİPİD METABOLİZMASI KAYNAKLI DEĞİŞİKLİKLERİN ARAŞTIRILMASI

Gök, Seher

Doktora, Biyoloji Bölümü

Tez Yöneticisi: Prof. Dr. Feride SEVERCAN

Temmuz 2017, 113 sayfa

Geleneksel kemoterapötik ajanlar, meme tümörü gelişimini baskılayabilmesine rağmen, çoğunlukla etki mekanizmalarında belirsizdirler ve normal dokular için toksik etkilere sahiptirler. Bunun yerine, tümör hücrelerinin sağlıklı hücrelere göre E Vitamini (EV) ve sentetik türevlerinin bazı biçimlerine daha duyarlı oldukları bildirilmiştir. İlaç- hücre etkileşimlerinin araştırılması ve kanser model hücrelerinde sitotoksik aktivitenin ve biyolojik etkilerin altında yatan mekanizmanın anlaşılması, ilaç keşfinin klinik öncesi evresinde gereklidir. Yan zincir modifikasyonuna sahip bir α -tokoferol türevi olan TC6OH'ın ön araştırmalarda anti-kanser aktiviteye sahip olduğu gösterilmiştir. EV ve EV analoglarının yağda çözünen lipofilik moleküller olmaları sebebiyle, lipit metabolizmasını ve ilgili yolları modüle ederek işlevlerini yerine getirdiği hipotezi ileri sürülmüştür. Bu çalışma, α -tokoferol'ü referans bileşik olarak kullanarak EV analogunun hücredeki etkisini değerlendirmeyi amaçlamaktadır. Östrojen reseptörü (ER) pozitif meme kanseri, MCF7 hücre hattında, analogun, hücre metabolizması, hücre lipitlerin biyofiziksel özellikleri ve hücrelerin fonksiyonel özellikleri üzerine etkileri 48 saatlik analog maruziyetinde izlendi. Analogun hücre döngüsünü kesintiye uğratarak, kontrollü hücre ölümünü

tetiklediđi, metastatik özellikleri baskıladıđı ve farklılaşmaya neden olduđu ortaya konarken, aynı dozlarda analogun MCF10A meme epitel hücreleri üzerinde sitotoksik etki göstermediđi ortaya konuldu. Ayrıca, analog tedavisinin hücresel yağ asidi ve kolesterol düzeylerini arttırdıđı, zar dinamiklerini deđiřtirdiđi ve apoptotik süreçlerde ilişkili olduđu düşünölen lipit peroksidasyonunu azalttıđı gözlemlendi. Sonuç olarak, Analog uygulamasının, mitokondriyal zar potansiyelini deđiřtirerek, lipit sentez, taşıınma ve yıkım yollarını farklılaştırarak ve aynı zamanda MCF7 hücrelerindeki bazı anti-apoptotik ve büyüme faktörüne bađlı proteinlerin ifadesini azaltarak tümör hücresi apoptozunu indüklediđi belgelenmiřtir. ER pozitif hücrelerin hali hazırdaki tedavilere gösterdiđi ilaç direnci nedeniyle, bu çalışmanın bulguları translasyonel deđerdedir.

Anahtar Sözcükler: E Vitamini Analodu, tokoferol, lipit metabolizması, meme kanseri, spektroskopi

Dedicated to, My Ancestors

ACKNOWLEDGEMENTS

I wish to express my sincere thanks to my supervisor Prof. Dr. Feride Severcan for her valuable guidance, encouragement, support and comments throughout the research.

I wish to extend my thanks to Assoc. Prof. Dr. Çağdaş D. Son and Assist. Prof. Dr. Özgür Şahin, for their constructive contributions, as a member of my thesis follow-up committee.

I would also like to thank to Scientific and Technological Research Council of Turkey (TÜBİTAK) for supporting this research financially (Project Number: 114Z424).

I would like to extend my special thanks to Dr. Nihal Özek who has assisted me throughout my graduate studies. She is always there whenever I need for anything.

I would like to express my thanks to my lovely family for their motivation, continuous support and prayers. My father is the person who always supported me for my educational decisions since I was a child. My mother, is the one who raised me with her endless love. My brother, thanks to you for being supportive.

I would like to also thank the many other people who have assisted me in some way or another in our lab group.

TABLE OF CONTENTS

ABSTRACT	v
ÖZ	vii
ACKNOWLEDGEMENTS	x
TABLE OF CONTENTS	xi
LIST OF TABLES	xiv
LIST OF FIGURES	xv
LIST OF ABBREVIATIONS	xviii
CHAPTERS	
1. INTRODUCTION	1
1.1. Biology of Breast Cancer	1
1.2. Breast Cancer and Lipid Metabolism	2
1.3. Treatment Options for Breast Cancer	5
1.4. Role of Vitamin E in Cancer Research	8
1.4.1. Structure of Vitamin E	8
1.4.2. Cellular uptake	9
1.4.3. Therapeutic use of Vitamin E in Cancer	10
1.5. Novel Vitamin E Analog	12
1.6. Use of Spectroscopic Techniques for Drug Research	13
1.7. Scope of the Study	15
2. MATERIALS AND METHODS	17
2.1. Cell Culture	17
2.1.1. VE Analog Treatment Procedure	17
2.2. Cell Response Assays	18
2.2.1. XTT Cell Viability assay	18
2.2.2. BrdU Cell Proliferation Assay	18

2.2.3. Annexin V-FITC / PI staining.....	19
2.2.4. JC-1 Staining.....	19
2.3. Cell Motility Measurements	20
2.3.1. In vitro scratch wound healing assay	20
2.3.2. Boyden chamber cell migration assay	20
2.4. Lipid Droplets Staining	21
2.5. Fatty Acid Metabolism PCR Array	21
2.5.1. RNA isolation	21
2.5.2. Agarose gel electrophoresis of RNA	21
2.5.3. cDNA synthesis	22
2.5.4. RT PCR Array.....	22
2.6. ATR-FTIR Spectroscopy.....	23
2.6.1. Sample Preparation	23
2.6.2. Data Collection	23
2.6.3. IR Data analysis	24
2.6.4. Chemometrics	24
2.7. Electron Spin Resonance (ESR) Spectroscopy	25
2.8. Measurement of Lipid Peroxidation	27
2.9. Western Blotting and Antibodies	28
2.10. Protein Array	29
2.11. Statistical Analysis	29
3. RESULTS AND DISCUSSION	31
3.1. The Effect of Analog Treatment on Cell Proliferation and Apoptosis.....	31
3.1.1. XTT Assay:.....	31
3.1.2. BrdU Assay:.....	34
3.1.3. Annexin V – PI affinity assay:.....	35
3.1.4. JC-1 Staining:.....	36
3.2. The Effect of Analog Treatment on Migration Ability of Cells.....	38
3.2.1 Wound Healing Assay:	38

3.2.2. Boyden Chamber cell migration assay:	39
3.3. The Effects of Analog Treatment in Lipid Content and Structure	40
3.3.1. VE Analog induces lipid droplet formation.....	40
3.3.2. Monitoring changes in cellular lipids by spectroscopic techniques	41
3.3.3 The effect of VE Analog on lipid peroxidation	64
3.3.4. Assessment of Changes in Fatty Acid Metabolism Gene Transcripts via Quantitative RT-PCR Array	67
3.4. Effect of VE Analog in Protein Level	73
3.4.1. Western Blot Analysis	73
3.4.2. Protein Array.....	77
4. CONCLUSION	83
REFERENCES.....	87
APPENDICES	
APPENDIX A	103
APPENDIX B	105
CURRICULUM VITAE	107

LIST OF TABLES

TABLES

Table 1. Classification of breast cancer types	5
Table 2. The name and the chemical structures of spin labels used in the current study.	25
Table 3. The list of antibodies used for Western Blot analysis.....	28
Table 4. Band assignments of main absorptions in IR spectra of MCF7 cells based on the literature (Cakmak et al, 2011; Ozek et al, 2010; Severcan & Haris, 2012).....	50
Table 5. Genes over-expressed in analog treated vs control and tocopherol vs control groups.....	70
Table 6. Genes under-expressed in analog treated vs control and tocopherol vs control groups.....	71

LIST OF FIGURES

FIGURES

Figure 1. Simplified overview of lipid metabolism. (Adapted from Barnard, 2014) ..	3
Figure 2. Lipids regulate apoptotic signaling in the cells. Adapted from	4
Figure 3. Structure of the natural isoforms of Vitamin E.	9
Figure 4. 2,5,7,8 – tetramethyl-2-(4'-methyl-3'-pentenyl)-6-acetoxy chromane	12
Figure 5. Typical biological spectrum of human breast carcinoma tissue, showing biomolecular peak assignments from 3000–800 cm^{-1} , where ν = stretching vibrations, δ = bending vibrations, s = symmetric vibrations and as = asymmetric vibrations. (Adopted from Baker et. al., 2014).....	14
Figure 6. Growth inhibition curve for 12, 24, 48 and 78 h analog and α -tocopherol treated MCF7 cells.	32
Figure 7. (A) Dose response curve of 12h, 24h, 48h and 72h different concentration treated MCF7 cells. (B) Average IC_{50} calculations for the analog treatment dose (n=12).....	33
Figure 8. Growth inhibition curve for 48h analog and α -tocopherol treated MCF-10A cells (n=6).	33
Figure 9. % change in cell proliferation in response to analog and α -tocopherol treatment for 48 h (n=6; *p<0.05, ***p<0.001)	34
Figure 10. Annexin V / PI staining of Control (A), Analog (B) and α -tocopherol (C) treated cells (n=4 for each group)..	35
Figure 11. Percentages of apoptotic events. e. apop.: shows the number of early apoptotic cells, l. apop.: shows the number of late apoptotic cells.	36
Figure 12. Flow cytometry readings of JC-1 staining. Mitochondrial membrane potential changes are represented for Control (A), Analog (B) and α -tocopherol (C) treated cells.....	37
Figure 13. Representative pictures taken at different time points showing wound closure in response to 150 μM analog and α -tocopherol treatment.	38

Figure 14. Quantification of cell motility in the in-vitro scratch wound healing assay.	39
Figure 15. Transwell migration assay. A: representative pictures of cell migration for experimental groups, B: number of cells migrated (n=3 for each group).	40
Figure 16. Oil Red O stained MCF7 cells. Images were taken with 20X objective. .	41
Figure 17. PCA PCA loading (A) and scatter plot (B) for experimental groups based on the IR data in the 4000-650 cm ⁻¹ spectral region.	43
Figure 18. PCA loading (A) and scatter plot (B) for experimental groups based on the IR data in the 3000-2800 cm ⁻¹ spectral region.	44
Figure 19. PCA loading (A) and scatter plot (B) for experimental groups based on the IR data in the 1700-1505 cm ⁻¹ spectral region.	45
Figure 20. PCA loading (A) and scatter plot (B) for experimental groups based on the IR data in the 1150-900 cm ⁻¹ spectral region.	46
Figure 21. Hierarchical cluster analysis of experimental groups in the 3000-2800 cm ⁻¹ spectral region.	47
Figure 22. Average absorption ATR-FTIR spectrum of experimental groups in the 4000-650 cm ⁻¹ spectral range.	48
Figure 23. Average absorption (A) and second derivative (B) ATR-FTIR spectra of experimental groups in 3025-2800 cm ⁻¹ region.	51
Figure 24. Band area values of (A) CH ₂ antisymmetric, (B) CH ₂ symmetric and (C) CH ₃ antisymmetric bands.	52
Figure 25. Area ratio of CH ₂ antisymmetric / CH ₃ antisymmetric bands.	53
Figure 26. Wavenumber (A) and Bandwidth (B) changes of CH ₂ antisymmetric stretching band in experimental groups.	55
Figure 27. Band area changes of olefinic band (3009 cm ⁻¹) in the experimental groups.	56
Figure 28. Representative absorbance (A) and second derivative (B) spectra of the experimental groups in the 1750-1500 cm ⁻¹ region.	57
Figure 29. Representative absorbance (A) and second derivative (B) spectra of the experimental groups in the 1500-900 cm ⁻¹ region.	58
Figure 30. Band Area changes of the C=O stretching (1746 cm ⁻¹) (A) and CO-O-C antisymmetric stretching (1172 cm ⁻¹) (B) bands in the experimental groups.	59

Figure 31. Representative 16-DSA labeled ESR spectra of MCF7 cells (A) and relative correlation time (τ_c) changes in the experimental groups (B)	61
Figure 32. Representative 5DSA labeled ESR spectra of MCF7 cells (A) and relative changes in the order parameter (S) for the experimental groups (B).....	62
Figure 33. (A) MDA level change in the experimental groups, (B) MDA standard curve. The average of the control group was considered as 100%.	64
Figure 34. (A) 8-isoprostane level change in the experimental groups, (B) 8-isoprostane standard curve	65
Figure 35. RNA integrity and gDNA contamination test using agarose gel electrophoresis of isolated RNA isolated from the control, analog and α -tocopherol treated MCF cells.	67
Figure 36. The scatter plot compares the normalized expression of genes on the array between the two selected groups; A: analog vs control, B: α -tocopherol vs control. 68	
Figure 37. The clustergram shows non-supervised hierarchical clustering of the entire dataset to display a heat map with dendrograms indicating co-regulated genes across groups.....	69
Figure 38. Changes in protein expression levels in Control (C), Analog (A) and α -tocopherol (T) treated groups.....	74
Figure 39. Changes in protein expression levels in Control (C), Analog (A) and α -tocopherol (T) treated groups.....	76
Figure 40. Proteome profiler array expression patterns of experimental groups. (A) Dot blot, (B) 3D representation.....	78
Figure 41. Changes in the protein expression levels of selected genes in the control, analog and α -tocopherol treated groups.	79

LIST OF ABBREVIATIONS

ATR-FTIR	Attenuated Total Reflectance Fourier Transform Infrared
DSC	Differential Scanning Calorimetry
ELISA	Enzyme Linked-Immunosorbent Assay
ENO-2	Enolase g
ER	Estrogen Receptor
ESR	Electron Spin Resonance
FBS	Fetal Bovine Serum
FTIR	Fourier Transform Infrared
IC ₅₀	The half inhibitory concentration
IR	Infrared
SDS	Sodium Dodecyl Sulfate
PBS	Phosphate buffered saline
PCR	Polymerase Chain Reaction
PI	Propidium Iodide
τ	Correlation Time
T _m	Main phase Transition Temperature
α -TOS	α tocopheryl succinate
XTT carboxanilide)	(2,3-bis-(2-methoxy-4-nitro-5-sulfophenyl)-2H-tetrazolium-5-
VE	Vitamin E
VES	Vitamin E succinate
$\Delta\psi$ _m	Mitochondrial inner trans-membrane potential

CHAPTER I

INTRODUCTION

1.1. Biology of Breast Cancer

Breast cancer defined as the neoplastic differentiation of breast tissue, has high incidence rate among women (Jemal et al, 2011). High metastatic potential and drug resistance to the chemotherapy of breast cancer cases results in the high level of incidence and the mortality rates.

Hormones, high lipid diet, reactive oxygen species and stress are primary risk factors. Majority of the cases arise sporadically but family history is relevant in 5% of the cases. The genes, BRCA1, BRCA2, p53, STK11/LKB1, PTEN and ATM are involved in hereditary breast cancers (Baselga & Norton, 2002). The role of specific receptor in breast cancer pathogenesis has been widely investigated in order to find potential therapeutic targets. Estrogen receptor is the nuclear receptor controlling the transcription of certain genes that play pivotal roles in disease progression. Another class is the epidermal growth factor (EGF) family tyrosine kinase receptors, activation of which results in malignant transformation and proliferation (Baselga & Norton, 2002).

A major group of breast malignancies (95%) arises from epithelial cells and characterized as adenocarcinomas which are further classified as carcinoma in situ (CIS) and invasive carcinomas. CIS is the neoplastic proliferation of ducts and lobules whereas invasive carcinoma penetrates through the basement membrane into the stroma. Other small class accounts for approximately 5% including metaplastic and invasive micropapillary breast cancer (Schatten, 2013).

1.2. Breast Cancer and Lipid Metabolism

Metabolic reprogramming is the major distinguishing feature of cancer. Increased glucose uptake and glycolysis utilization (Warburg effect) and increased glutamine consumption to supply the need of carbon and amino-nitrogen for nucleotide, lipid and amino acid synthesis are well established signs of carcinogenesis (Son et al, 2013; Warburg, 1956; Ying et al, 2012). Depending on the recent data, alterations in lipid and cholesterol associated pathways are underlined in cancer formation (Ackerman & Simon, 2014; Baenke et al, 2013; Cruz et al, 2013).

Lipids compass a wide class of molecules with unique chemical structure in respect to backbone structure, chain length, and degree of unsaturation. Lipids composed of phospholipids, glycerides, sterols, waxes and lipid-soluble vitamins. All the lipid classes support cell structure, involved in signaling process and have role in energy storage and synthesis as a common biological function. Changes in several lipid classes have been linked to various cancers. These alterations can lead to change in ligand–receptor interaction, antigen presentation, endocytosis, lipid-lipid and lipid-protein interactions, membrane fluidity and domain formation (Barnard, 2014). Simplified overview of overall lipid metabolism in cell is given in Figure 1.

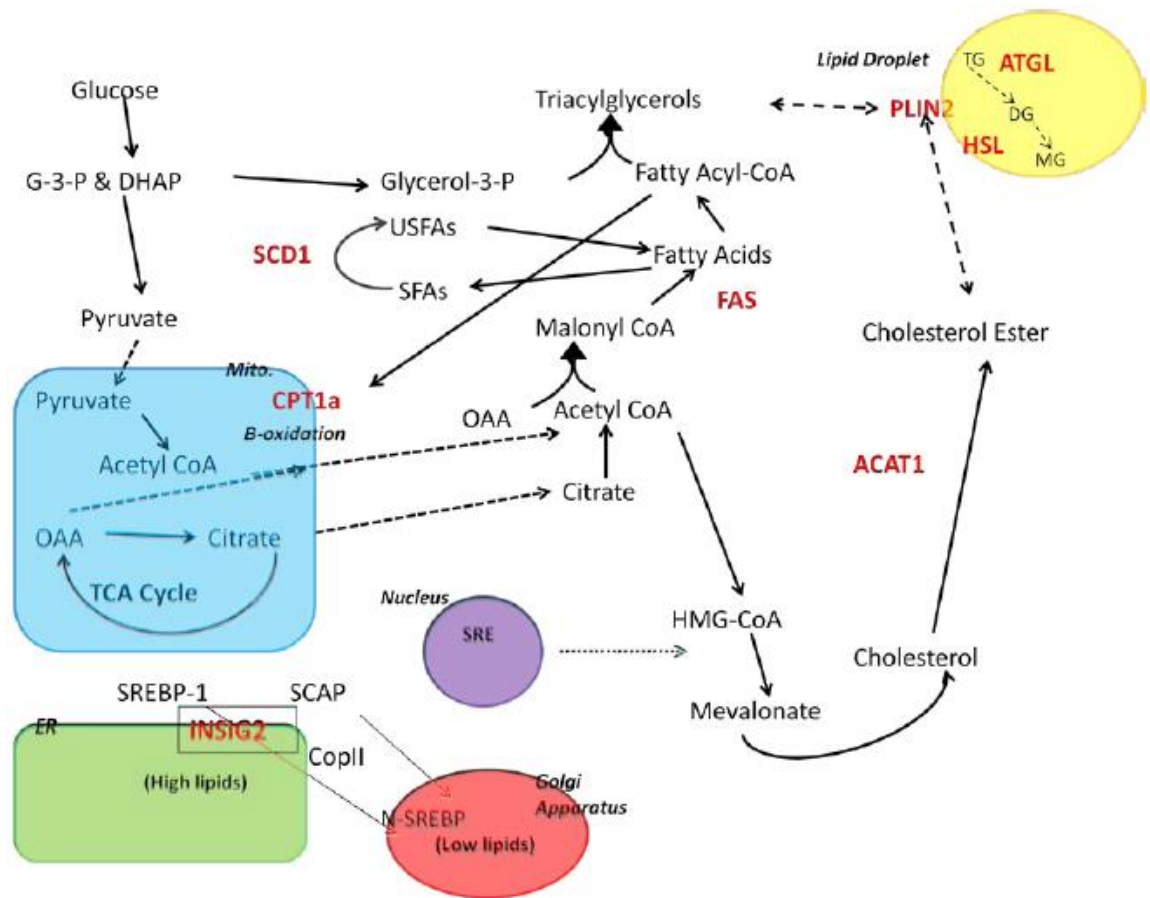


Figure 1. Simplified overview of lipid metabolism. (Adapted from Barnard, 2014)

In the past, lipids had been seen, as a passive component of membrane structure. Evident data has been exerted their multiple roles in the regulation of cellular signal transduction cascade. Free oxygen radicals produced by these factors, cause the oxidative damage of biomolecules and give a way to neoplastic transformations. Increase in lipid metabolism is defined as carcinogenesis sign in breast cancer (Blancato et al, 2004; Menendez & Lupu, 2007). For instance, there was no change in HER2/neu normal breast epithelial cells while HER2/neu positive breast cancer cells gaining lipogenic phenotype (Kourtidis et al, 2009). Also, it was reported that, tumor cells activate de novo lipid synthesis pathways.

Lipid metabolism is very complex and is regulated by a complex signaling network in the cells. The same lipid molecule, via different signaling pathways or under different conditions, can generate different metabolites. Some lipids directly induce

caspase activation leading to programmed cell death (Huang & Freter, 2015). The summary of lipid classes which can regulate different caspase dependent apoptosis is given in Figure 2.

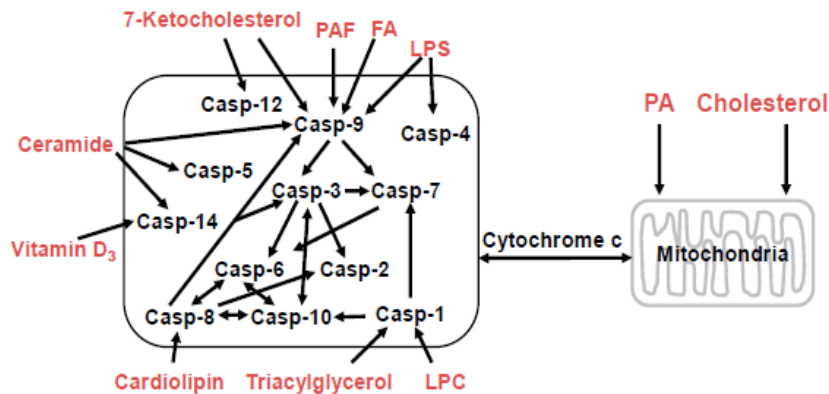


Figure 2. Lipids regulate apoptotic signaling in the cells. Adapted from (Huang & Freter, 2015)

Dysregulation of numerous cellular mechanisms like altered cell signaling, cellular trafficking, escape from growth arrest and enhanced cell migration ability could yield breast tumor formation. New findings suggest that, the lipid rafts play active role in all of these complex events in breast carcinogenesis (Cary & Cooper, 2000; Nabi & Le, 2003). Lipid rafts are the cholesterol & sphingolipid rich membrane domains. Critical cellular regulatory proteins which are readily altered due to carcinogenesis, are clustered in these specialized membrane domains (Mollinedo & Gajate, 2015; Pike, 2003). In addition, lipid rafts are amenable to modification by diet and nutrition (Yaqoob, 2009) and it was also shown that fatty acid supplementation make breast tumor cells more sensitive to the effects of anti-cancer drugs both in vivo and in vitro by altering raft formation (Bougnoux et al, 2010; Germain et al, 1998).

1.3. Treatment Options for Breast Cancer

Gene expression profiling has helped to shedding light on the heterogeneity and complexity of breast cancer at molecular level. Based on the current data breast cancer has classified as luminal A (ER+, PR-/+, HER2-low), luminal B (ER+, PR-/+, HER2+), basal like (ER-, PR-, HER2-), Her2-positive (ER-, PR-) and normal like subtypes. Each subtype gives different response to therapy. Luminal A and B types are highly responsive to the hormonal therapy such as tamoxifen while HER2 positive subtype can be treated with targeted antibodies like trastuzumab or tyrosine kinase inhibitors like lapatinib. ER, PR and HER2 negative basal type tumors are aggressive, have poor diagnose and treatment rates (Holliday & Speirs, 2011). The Table 1, summarizing the molecular classification of breast cancer types is given.

Table 1. Classification of breast cancer types

Classification	Immunoprofile	Characteristics
Luminal A	ER+, PR-/+, HER2-low	Endocrine responsive, often chemotherapy responsive
Luminal B	ER+, PR-/+, HER2+	Endocrine responsive, variable to chemotherapy. Trastuzumab responsive
Basal	ER-, PR-, HER2-	EGFR+, endocrine non-responsive, often chemotherapy responsive
Claudin-low	ER-, PR-, HER2-	E-cadherin and Claudin3 low. Intermediate responsive to chemotherapy
HER2 positive	ER-, PR-	Trastuzumab and chemotherapy responsive

Breast cancer treatment strategy generally involves; surgery, radiation therapy, hormonal therapy, targeted therapy and chemotherapy. The type of the treatment is determined according to the size and location of tumor, stage of cancer, cell turnover rate, status of hormones and their receptors, status of axillary lymph nodes and

menopausal status as well as the age of patient, general health conditions and patient preferences. In chemotherapy, several powerful drugs have been used to target and eliminate the fast-proliferating breast cancer cells. Although chemotherapy is frequently used with other treatments such as surgery, it also may have used as the primary treatment, when surgery is not an option (Holliday & Speirs, 2011).

Chemotherapy is usually given as a combination therapy (polychemotherapy). Frequently used chemotherapeutic agents are anthracyclins (doxorubicin, Daunorubicin, Mitoxantrone, Idarubicin), alkylating agents (cyclophosphamide), anti-metabolites (5-fluorouracil) and anti-microtubules (paclitaxel, docataxel). In advanced cases, new cytotoxic agents like vinca alkaloids (vinorelbine), pyrimidine analogs (gemcitabine) and anti-metabolites (capecitabine) have been used (Baselga & Norton, 2002; Malhotra & Perry, 2003).

- *Anthracyclines* are a class of antibiotics. Structurally look like an amino sugar with glycoside group. They act as a Topoisomerase inhibitors and DNA intercalating agents.
- *Alkylating agents* are the drugs which able to covalently bind with amino, carboxyl and phosphate groups of nucleic acids and proteins eventually impair their function.
- *Anti-metabolites* are the synthetic analogs of molecules which are needed for nucleic acid synthesis. They inhibit the cellular proliferation at S phase of the cell cycle.
- Anti-microtubules also called as Taxanes, able to stabilize GDP-bound tubulin in the microtubule formation thereby preventing the depolymerization of microtubules. Cell cycle is inhibited at M phase.
- *Vinca alkaloids* are the drugs that inhibit mitotic spindle formation by the prevention of tubulin polymerization.

Estrogen receptors are ligand gated transcription factors of the nuclear receptor super family regulators. ER activity can be regulated by hormonal and non-hormonal ligands. Endocrine therapy is the standard method for the hormone receptor positive breast cancer patients, which represents the majority of all breast cancer cases. Synthetic steroidal and non-steroidal ER antagonists have designed to inhibit breast cancer cell proliferation, to treat hormone responsive tumors. An anti-estrogen

Tamoxifen is a selective ER modulator which has been widely used as a first line treatment for ER-positive breast cancer. However, side effects and acquired drug resistance limit to efficacy and use of ER antagonists. (Thomas & Gustafsson, 2011). Aromatase inhibitors like anastrozole, exemestane and letrozole can also be used against hormone sensitive breast tumors. They able to stop production of estrogen from by blocking the aromatase enzyme. However, in premenopausal woman aromatase inhibitors have a limited ability to reduce circulating estrogen because they have large number of aromatase substrate present in ovary. Therefore aromatase inhibitors are mainly used to treat postmenopausal women (Fabian, 2007). Another last generation ER positive endocrine treatment agent Fulverstrant, is an analog of estradiol which able to down regulate ER via disrupting ER dimerization and increasing the degradation of unstable drug-ER complex. Fulverstrant is highly effective following the failure of previous tamoxifen and aromatase inhibitor therapy. However, after prolonged therapy resistance develops in majority of cases. It has been suggested that *miR-221 / 222* play a prominent role in the acquisition of fulverstrant resistance (Rao et al, 2011).

In addition to the acquired drug resistance and insensitivity, other detrimental consequences were reported about hormonal therapy. It has been known that the full extent of estrogen's activity in the brain is complex network and have not fully understood yet. Results coming from research showed that endocrine therapy appear to be associated with cognitive deficits such as impairments in memory, executive functions and speed of cognitive processing (Lee et al, 2016). Therefore, it is important to approach ER positive breast cancer therapy from a different standpoint rather than hormonal therapy.

Novel strategies are needed to produce effective chemotherapy without the harmful side-effects that accompany high dose chemotherapy. One such strategy is the potentiation of chemotherapy with agents that are well tolerated by the organism and have the capability of lowering the threshold of chemotherapy-induced cell death.

Estrogen receptor expressing, hormone sensitive MCF7 cell line has been commonly used in the world as a model to study hormonal response in the lab. (Holliday & Speirs, 2011). As a model system to investigate new treatment option for ER positive breast cancer cases, experiments in this study were conducted with MCF7 cells.

1.4. Role of Vitamin E in Cancer Research

1.4.1. Structure of Vitamin E

The role of vitamins as a protective and therapeutic agent for cancer has been widely studied in the respects reported in previous part (Mamede et al, 2011). There are many researches about the applicability of Vitamin E (VE) and its natural derivatives, like α , β , γ and δ tocopherols, on cancer therapy (Yang et al, 2012).

Vitamin E is a generic term used for eight lipophilic forms including α , β , γ , δ tocopherols and tocotrienols. Only α -tocopherol meets the VE requirement of human out of four tocopherols and four tocotrienols. The structural difference between both groups of isoforms is that, tocopherols have a saturated phytyl chain while tocotrienols have the unsaturated chain (Figure 3). Natural VE isoforms composed of three main structural moieties:

- (1) functional domain; redox active hydroxyl group responsible for the antioxidant ability and apoptotic activity of the VE derivatives,
- (2) signaling domain; composed of aromatic rings, has role in signal regulation,
- (3) hydrophobic domain which binds the VE molecule to the biological membranes and lipoproteins (Neophytou & Constantinou, 2015).

The small structural differences between VE isoforms have a significant impact on their biological activities and fate inside the body. Due to the structural specificities, it tends to interact with hydrophobic domains of lipids and proteins. In organisms, the major biological function of VE is accepted as the protection of membrane components from the oxidative damage (Mustacich et al, 2007). However, in addition to the antioxidant properties, VE is thought to have molecular functions independent of radical scavenging pathways. α -tocopherol has been associated with the regulation of protein kinase C which in turn involved in the proliferation and differentiation of smooth muscle cells, monocytes and human platelets. Data of VE metabolism mainly come from in vitro studies.

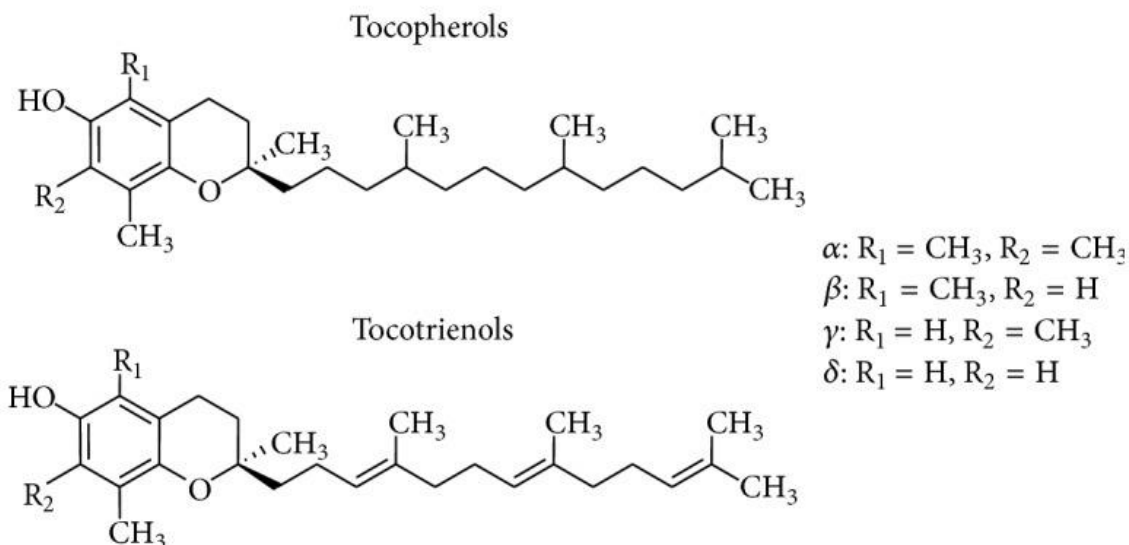


Figure 3. Structure of the natural isoforms of Vitamin E (Reproduced from (Neophytou & Constantinou, 2015)).

1.4.2. Cellular uptake

The explanations about the cellular uptake of VE mainly have been coming from liver studies, as liver is the major organ for VE regulation in the body. Although the data suggests that there are no specific mechanisms of α -tocopherol uptake but, rather, it takes the advantage of well-known lipid uptake pathways. It has been suggested that tocopherol molecule can flip-flop out of the membranes because of its lipophilic character (Mustacich et al, 2007). Regulated transfer of VE may also be controlled by lipid transfer proteins and lipases, receptor mediated lipoprotein endocytosis, selective uptake and scavenger receptor class B type I (SR-BI) receptors (Mardones & Rigotti, 2004). Although, all of mechanisms have seem to take part in α -tocopherol uptake, the relative importance of each pathway dependent primarily on the source of lipoprotein and the type of cell or tissue involved. In addition, it is worth to note that, there are similarities between α -tocopherol and cholesterol

transport paths. α -tocopherol cellular transport pathways involve cell surface receptors and transporters which are those observed in cholesterol transport into and out of cell (Mardones & Rigotti, 2004).

1.4.3. Therapeutic use of Vitamin E in Cancer

Therapeutic use of VE either alone or in combination with other anticancer agents has become a subject of great interest. Traditional chemotherapeutic agents, while effective in suppressing the growth and progression of many types of cancer, are relatively nonspecific in their mechanism of action and characteristically have toxic effects on both normal and neoplastic tissues. In contrast, tumor cells have been shown to be significantly more sensitive than normal cells to the anticancer effects of specific forms of VE. Cell culture studies have shown that treatment with natural forms and synthetic derivatives of VE significantly inhibits growth and initiates apoptosis in neoplastic cells using treatment doses that have little or no effect on normal cell growth or viability (McIntyre et al, 2000a; Neuzil et al, 2001a; Weber et al, 2002).

(You et al, 2001) reported that a VE derivative; RRR- α -Tocopheryl succinate (VES) induced differentiation in MCF7 and MDA-MB-435 cells via triggering β -casein mRNA expression. It was reported that neither α -tocopherol nor α -tocopheryl acetate could induce apoptosis in variety of cell types (Alleva et al, 2001; Kogure et al, 2001; Neuzil et al, 2001b; Weber et al, 2003). Cell culture experiments using α -tocopherol on a series of well-established cancer cell lines that included two erythroleukemia (HEL and OCIM-1) cell lines and a hormone-responsive breast (MCF-7) and prostate cancer (CRL-1740) cell lines showed that tumor cell proliferation was inhibited with only very high doses (mM) of this form of VE (Sigounas et al, 1997). The physiological significance of these studies is unclear. However, few studies have shown that γ -tocotrienol may have some protective action in the prevention of prostate cancer (Galli et al, 2004; Gysin et al, 2002). Cell culture experiments demonstrated that γ -tocopherol caused a down-regulation in cyclin D1

and E levels and induced a blockade cell cycle progression in DU-145 prostate carcinoma cells (Gysin et al, 2002). Others have also shown that δ -tocopherol displays apoptotic activity against pre-neoplastic and neoplastic mammary epithelial cells, but these effects were significantly less potent as compared to similar treatment with tocotrienols. These data also showed that the highly malignant cells were the most sensitive, whereas normal cells were the least sensitive to the apoptotic effects of these individual VE isoforms (McIntyre et al, 2000a; McIntyre et al, 2000b).

Investigations have also shown that combined treatment of VE with other chemotherapeutic agents resulted in a significant decrease in viable tumor cell number as compared to either treatment alone. Thus findings strongly suggest that VE can be used effectively to enhance therapeutic efficacy and reduce toxicity of other anticancer agents (Anderson et al, 2004a; Guthrie et al, 1997; Kline et al, 2004; Zhang et al, 2004; Zu & Ip, 2003).

The synthesis and testing of novel VE compounds for anticancer efficacy is an ongoing endeavor by several laboratories (Anderson et al, 2004a; Anderson et al, 2004b; Arya et al, 1998; Birringer et al, 2003; Lawson et al, 2003; Neuzil et al, 2001b; Shiau et al, 2006; Thompson & Wilding, 2003; Tomic-Vatic et al, 2005). To date, two VE analogs, VES (Vitamin E succinate) and α -TEA (α -Tocopheryloxyacetic acid), have been studied in greatest detail and they have shown potent anticancer properties in preclinical animal models. VES administered intraperitoneally has been demonstrated to inhibit human breast, colon, and mesothelioma cancer and mouse lung, melanoma, and mammary cancer in animal models (reviewed by Wang et al., 2006). For another α -tocopherol analog, α -TOS, it has been shown that apoptosis is triggered by mitochondrial destabilization (Weber et al, 2003).

Taken the experimental evidence obtained from cell culture studies together, α -tocopherol treatment alone is not an effective anticancer agent, whereas tocotrienols and α -tocopherol derivatives appear to be strong candidates for use as cancer chemotherapeutic agents. This suggestion is even more attractive when taking into account the low toxicity displayed by tocotrienols and α -tocopherol derivatives against normal cells.

1.5. Novel Vitamin E Analog

A new VE analog; 2,5,7,8-tetramethyl-2-(4'-methyl-3'-pentenyl)-6-acetoxy chromane (TC6OH), was synthesized by the Department of Vitamins & Coenzymes Biochemistry of the Palladin Institute of Biochemistry, National Academy of Science of Ukraine, which can be utilized to produce medicaments, biological active ingredients, as well as food supplements and veterinary products (Figure 4).

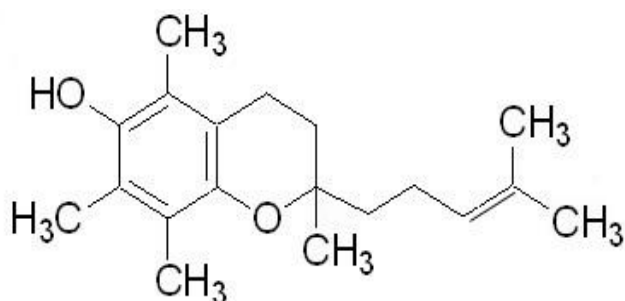


Figure 4. 2,5,7,8 – tetramethyl-2-(4'-methyl-3'-pentenyl)-6-acetoxy chromane

This analog of the VE possess additional biological and medical properties compared to the native VE. It was proposed that this new VE analog can be used for prophylaxis, as well as for treatment of variety of pathological states with oxidative stress etiology. It has been proposed that the product would provide effective protection against hypoxia, VE deficiency, intoxication, cancer, etc. This derivative of VE proposed to be used as an independent product, as well as the component of an existing medications and therapies for treatment of disease and pathological states in human or in animals. Innovative aspects and main advantages of the product suggested by the producer are:

- increased viability at stress conditions;
- normalized lipid structure of the cell membrane;
- regulation of free-radical processes in cells and organism;

- effect on activity of the antioxidant enzymes.

It has been hypothesized that the cancer cells, due to their accelerated metabolism, can accommodate much higher amounts of VE analog than the normal healthy cells thus the detrimental effects could likely be observed more in cancer cells.

At the Department of Vitamins and Coenzymes Biochemistry of the Palladin Institute of Biochemistry, experiments performed on Lewis Lung carcinoma animal model have clearly demonstrated that, this compound drastically decreased tumor size and level of metastasis. When the results were compared with those of Cisplatin, VE derivative (LD50: 5000mg/kg for rat) is 600 times less toxic than Cisplatin (LD50: 8mg/kg for rat). In addition, the side effects like hair loss, nephrotoxicity (kidney damage) and vomiting that had been observed as a result of Cisplatin treatment were not occurred in VE analog treatment. In addition, VE analog offers approximately 200 times cheaper treatment option. Analog was also tested on Walker 256 breast carcinoma Wistar rat models and the results were compared with those of doxorubicin treated group. Similar in lung cancer model, analog decreased breast tumor size in rats and less toxic than doxorubicin. Additionally, it doesn't alter white blood cell count in the treated group while doxorubicin caused severe decrease. Although the TC6OH has been yielded positive results in cancer treatment, the molecular explanations at cellular level are still missing.

1.6. Use of Spectroscopic Techniques for Drug Research

Screening for the mode of action of anti-cancer drugs has some technical challenges that are beyond the practical capability of conventional molecular biology methods. At this point, spectroscopic techniques open new windows for exploratory drug-cell interaction studies.

As a new perspective, infrared spectrum of cells treated by anti-cancer drugs could present an opportunity to obtain fingerprint of all molecules that forms to cells, and offer to observe metabolic changes induced by drug exposure with high sensitivity. Middle IR (MID-IR) spectroscopy measurements based on the absorption of MID-IR

light in the electromagnetic spectrum by vibrational transitions in covalent bonds. While the wavenumbers in the spectrum relate to the nature of these covalent bonds including their structure and the molecular environment, the intensities / areas under the curve, give quantitative information (Severcan & Haris, 2012). Infrared spectrum of a cell is complex with sum of the contributions coming from proteins, lipids, nucleic acids and other chemical species present in the cells (Figure 5). These spectra could be used as signatures to monitor global effects of drug on cell constituents (Severcan & Haris, 2012).

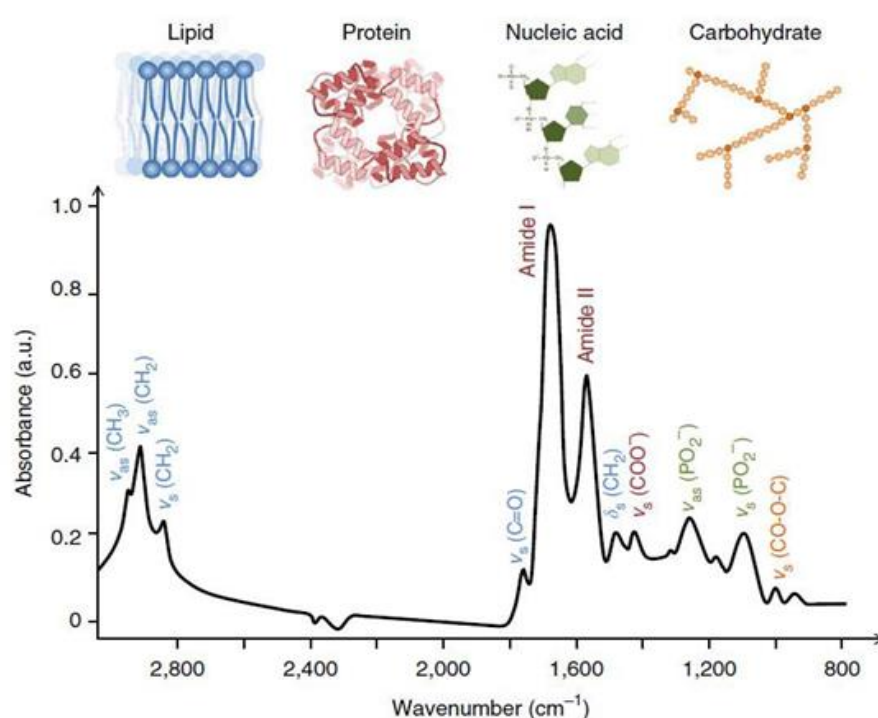


Figure 5. Typical biological spectrum of human breast carcinoma tissue, showing biomolecular peak assignments from 3000–800 cm^{-1} , where ν = stretching vibrations, δ = bending vibrations, s = symmetric vibrations and as = asymmetric vibrations. (Adopted from Baker et. al., 2014).

In this study, it has been suggested that the cells exposed to potential anti-cancer drug will have metabolic modifications which are possibly correlated with drug's cellular mode of action. The wealth of information present in IR spectra related to

drug-cell interaction was feasibly demonstrated in previous studies (Gasper et al, 2009; Inan Genc et al, 2016).

Throughout the present study, information coming from IR spectroscopy evaluated as fingerprints of all molecules that constituent the cell and detects subtle metabolic changes which in turn shed light on the chemical modifications induced upon analog and α -tocopherol treatment.

Another spectroscopic technique applied in this study is the Electron Spin Resonance spectroscopy which measures the absorption of microwave radiation corresponding to the energy splitting of an unpaired electron in any chemical system, under strong magnetic field. Analysis of the line shapes and positions in the ESR spectrum give information about the rate of motion of the spin label, the structure, order, viscosity and polarity of the system (Campbell & Dwek, 1984).

Measurement yield structural and dynamic information even from continuing chemical or physical processes without influencing the process itself. This makes ESR spectroscopy one of the ideal analytical technique in biological studies. ESR is used to investigate membrane properties and drug-membrane interactions especially for the determination of membrane order, fluidity and localization of drug into bilayer. An advantage of the technique is its sensitivity which allows to studying drug-membrane interactions at molecular or sub-molecular levels. In previous studies membrane order and dynamics have been studied as well as effects of VE (Severcan & Cannistraro, 1988; Severcan & Cannistraro, 1989) and other drugs on membrane phase behavior and permeability (Deo & Somasundaran, 2002; Sade et al, 2012; Severcan & Cannistraro, 1988; Severcan & Cannistraro, 1989; Severcan & Cannistraro, 1990; Vishnyakova et al, 2000). Similarly, in this study, the effect of VE analog on cell membrane was investigated via ESR measurements.

1.7. Scope of the Study

TC6OH, being a lipophilic compound, is also a potential modulator of membrane-lipid structure and dynamics. This dissertation focuses on investigating the biological

functions of new vitamin E analog (TC6OH) in MCF7 breast cancer cells, by performing cell response assays and identifying the major effects of TC6OH on cellular lipids at genetic and metabolic levels. For that purpose, we have treated MCF7 cell line with TC6OH. Through the experiments same dose of α -tocopherol treated group was used as a reference, allowing us to delineate what kind of effect is caused by the change in the structure of the tocopherol chain even though the same amount of substance is present in the cell system.

CHAPTER II

MATERIALS AND METHODS

2.1. Cell Culture

Human breast cancer MCF7 cells were obtained from Şap Institute (Ankara, Turkey). MCF7 cells were cultured in phenol red free complete DMEM (Biochrom AG, Germany) culture medium supplied with 10% Fetal bovine serum (Biowest), 1% penicilin/streptomycin/amphotericin (Lonza, Basel, Switzerland).

Human breast epithelial MCF10A cells were kindly donated by Dr. Sreeperna Banerjee. MCF10A cells were cultured in DMEM F12 (Biowest) medium supplied with 5% horse serum (Biochrom, AG, Germany), 100 ng/ml cholera toxin (sigma), 20 ng/ml Epidermal growth factor, 10 µg/ml insulin, 0.5 µg/ml hydrocortisone (Sigma) and 1% penicilin/streptomycin/amphotericin (Lonza). All the cells were incubated in humidified atmosphere with 5% CO₂ at 37°C.

2.1.1. VE Analog Treatment Procedure

α-tocopherol and tocopherol analog was weighed and solved in absolute cell culture grade ethanol then 1mM stock solution was prepared with culture medium decreasing the EtOH concentration to 0.5%. After the cells were reached 75-80% confluency, they were treated with relevant concentrations. Final EtOH concentration was not more than 0.05% for treated cells. All dilutions prepared in culture medium. The same amount of EtOH was also added to the related control groups. Drug solutions were freshly prepared for each week.

2.2. Cell Response Assays

2.2.1. XTT Cell Viability assay

Cell viability was determined by XTT assay (Roche) according to manufacturer's instructions. 1×10^4 cells were seeded in 96-well plate (Greiner) suspending in 100 μ l culture medium. Cells were incubated for 24 h then medium was discarded. Freshly prepared treatment medium (100 μ l) was added to each well. Varying μ M drug concentrations were applied for 12, 24, 48 and 72 hours separately. After incubation, 50 μ l XTT reagent was added to each well and absorbance was measured at 570 nm with Multiskan microplate reader (Thermo Scientific, USA). Background absorbance was recorded at 670 nm and subtracted from the Absorbance values at 570 nm.

Cell viability curves were constructed for each plate. Absorbance of untreated (control) cells was used as 100% viability. IC_{50} values for each plate were calculated by linear regression analysis.

2.2.2. BrdU Cell Proliferation Assay

Cell proliferation was measured via BrdU incorporation assay according to the manufacturer's instructions (Roche, Mannheim, Germany). 1×10^4 cells were seeded in 96-well plate. After the treatments, labeling, fixation and detection steps were followed. BrdU incorporates instead of thymidine in newly synthesized DNA in proliferating cells. Assay principle depends on the spectroscopic detection of BrdU level. Absorbance was recorded at 370 nm and subtracted from the background absorbance recorded at 492 nm.

2.2.3. Annexin V-FITC / PI staining

Apoptosis characterized by cytoplasmic and nuclear condensation, DNA degradation and the loss of membrane asymmetry. In the early stage of apoptosis phosphatidylserine (PS) molecules turns from inner to the outer surface of plasma membrane. Annexin V dye has high affinity to PS molecules. By following Annexin V signal in flow cytometry, it can be possible to detect the ratio of apoptotic cells in a cell population. Cells were cultered and treated in 6-well plates then trypsinized and collected as well as their supernatants. Cells were washed with PBS and supernatant was discarded. Annexin V staining were conducted by FITC Annexin V apoptosis detection kit (BD Pharmingen™ Catalog # 556547) following the manufacturer's instructions and read by flow cytometer (BD Accuri™ C6, Germany). 20000 cells were analyzed per single measurement.

2.2.4. JC-1 Staining

Apoptosis also causes mitochondrial changes. As a result of the Nitric oxide gas production, increase in the permeability of mitochondrial membrane causes membrane potential changes. Mitochondrial membrane potential change was followed with the help of JC-1 stain. Healthy cells have high membrane potential thus JC-1 dye can form aggregated compounds and give red fluorescence whereas apoptotic cells have lower mitochondrial membrane potential which causes JC-1 dyes to remain in monomeric state. Monomeric JC-1 gives green fluorescence. Cells were cultered and treated in 6-well plates then trypsinized and collected as well as their supernatants. Cells were washed with PBS and supernatant was discarded. JC-1 staining is conducted by BD JC-1 kit following the kit instructions and read by flow cytometer in red (FL-2) and green (FL-1) fluorescence channels. Mitochondrial depolarization was determined by following the green/red fluorescence ratio.

2.3. Cell Motility Measurements

2.3.1. In vitro scratch wound healing assay

Effect of analog treatment on cellular motility was measured by in vitro scratch wound healing assay. Non-treated cells were inoculated in 6-well plate and incubated up to they become confluent. Then each well was scratched with a sterile 1000 μ l pipette tip. Cells were washed 2X with PBS after scratching to remove debris then incubated in treatment medium for 48h. Subsequent images were taken at the time of 0, 12th, 24th and 48th hours with inverted light microscope (Olympus, Hamburg, Germany). Images were analyzed with ImageJ 1.42 (<http://rsbweb.nih.gov/ij/>) program to measure the distance between wound edges.

2.3.2. Boyden chamber cell migration assay

Migration capacity of treated and non-treated cells was measured by in vitro Boyden chamber assay. Boyden chambers with 8 μ m pore size (Corning, USA) were used. 5×10^4 MCF7 cells in 0.5 ml serum free DMEM medium were inoculated to the upper chamber of transwell. Treatment was done in the time of inoculation and allowed to migrate for 48 h. Serum rich medium was used as a chemo-attractant in the lower chamber. Chambers were fixed with 4% paraformaldehyde for 2 min, washed with PBS, permeabilized with absolute Methanol for 20 min, washed twice and stained with Giemsa stain for 15 min. After the last wash with PBS twice, migrated cells were observed under light microscope with 20x objective. 3 fields per membrane were counted.

2.4. Lipid Droplets Staining

MCF7 cells were cultured in complete media in triplicate 60 mm culture dishes and treated with vehicle, α -tocopherol and α -tocopherol analog for 48 h. After the treatment, the media was aspirated and cells were fixed with 4% paraformaldehyde for 10 min at room temperature. Cells were washed two times with PBS. Oil red O dye was dissolved in isopropanol for making 0.5% stock solution. 3:2 ratio of filtered Oil Red O in isopropanol to water was added to the cells and allowed to stand for 10 min. Cells were washed with distilled water and observed under microscope.

2.5. Fatty Acid Metabolism PCR Array

2.5.1. RNA isolation

Total RNA was extracted from cells by using RNeasy Minikit (Qiagen, Hilden, Germany) according to the manufacturer's instructions. The purity and quantity of isolates were determined via Nanodrop (Thermo-Fisher Scientific, USA) spectrophotometer at 260 and 280 nm wavelengths. RNA concentrations of > 350 ng/ μ l and Absorbance ratios of $260 / 280 > 1.8$ and $260/230 > 1.7$ were used for further applications. Isolated RNA was kept at -80°C until cDNA synthesis.

2.5.2. Agarose gel electrophoresis of RNA

To check the integrity of isolated RNA, agarose gel electrophoresis was conducted. 1mg agarose powder was dissolved in 50 ml 1x TAE buffer by heating the mixture in microwave. 4 μ l of Ethidium Bromide was added into the cooled solution. 2 μ l RNA

sample was loaded to the wells by mixing with 2 μ l of 2x RNA loading dye (Fermantas, Lithuania). RNA was run at 100V for 30 min and visualized under UV.

2.5.3. cDNA synthesis

cDNA was synthesized from total RNA with RT² First Strand Kit (Qiagen) by following the manufacturer's instructions. 3 μ g starting RNA was used per 20 μ l synthesis reaction. Reaction conditions are as follows;

1 hour at 42 °C + 5 minutes at 70 °C

2.5.4. RT PCR Array

cDNA product was mixed with RT² SYBR Green ROX FAST mastermix (Qiagen) and nuclease free water was added to the mixture according to the instructions. 20 μ l of prepared PCR mix was pipetted robotically to each well of Human Fatty Acid Metabolism RT² Profiler PCR Array (SABioscience, Frederick, MD, USA) using QIAgility®. RT² Profiler PCR Array was sealed with Rotor-Disc Heat Sealing Film using Rotor-Disc Heat Sealer. RT Thermal cycler (Applied Biosystems, Foster City, CA) was programmed as;

10minutes initial incubation at 95°C + 40 cycles of [30 seconds at 94°C + 30 seconds at 65°C + 30 seconds at 72°C].

All the data analyses were conducted via online Qiagen RT² profiler PCR array data analysis center. Lower limit of detection (C_T cut-off) was set to 33. For the normalization of data, the optimal set of internal control genes for the analysis from the full panel on the PCR array was automatically selected. Software measures and identifies the genes with the most stable expression. The C_T values for these genes are geometrically averaged and used for $\Delta\Delta C_T$ calculation. Relative quantitation of

the expression for each gene was determined for each group by comparing to the untreated (control) group using the $\Delta\Delta C_T$ method. Results are represented as fold change in expression of each gene comparing to the control. Fold regulation and p-value cut off were set to 2 and 0.05 respectively. Total gene list is given as a table in Appendix B.

2.6. ATR-FTIR Spectroscopy

2.6.1. Sample Preparation

Control, analog and α -tocopherol treated cells were cultured for 48h. 6 independent growths were done for each group. Cells were washed with PBS, trypsinized and counted with hemocytometer under light microscope. 2 million cells were centrifuged for 5 min at 1000g. Pellet was resuspended in 10 μ l PBS and incubated on ice during ATR-FTIR measurements.

2.6.2. Data Collection

2 μ l cell + PBS mix was placed on ZnSe ATR crystal (*Perkin-Elmer Inc.*, Norwalk, CT, USA, equipped with ATR accessory). Spectrum of air was used as a reference and automatically subtracted from the sample spectrums. Samples on crystal were dried by mild N_2 flux for 5 min. to remove bulk water then scanned over 4000-650 cm^{-1} spectral range with 100 scan number per sample at 4 cm^{-1} resolution. 3 spectra were collected for each sample. Average of these 3 spectra was used for further analysis. Data collection and manipulation was carried out via spectrum 100 software.

2.6.3. IR Data analysis

In spectral data analyses, second derivative raw spectra were used to increase band resolution. Second derivative spectra were obtained by Savitzky-Golay algorithm. Band assignments for the analyzed bands are given in Table 3 in results and discussion part. Band frequency and bandwidth values were calculated using OPUS 5.5 software (Bruker Optics, GmbH) by peak picking method. Band areas were calculated from the non-derivative, baseline corrected spectra by Spectrum 100 software using band automatic band area calculation menu. For the representative figures vector normalized, baseline corrected spectra were used.

2.6.4. Chemometrics

Chemometric analyses were conducted via *Unscrambler X 10.3 (Camo Software, Norway)* multivariate analysis (MVA) software. Second derivative vector normalized absorbance spectra were loaded for Principle Component Analysis (PCA) and Hierarchical Cluster Analysis (HCA). Detailed information about the PCA and HCA was previously given (Bozkurt et al, 2010; Gok et al, 2016; Gok et al, 2015). Mean centered PCA was applied over the range of whole IR (4000-650 cm^{-1}), CH-Lipid (3000-2800 cm^{-1}), protein (1700-1500 cm^{-1}) and nucleic acid (1150-900 cm^{-1}) regions. Results were presented as loading and score plots.

HCA was conducted over the range of 3000-2800 cm^{-1} . Ward's algorithm calculated the squared Euclidian distance between the samples. Clustering depends on the relative distance among the spectra. Results were presented as dendrograms.

2.7. Electron Spin Resonance (ESR) Spectroscopy

ESR spin labeling technique is used for the collect information about membrane polarity and fluidity (permeability) changes and lipid phase transitions in biological systems. ESR is a suitable technique for materials that have unpaired electrons. If the biological system of interest has not unpaired electrons for ESR measurements, molecules that contain unpaired electrons are used. This technique is called as spin-label probe ESR spectroscopy. The most widely used molecules that contain free radicals are nitroxide radicals. Nitroxides have stable structures and able to give information about the environment where they stand in, without giving any significant changes to the environment. Doxyl stearic acids are lipophilic nitroxides, can have various chain lengths (5-DSA, 12-DSA, 16-DSA etc) thus able to give information about different parts of membrane (Kocherginsky N., 1995). Chemical structures of the spin labels used in this study, were given in Table 2,

Table 2. The name and the chemical structures of spin labels used in the current study.

Name	Chemical Structure
<u>5-doxyl stearic acid (5-DSA)</u> (2-(3-carboxypropyl)-2-tridecyl-4,4-dimethyl oxazolidine-3-oxyl)	
<u>16-doxyl stearic acid (16-DSA)</u> (2-(14-carboxytetradecyl)-2-ethyl-4,4-dimethyl oxazolidine-3-oxyl)	

In the current study, 5-doxyl stearic acid and 16-doxyl stearic acid were used to label the outer (upper part of acyl chains) and inner (lower part of the acyl chains) part of membrane respectively. 10^{-2} M DSA labeling stock solution was prepared in absolute ethanol and stored in -20°C . 10^7 cells /ml cells in PBS were incubated in 10^{-4} M

labeling solution for 60 min at 37°C. Unbound spin labels were removed by extensive PBS washing (6 times). Labeled samples were placed in capillary glass tubes and ESR spectra were collected immediately by Bruker ESR EMX spectrometer (Bruker, Germany) at X band, 9.85 GHz, 100G sweep width, 0.5 Gauss modulation amplitude and 10mW microwave power. The resonator in a microwave spectrophotometer is called cavity. The cavity containing the sample placed in a magnetic field that is “swept” through the resonance condition. Detection is improved by modulating the magnetic field. The detected signal appears as a first derivative of the absorption line.

Membrane fluidity information was obtained by calculating the rotational correlation time (τ_c) from the 16-DSA labeled sample spectra using formula 1.

$$\tau_c = 6.5 \times 10^{-10} W_0 \left[\left(\frac{h_0}{h_{-1}} \right)^{\frac{1}{2}} - 1 \right] \quad (1)$$

where $K = 6.5 \times 10^{-10} \text{ s G}^{-1}$ is a constant depending on microwave frequency and the magnetic anisotropy of the spin label, W_0 is the peak-to-peak width of the central line, and $\frac{h_0}{h_{-1}}$ is the ratio of the heights of the central and high field lines, respectively (Severcan & Cannistraro, 1989; Severcan & Cannistraro, 1990).

Amplitude of motion of the spin label is governed by its environment. The extent of fast motional averaging of the anisotropy can be defined by order parameter (S), where;

$S = \text{observed anisotropy} / \text{maximum anisotropy}$

Order parameter (S) was calculated by using the given formula (2) from the 5-DSA labeled sample spectra. Calculation of elements and the equation constants in the order formula are also given. $A_{//}$ and the A_{\perp} are apparent parallel and perpendicular hyperfine splittings.

$$S = \frac{A_{//} - A_{\perp}}{A_{zz} - 0.5(A_{xx} + A_{yy})} \times \frac{a_0'}{a_0} \quad (2)$$

$$A_{//} = A_{\max}$$

$$A_{\perp} = A_{\min} + 1.32 + 1.86 \log(1 - S_{app})$$

$$S_{app} = \frac{A_{\max} + A_{\min}}{A_{zz} - \frac{1}{2}(A_{xx} + A_{yy})}$$

$$a_0 = \frac{1}{3}(A_{//} + 2A_{\perp})$$

$$a_0' = \frac{1}{3}(A_{xx} + A_{yy} + A_{zz})$$

For 5 DSA,

$$A_{xx} = 6.3G$$

$$A_{yy} = 5.8G$$

$$A_{zz} = 33.6G$$

2.8. Measurement of Lipid Peroxidation

Some specific molecules like, Malondialdehyde (MDA), 4-Hydroxynonenal, 8-isoprostane and OxLDL are produced, as an end products of the lipid peroxidation and can be used as a marker to test peroxidation level in cell. In the current study, MDA and 8-isoprostane levels were measured by using assay kits, by following the manufacturer's instructions (abcam, ab118970 and ab175819 respectively). MDA

and 8-isoprostane quantity for each individual sample was determined with the help of standard curves.

2.9. Western Blotting and Antibodies

Cells were harvested by scraper on ice for protein isolation. Collected lysates were centrifuged and sonicated. Total protein isolation was done from the treated and non-treated cells by ReadyPrep™ protein extraction kit (Bio-Rad, catalog #163-2086) with the addition of protease inhibitor cocktail (Roche, Germany) and the protein concentration was determined via Bio-Rad RC DC protein Assay (catalog #500-0121) according to the manufacturer's instructions.

Protein extracts (50 µg) were denatured in 6X Laemmli buffer, separated on polyacrylamide gel (10%) and transferred to the PVDF membrane (Bio-Rad). Membranes were firstly blocked with skim milk in TBST buffer (5%) then incubated with the related antibody followed by HRP-conjugated secondary antibody incubation. β -actin was used as a loading control. List of antibodies used in western blot analyses are given in Table 3,

Table 3. The list of antibodies used for Western Blot analysis

Antibody	Company Name	Catalog Number
HMGCS1	abcam	ab87246
SREBP	abcam	ab28481
LIPE	abcam	ab103281
Vimentin	Cell signaling	5741
p-ERK	Cell signaling	4376
p-AKT Ser 473	Cell signaling	4058
Cleaved Caspase 3	Cell signaling	9664
Secondary (Anti-rabbit)	abcam	ab16284
β -Actin	abcam	ab49900

The bands were visualized by chemiluminescence detection kit (ECL, Biorad) and Chemi-Doc imaging systems. Signal accumulation mode was preferred for image capture. Pixel densities on each spot were determined by image processing program (ImageJ). Signal taken from the negative control spot was used as a background value and subtracted from the averaged signal of each spot and the corresponding signals on different arrays for treated and non-treated samples were compared to determine relative change in protein expression.

2.10. Protein Array

Total protein was isolated from cell lysates and concentration was determined by Biorad AC DC assay. Aliquots were stored at -80°C. Human XL oncology array kit (R&D systems, catalog #ARY026, Minneapolis, USA) was used to panel 84 human cancer related proteins simultaneously. The names and the coordinates of protein spots are given as table in Appendix A.

Membrane blocking, sample incubation, washing, antibody incubation and chemiluminescence detection were performed following the manufacturer's instruction without any modification.

2.11. Statistical Analysis

Each experiment was biologically repeated at least 3 times independently, with several technical replicates. Statistical analyses were conducted with GraphPad Prism (GraphPad Software Inc, USA). Normality of the data was checked by Kolmogorov-Smirnov test. As there are more than 2 normally distributed groups, significance was tested by One-way ANOVA with Tukey's post-hoc test. Results were presented as Mean \pm SEM. Significance was considered as * $p < 0.05$, ** $p < 0.01$ and *** $p < 0.001$.

CHAPTER III

RESULTS AND DISCUSSION

3.1. The Effect of Analog Treatment on Cell Proliferation and Apoptosis

4 types of cell viability and apoptosis assays were used thorough this study.

3.1.1. XTT Assay: Changes in the rate of cell proliferation in response to analog and α -tocopherol treatment were determined by XTT assay. Figure 6 represents the percent viability of treated MCF7 cells at increasing concentration of analog and α -tocopherol with different incubation time intervals. Reduction in the cell viability compared to the control (non-treated) reached statistical significance in response to analog treatment.

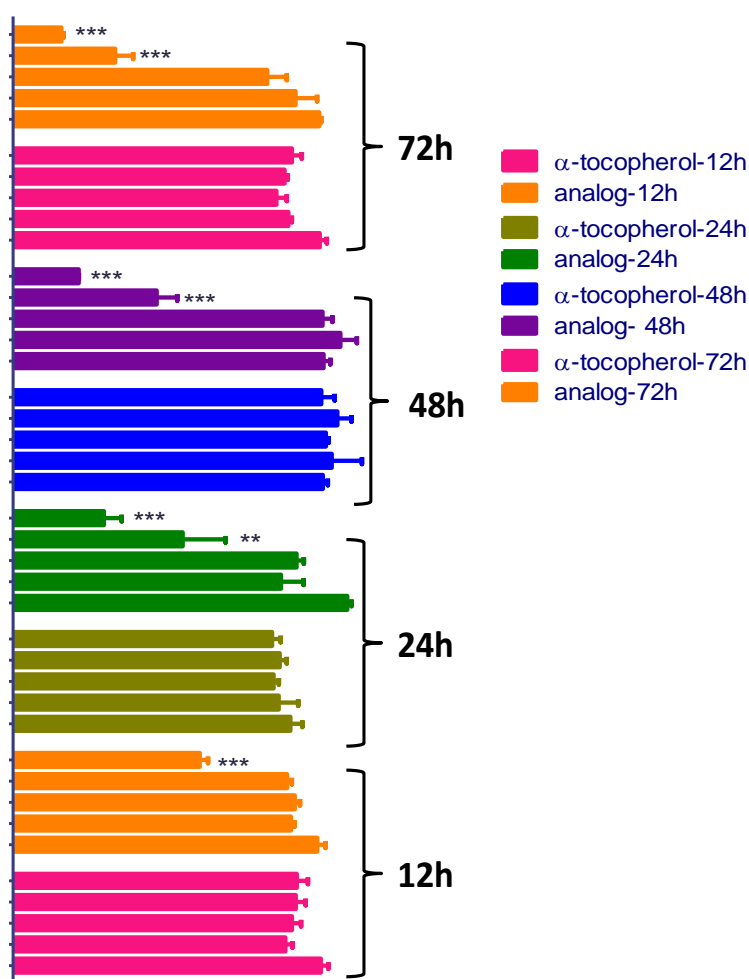


Figure 6. Growth inhibition curve for 12, 24, 48 and 78 h analog and α -tocopherol treated MCF7 cells. MCF7 cells were placed in 96-well plates and treated with 50, 100, 150 and 200 μ M analog and α -tocopherol. Cellular viability was determined for each time point by an XTT assay. Each time point represents the means \pm SEM (n=12; **p<0.01, ***p<0.001)

IC₅₀ (concentration that caused 50% inhibition of growth) values were calculated by extrapolating the curve. Average IC₅₀ values for analog treatment are given in Figure 7 for each time points. 150 μ M with 48 h incubation was determined as targeting dose for VE analog. Same dose was used for α -tocopherol treatment for comparison during the further experiments.

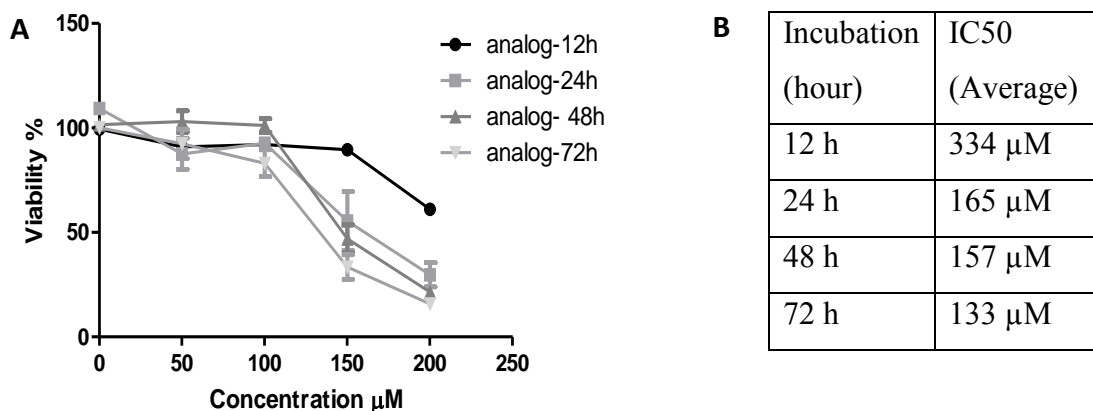


Figure 7. (A) Dose response curve of 12h, 24h, 48h and 72h different concentration treated MCF7 cells. (B) Average IC₅₀ calculations for the analog treatment dose (n=12).

XTT assay was performed for MCF-10A breast epithelial cells to observe the possible toxic effects of analog in non-cancerous cells. Figure 8 shows the 48h analog and α -tocopherol treatment from 0-300 μM dose interval.

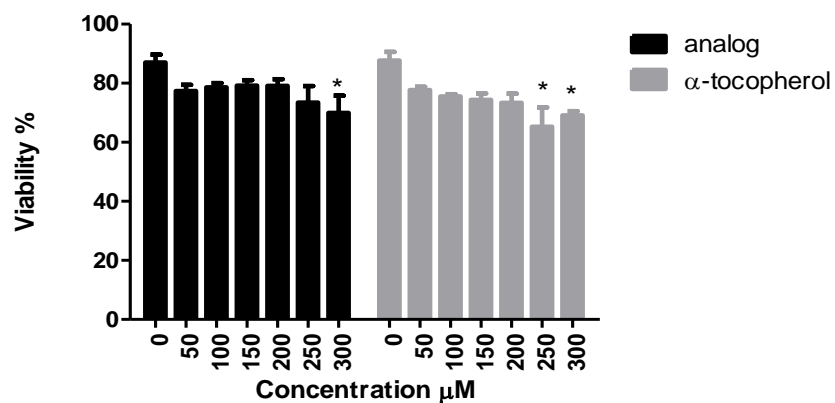


Figure 8. Growth inhibition curve for 48h analog and α -tocopherol treated MCF-10A cells (n=6).

As it can be seen from the Figure 8, analog treatment did not affect cell viability significantly up to 300 μ M. Results showed that growth inhibitory dose of analog for MCF7 cells did not significantly alter the cell viability of human breast epithelial MCF10A cells. It is open question that why VE analog is highly toxic towards cancer cells while not in normal cells. It can be speculated that physicochemical properties of VE analog could affect the selectivity. The VE analog is weak acid with low pKa value. Therefore, at physiological pH of normal cell interstitium, majority of the analog molecules exist in the deprotonated state. As a result, it can be expected that, molecule will cross the plasma membrane at low rate. On the other hand, the acidic pH of tumor cell interstitium causes the increased protonation of VE analog molecule which facilitates the free diffusion of analog throughout the plasma membrane. This hypothesis is consistent with the idea that the inducers of apoptosis which are weak acids may be selective anticancer agents due to their preferential uptake by tumor cells (Gerweck et al, 1999; Kozin et al, 2001).

3.1.2. BrdU Assay: To confirm the effect of analog treatment on cell proliferation, the chemiluminescent BrdU incorporation assay for 48 h was carried out.

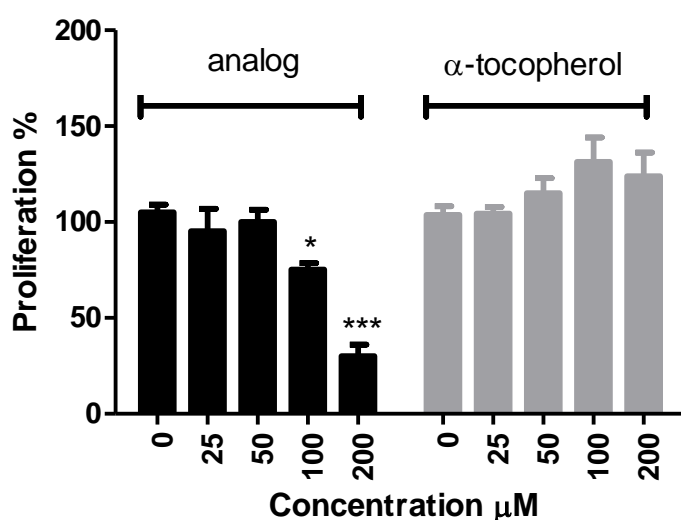


Figure 9. % change in cell proliferation in response to analog and α -tocopherol treatment for 48 h (n=6; *p<0.05, ***p<0.001)

Significant decrease in cell proliferation was observed in response to analog treatment at 100 μ M and 200 μ M concentrations for 48 hours whereas there is no significant change in response to α -tocopherol ($*p<0.05$ and $***p<0.001$) (Figure 9). Cellular proliferation results were in consistent with the cell viability results. It can be concluded that VE analog decreases cellular viability by inhibiting the DNA synthesis severely. On the other hand α -tocopherol has no significant effect on MCF7 cell viability as previously reported by others (Sigounas et al, 1997).

3.1.3. Annexin V – PI affinity assay: Flow cytometry readings showed that, analog treatment resulted in an increase in the number of early (lower right quadrant) & late apoptotic (upper right quadrant) cells compared to the α -tocopherol treated and control ones. The assay was repeated three times and the representative figures are shown in Figure 10.

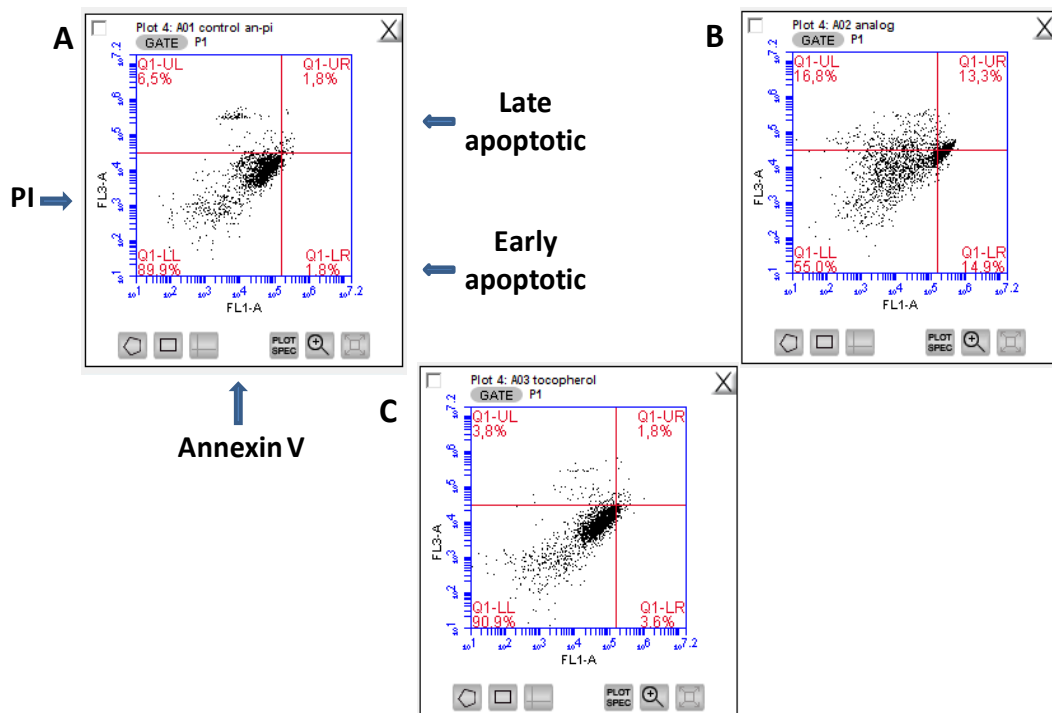


Figure 10. Annexin V / PI staining of Control (A), Analog (B) and α -tocopherol (C) treated cells (n=4 for each group). X axis represents Annexin V staining, Y axis represents PI staining. Early and late apoptotic cells are indicated by arrows.

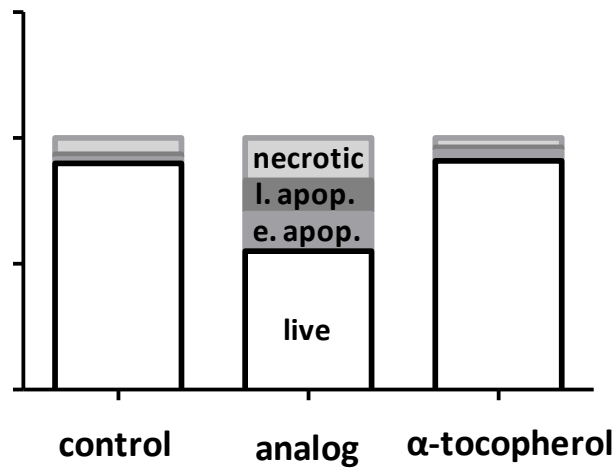


Figure 11. Percentages of apoptotic events. e. apop.: shows the number of early apoptotic cells, l. apop.: shows the number of late apoptotic cells.

The number of early and late apoptotic cell population was increased due to 48 h analog treatment compared to the untreated cells, whereas, there was no induction of apoptosis in the α -tocopherol treated population (Figure 11). Data coming from number of other researches clearly indicated that natural α -tocopherol displays little or no apoptotic activity (Kimmick et al., 1997; Kline et al., 2004; Neuzil et al., 2002b; Schneider, 2005; Sylvester and Shah, 2005b). Our findings also pointed out similar results.

3.1.4. JC-1 Staining: As can be followed from the Figure 12, the ratio of depolarized cells increased, due to the 48 h analog treatment whereas the control (A) and α -tocopherol (B) group nearly gave similar responses. This data documented that mitochondria are important for apoptosis triggered by VE analog.

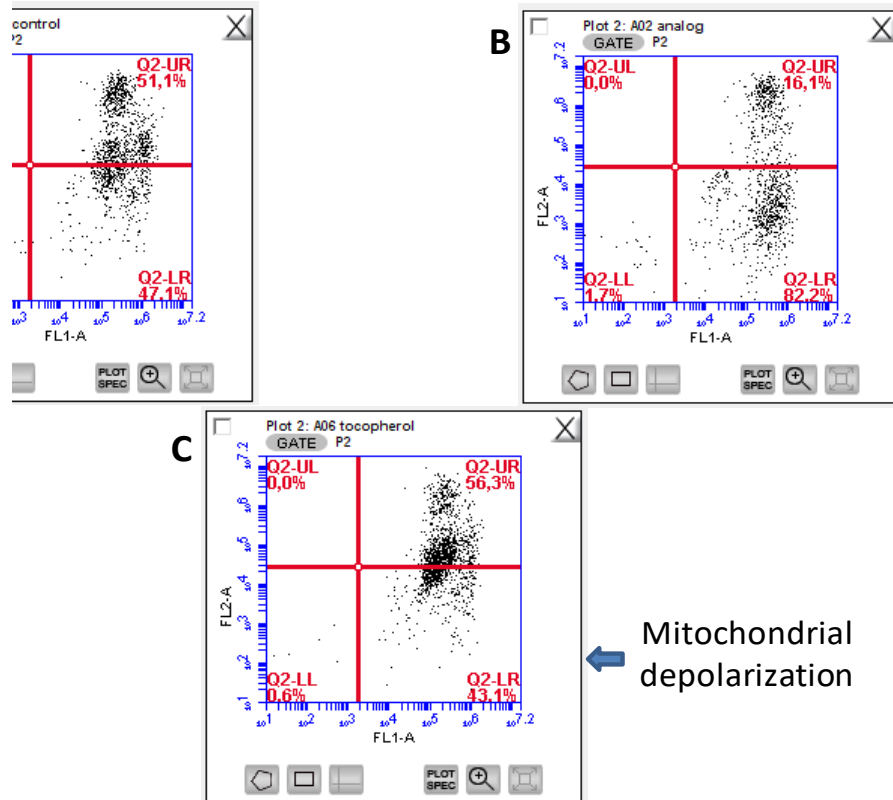


Figure 12. Flow cytometry readings of JC-1 staining. Mitochondrial membrane potential changes are represented for Control (A), Analog (B) and α -tocopherol (C) treated cells (n=4 for each group). Mitochondrial depolarization causes cells to migrate through lower right quadrant.

Apoptosis can take place following either extrinsic or intrinsic pathways. Extrinsic pathway begins when there is a lethal signal in the extracellular environment of the cell while intrinsic pathway is triggered by intracellular injury. Regarding the experimental results, VE analog induced apoptosis can be classified as both intrinsic, involving signaling responses from mitochondrial pathway and extrinsic, involving the responses from structural and compositional changes on the cellular membrane which were reviewed below. It was previously showed that, α -TOS, causes mitochondrial permeabilization throughout Noxa-Bak axes and induces apoptosis in several cell lines (Prochazka et al, 2010). This might be the common mechanism for TC6OH which acts as a mitochondrial destabilizing agent.

3.2. The Effect of Analog Treatment on Migration Ability of Cells

3.2.1 Wound Healing Assay: Experimental results showed that Analog treatment caused a reduction in cell motility, represented as wound closing confluent MCF7 cells. Analog treated cells were not able to close the wound in culture dish as compared to untreated and α -tocopherol treated cells (Figure 13).

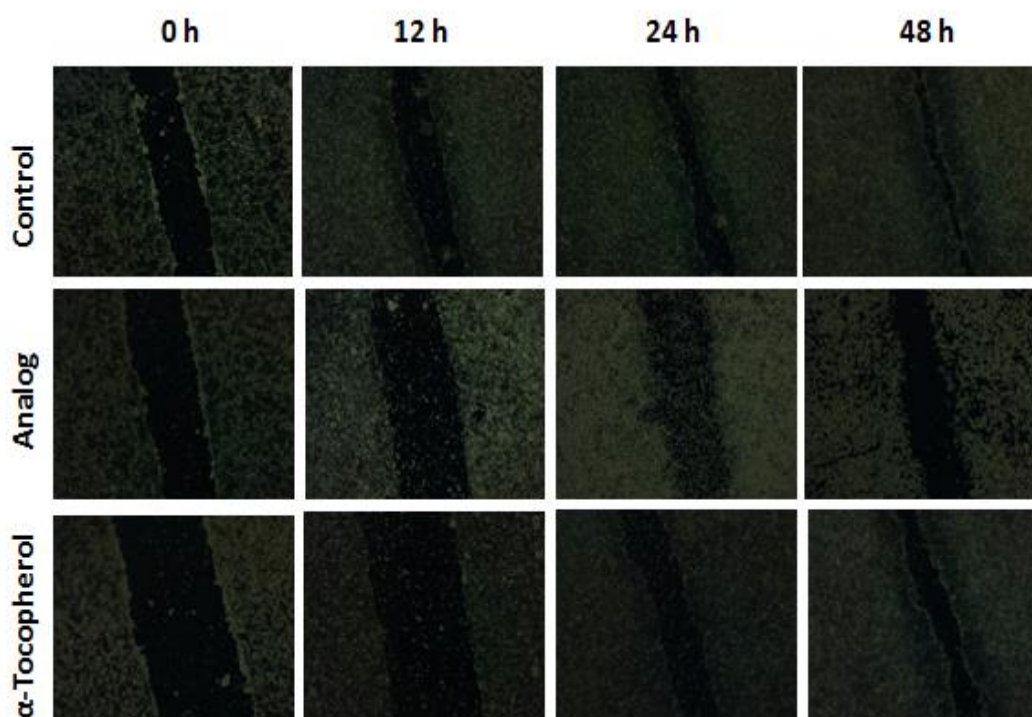


Figure 13. Representative pictures taken at different time points showing wound closure in response to 150 μ M analog and α -tocopherol treatment. Analog treated cells are not able to close the wound in the confluent culture flask when compared to untreated and α -tocopherol treated cells.

Area change during wound closure was quantitatively evaluated and shown in Figure 14. Cellular motility was not affected significantly in response to α -tocopherol treatment while significantly reduced under analog treatment.

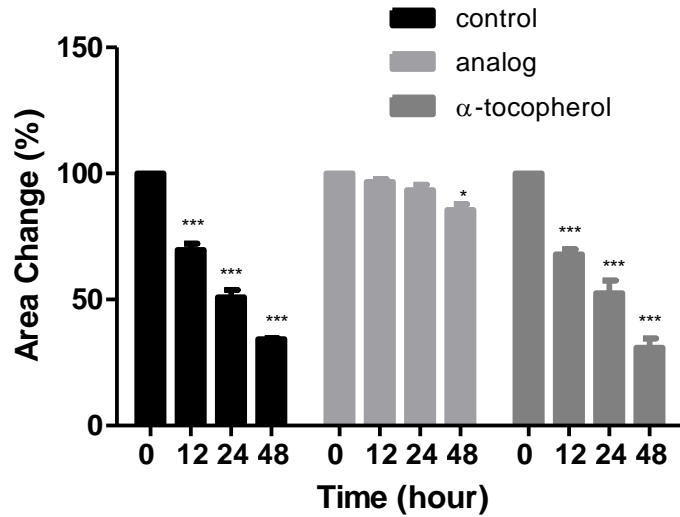


Figure 14. Quantification of cell motility in the in-vitro scratch wound healing assay (n=3 for each group; *p<0.5, ***p<0.001).

3.2.2. Boyden Chamber cell migration assay: In order to monitor the effect of analog treatment on cell migration, in vitro transwell migration assay was conducted. At the end of 48 h incubation, number of migrated cells was significantly decreased in the analog treated wells as compared to the control and α -tocopherol (Figure 15). Parallel results with the wound healing assay were observed. VE analog treatment had remarkable effect on migration ability of MCF7 cells.

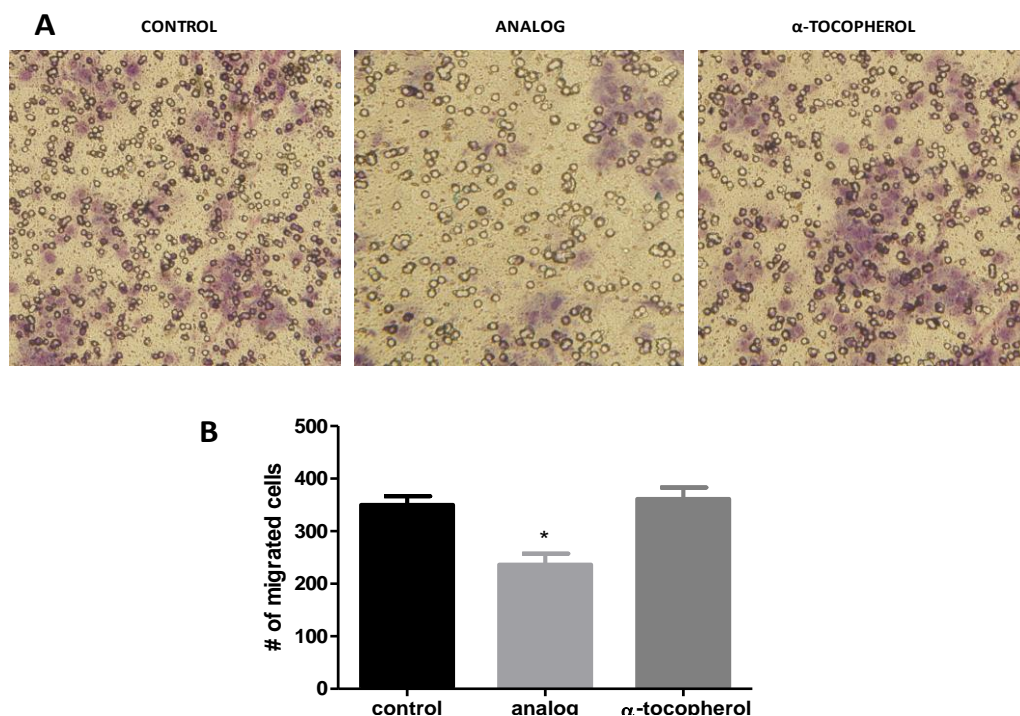


Figure 15. Transwell migration assay. A: representative pictures of cell migration for experimental groups, B: number of cells migrated (n=3 for each group).

3.3. The Effects of Analog Treatment in Lipid Content and Structure

3.3.1. VE Analog induces lipid droplet formation

In cancerous cells, excessive lipid and cholesterol are stored in lipid droplets. Fatty acids are the valuable energy source for cells in addition to the glucose and glutamine. Fatty acids can be obtained from accumulating lipid droplets by hydrolyses in cytoplasm.

To visualize changes in lipid content qualitatively, cells were stained with Oil Red O. As it can be followed from the Figure 16 the number of lipid droplets, give positive oil red o, is more in the analog and α -tocopherol treated groups than control. Results

give clues about the increase in total lipid amount in analog and α -tocopherol treated cells.

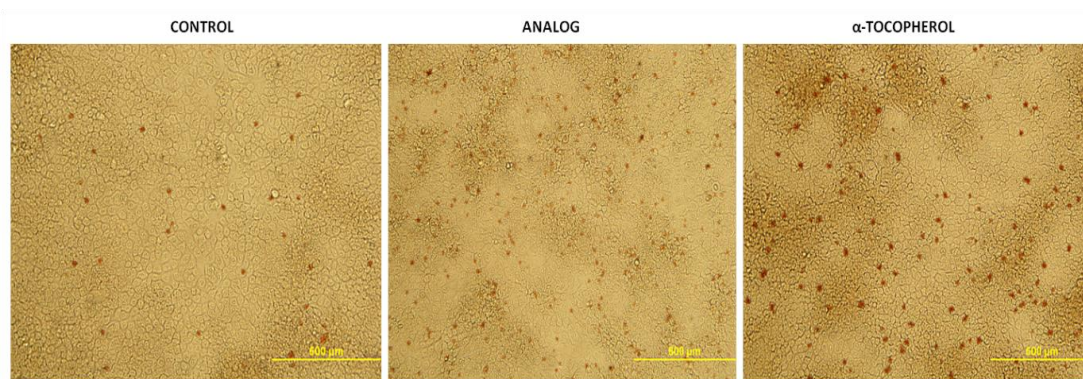


Figure 16. Oil Red O stained MCF7 cells. Images were taken with 20X objective.

3.3.2. Monitoring changes in cellular lipids by spectroscopic techniques

Two non-invasive biophysical techniques, ATR-FTIR and spin label ESR spectroscopies were used for investigation of the alterations caused by VE analog on lipid content, structure and dynamics in cell system. This dissertation is mainly focused on lipids. The diversity of lipids in terms of their physicochemical properties makes their analysis complicated. There are limited number of analytical methods like mass spectroscopy to monitor full lipid profile of cell (Fahy et al, 2011). However, a rapid method for quantitative analyses is needed.

3.3.2.1. Infrared Spectroscopy

FTIR spectra is plotted as absorbance as a function of wavenumber. For lipid analyses two major regions are used. The wavenumber region from $3050\text{-}2800\text{ cm}^{-1}$ contains C-H stretching contributions mainly originated from the hydrocarbon chains. The other region located in the low wavenumber below 1800 cm^{-1} is called fingerprint region. This region monitors polar head groups or the region near to polar

head group of saturated lipids, bending motion of lipid acyl chain and triglycerides/cholesterol ester in addition to proteins and nucleic acids. It has been shown that IR spectra has been used for signature of various lipid classes and structural details of biomembranes and lipid assemblies (Derenne et al, 2013)

3.3.2.1.1. Chemometric Analysis

Quantitative and qualitative analyses conducted so far have showed that there was structural, compositional and functional changes at molecular level due to the treatment. Spectroscopy based methods yield massive data which require multidimensional multivariate analyses to extract specific and meaningful information. PCA and HCA are unsupervised multivariate analysis methods give a way to explore data without preliminary information about the sample of interest (Gasper et al, 2009). PCA analysis was firstly conducted in whole IR region (4000-650 cm^{-1}) in order to reduce the number of variables that is going to be further explored. As it can be followed from the loading plot (Figure 17A) dramatic changes were agglomerated mostly in CH (3030-2800 cm^{-1}), amide (1700-1500 cm^{-1}) and nucleic acid (1200-1000 cm^{-1}) specific vibrations.

Loading plots indicate the frequency values which contribute to the variations described in each principal component. Each spectrum which consists of hundreds of absorbance values is reduced by linear transformation and represented as a single point in multidimensional space in PCA score plots. The peaks observed in the loading spectra explain the basis of the discrimination between the groups. Clustering of the groups for first 2 Principal Components (PCs) can be followed from the score plots (Figure 17B) in 2D representation. Score plots are constructed depending on the PCs. Variations between the sample groups are presented by PCs. PC-1 is the variable which explains the variation first best while the PC-2 is the second best and so on.

The percentages of PCs represented in brackets shows the fraction of total variance described by the PC. 78% of the spectral variance was thus explained by the data reported in Figure 17.

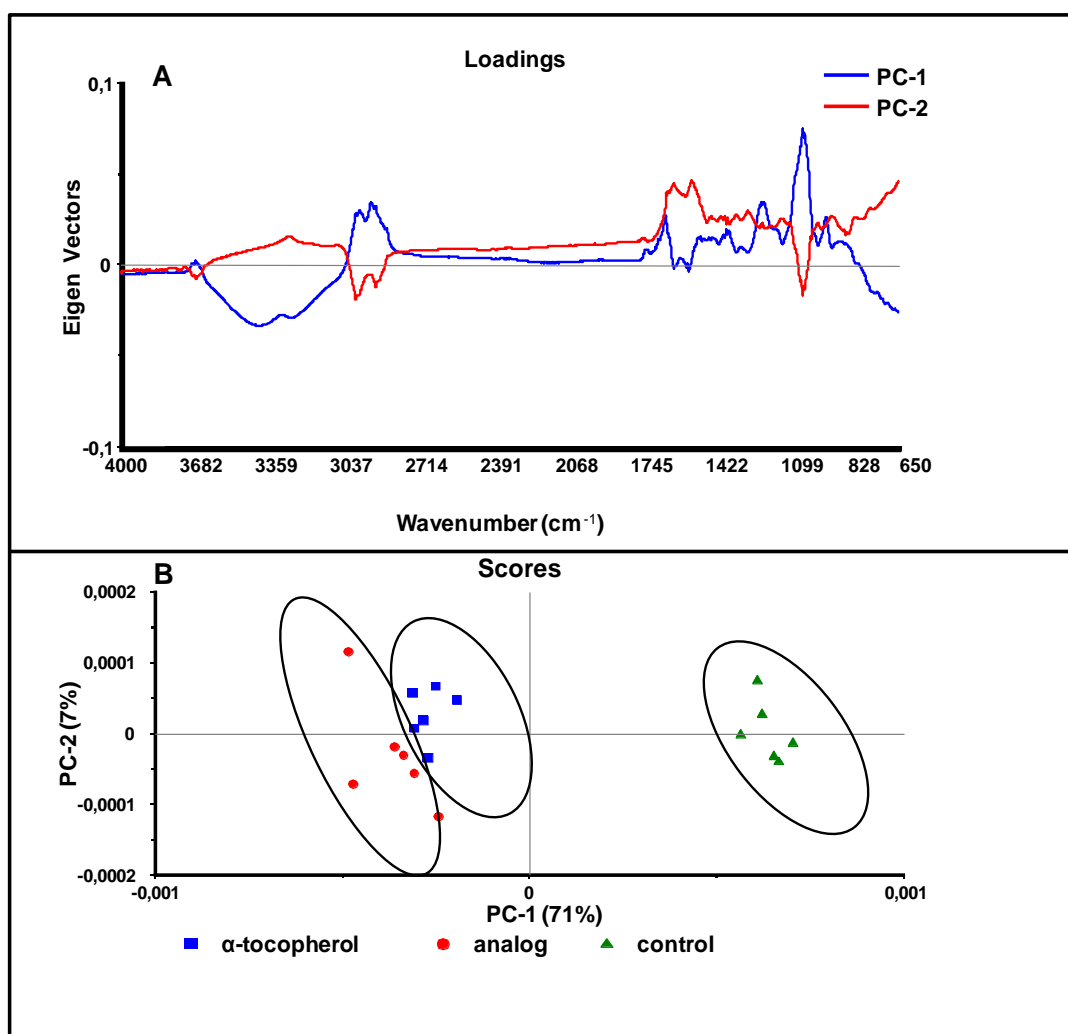


Figure 17. PCA PCA loading (A) and scatter plot (B) for experimental groups based on the IR data in the 4000-650 cm⁻¹ spectral region.

Depending on the variations taken from the loading plot in the whole IR region, PCA was further applied to the second derivative, vector normalized spectra over the range of C-H stretching (lipid) region. Loading and score plots for lipid region are given in Figure 18A and B respectively.

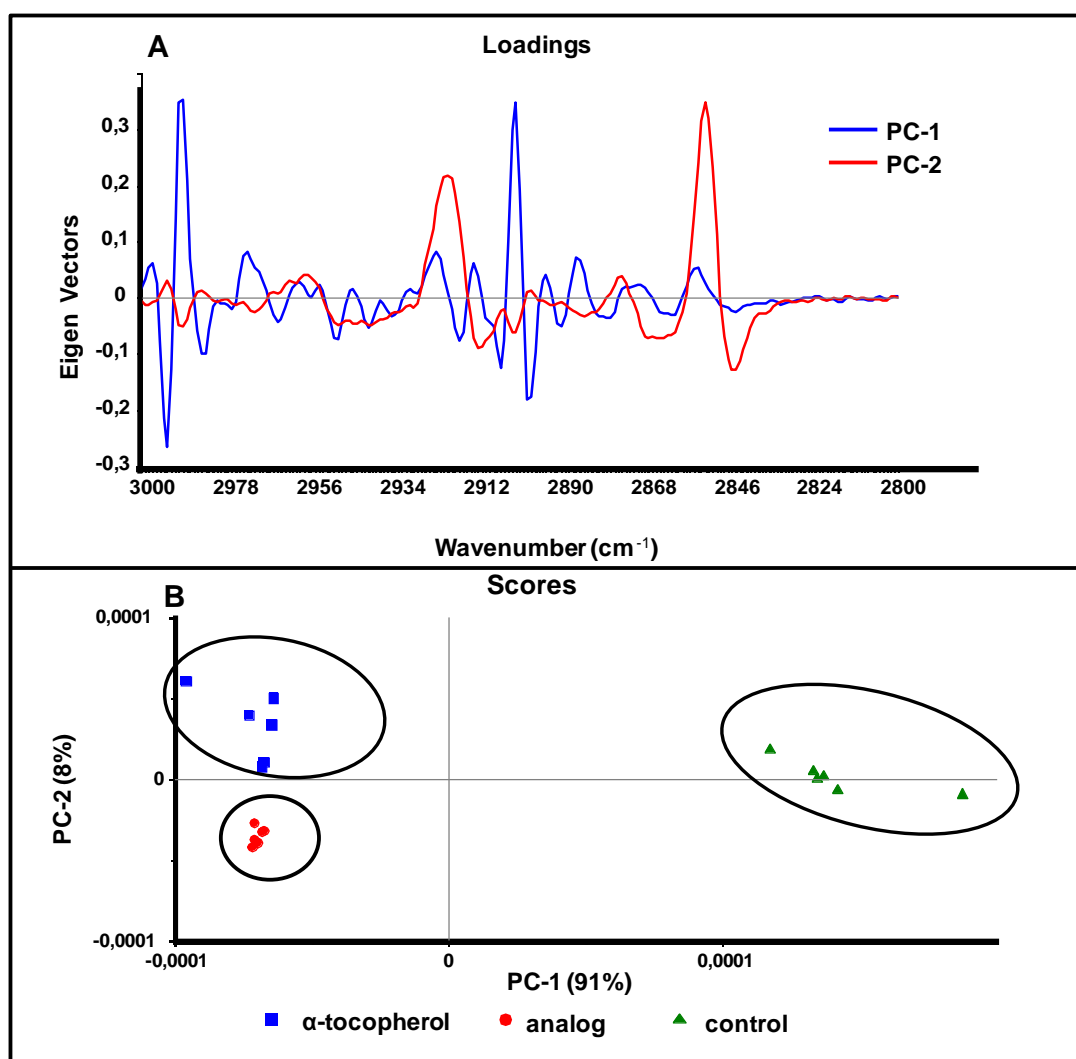


Figure 18. PCA loading (A) and scatter plot (B) for experimental groups based on the IR data in the 3000-2800 cm⁻¹ spectral region.

Score plots shows that control, analog and α-tocopherol treated cells clearly differentiated from each other in the whole IR and lipid regions. The success of differentiation in lipid region was increased as expected, meaning that drug induced changes were followed in cellular lipids. The PC values in the lipid region were increase to PC-1: 91% vs PC-2: 8% which are 71% vs 7% respectively in whole IR region.

To check the cellular differentiation in terms of protein and nucleic acid content, PCA was conducted over two other spectral regions. Figure 19 shows the

differentiation of the groups based on the amide bands. As it can be followed, discrimination power in protein region was less than the lipid region with the PC-1: 71% vs PC-2: 12%.

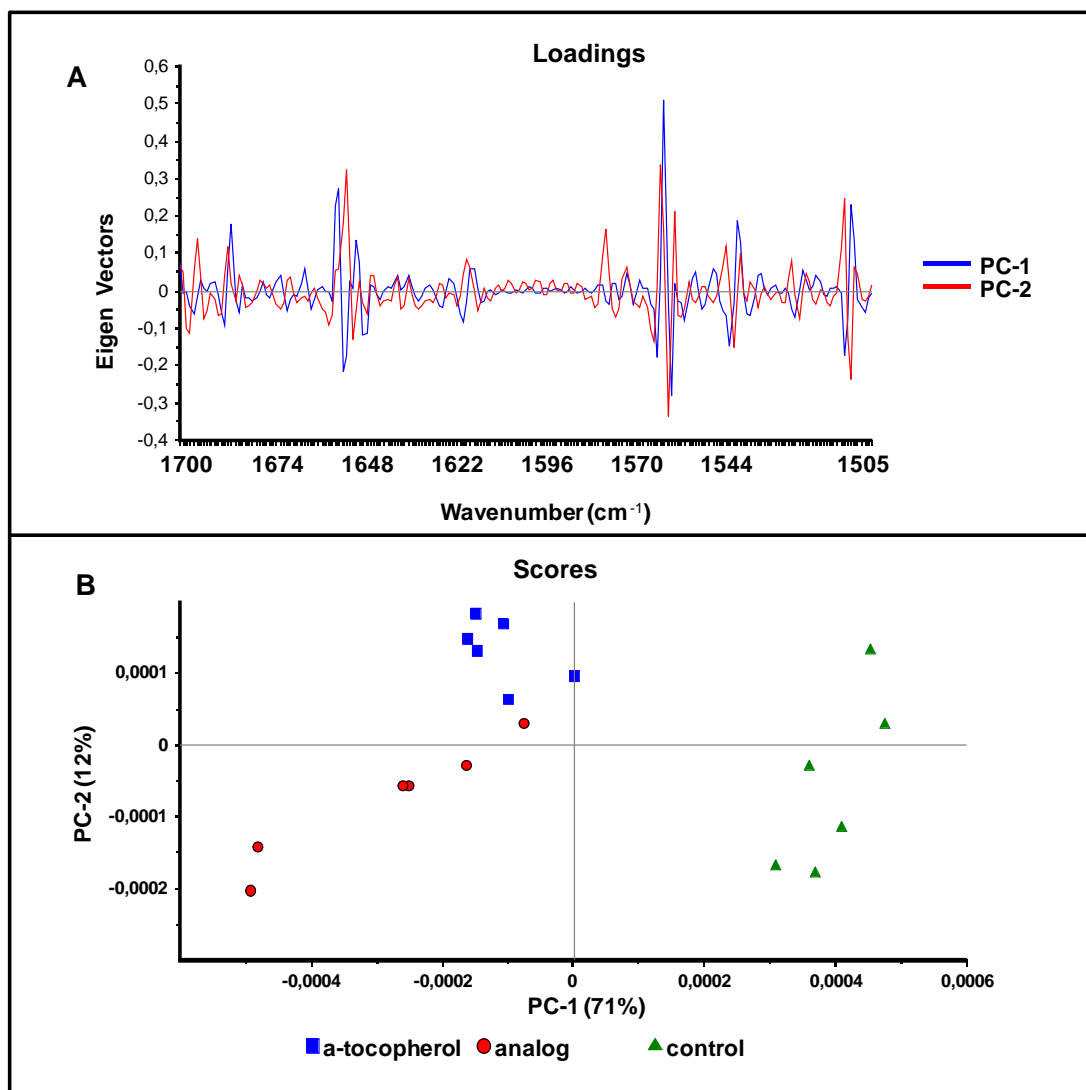


Figure 19. PCA loading (A) and scatter plot (B) for experimental groups based on the IR data in the 1700-1505 cm⁻¹ spectral region.

On the other hand, differentiation power reached the high value in the 1150-900 cm⁻¹ spectral region which is mainly composed of nucleic acid (DNA + RNA) specific vibrations (Figure 20) with the PC-1: 97% vs PC-2: 1.

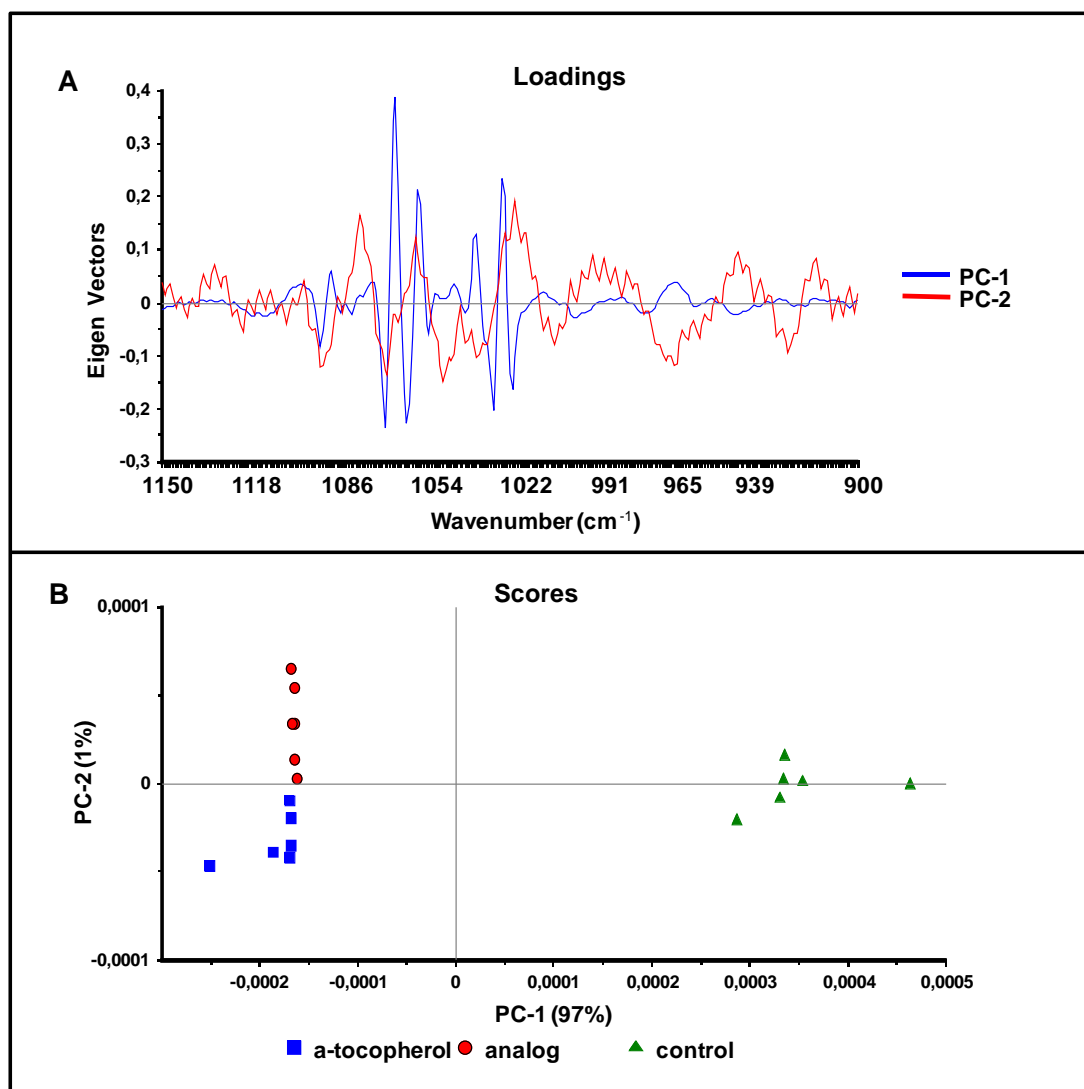


Figure 20. PCA loading (A) and scatter plot (B) for experimental groups based on the IR data in the 1150-900 cm⁻¹ spectral region.

Usually, the first 3PCs explain 99% of the variance. When the sum of PC-1 and PC-2 was calculated, the total explained variance is highest in lipid region with the 99% with first 2 PCs. Overall PCA results showed us that there were intense changes in lipid, protein and nucleic acid structure & content of experimental groups however lipid specific changes were dominated. Therefore, further infrared analyses were mainly conducted on lipid specific vibrations.

The other chemometric approach, HCA, aims to group samples depending on their characteristics. PCA generally used for to explore general relationships among the data however, to show whether the samples give clear differentiation or not,

additional cluster analysis should be conducted. Ward's algorithm was preferred together with Euclidian distances for dendrogram construction. Ward's algorithm searches to find the most homogeneous groups which mean that only two groups that show the smallest growth in heterogeneity factor are merged. The similarity of samples is indicated as heterogeneity value in the x axes of dendrogram. Increase in heterogeneity value shows the decrease in similarity index (Wang & Mizaikoff, 2008). In Figure 21, the clear splitting of all groups with high heterogeneity value can be seen. All samples of each group were clustered to its own class, in addition, the drug treated groups are agglomerated in different branch than the non-treated (control) group. HCA also proved that the lipid originated differentiation was dominant in the treated groups.

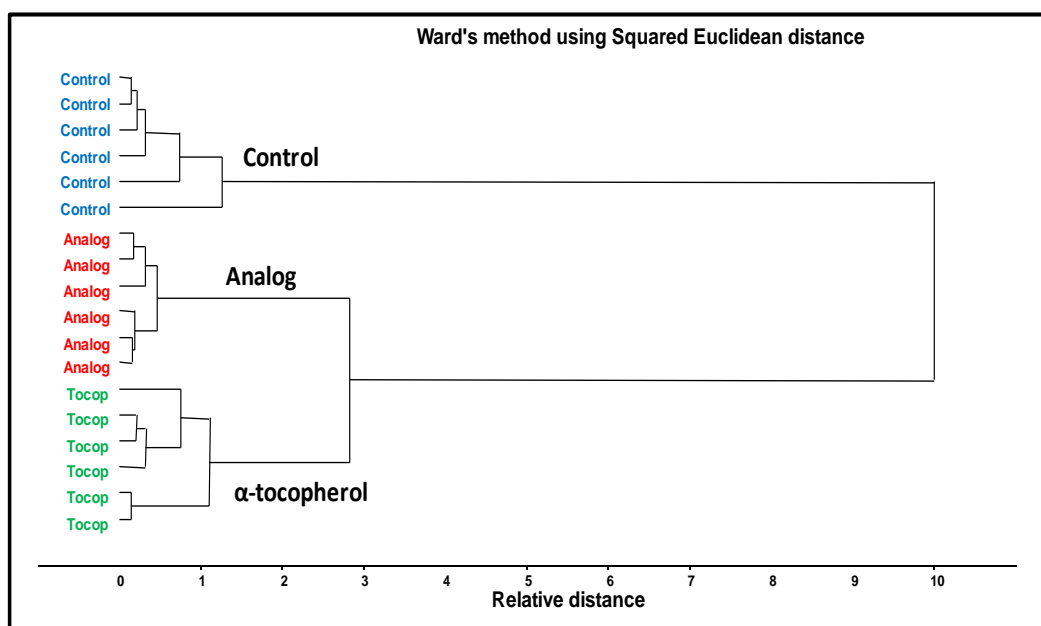


Figure 21. Hierarchical cluster analysis of experimental groups in the 3000-2800 cm^{-1} spectral region.

3.3.2.2. Spectral Analysis of IR Lipid Bands

In Figure 22, average absorption infrared spectra of the control, analog and α -tocopherol treated MCF7 cells are given.

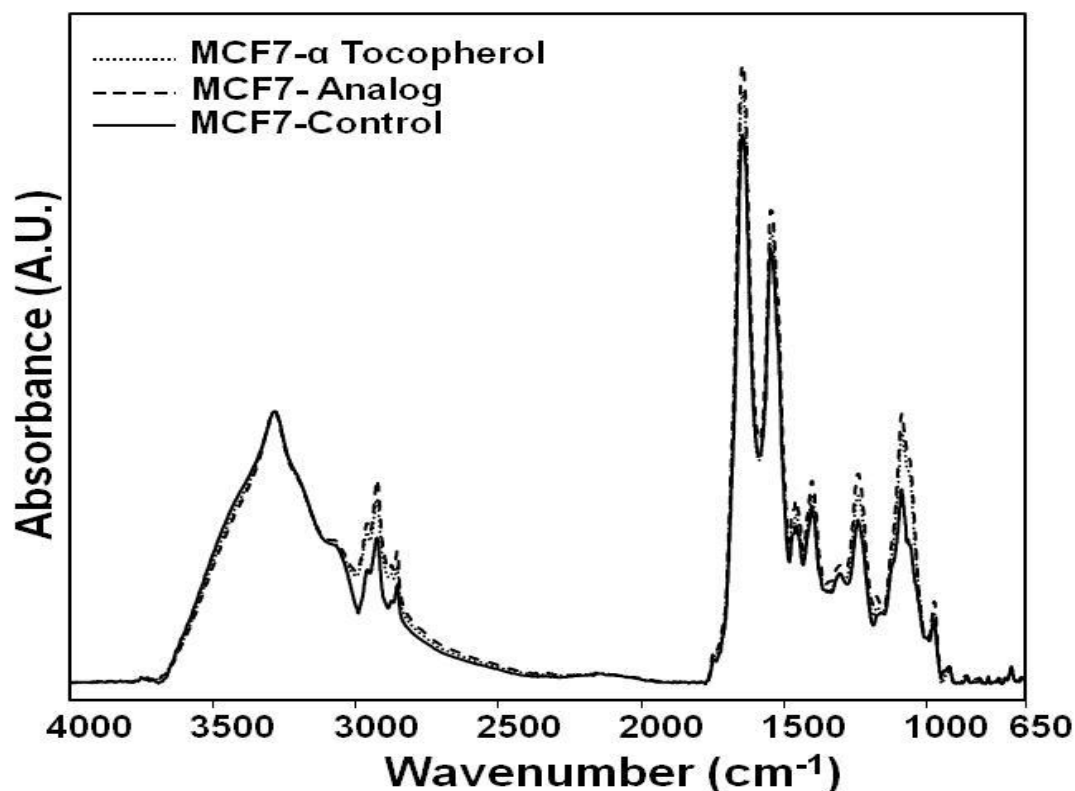


Figure 22. Average absorption ATR-FTIR spectrum of experimental groups in the 4000-650 cm^{-1} spectral range. Spectra were normalized with respect to amid A band.

There can be seen intensive alterations in the lipid bands (3025 -2800 cm^{-1}) between experimental groups. Cell has a complex spectrum composed of vibrations coming from the functional groups of different biological molecules like lipid, protein and nucleic acid. In order to characterize structural, compositional and functional changes due to the analog and α -tocopherol treatment, spectral wavenumber, band area and band width analysis were conducted for each experimental group in the C-H

stretching ($3025\text{-}2800\text{ cm}^{-1}$) and fingerprint ($1800\text{-}900\text{ cm}^{-1}$) regions. In Figure 23 the absorption (A) and second derivative (B) spectra of the C-H stretching (lipid) region are given. Second derivative spectra were used for band assignment in order to get better resolution. Assignments of the labeled bands in the second derivative spectrum can be found in Table 4.

Table 4. Band assignments of main absorptions in IR spectra of MCF7 cells based on the literature (Cakmak et al, 2011; Ozek et al, 2010; Severcan & Haris, 2012).

Band #	Wavenumber (cm ⁻¹)	Spectral assignment
1	3008	Olefinic =CH stretching: unsaturated lipids, cholesterol esters
2	2956	CH ₃ antisymmetric stretching: protein, lipid
3	2918	CH ₂ antisymmetric stretching: çoğunlukla lipid
4	2872	CH ₃ symmetric stretching: mainly proteins
5	2851	CH ₂ symmetric stretching: mainly lipids
6	1746	Ester C-O stretching: triglycerides, cholesterol esters
7	1651	Amide I: protein (%80 C=O stretching, α-helical structure)
8	1630	Amide I: protein (β-sheet)
9	1548	Amide II: protein (%60 N—H bending, %40 C—N stretching)
10	1469	CH ₂ scissoring: lipids
11	1454	CH ₂ asymmetric bending: mainly lipids and little contribution from proteins
12	1398	COO ⁻ symmetric stretching: fatty acids and aminoacids
13	1368	CH ₃ symmetric bending: lipids
14	1346	CH ₂ wagging: phospholipid, fatty acid and aminoacid side chains
15	1237	PO ₂ ⁻ asymmetric stretching: mainly nucleic acids with the little contribution from phospholipids
16	1172	CO-O-C asymmetric stretching: ester bonds in cholesteryl esters
17	1117	C—O stretching: ribose ring vibrations
18	1084	PO ₂ ⁻ symmetric stretching: nucleic acids and phospholipids; C-O stretching: glycogen, polysaccharides and glycolipids
19	1041	C-O stretching: , polysaccharides (glycogen)
20	1023	DNA
21	968	C-N-C stretching: RNA, DNA
22	934	Z-form DNA

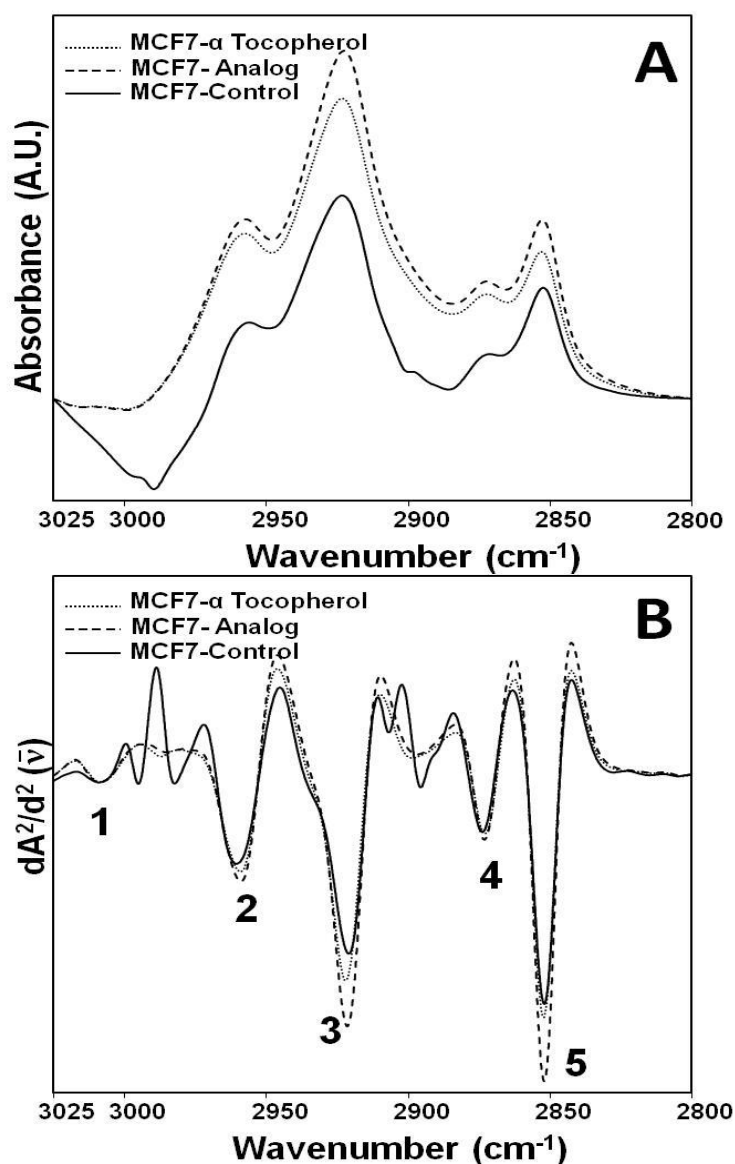


Figure 23. Average absorption (A) and second derivative (B) ATR-FTIR spectra of experimental groups in 3025-2800 cm⁻¹ region. Spectra for each experimental group are the average of 6 independent replicates.

3.3.2.2.1. The effect of VE Analog treatment on lipid amount in MCF7 cells

The C-H stretching region composed of mainly lipid originated CH₃ antisymmetric, CH₂ antisymmetric, CH₂ symmetric and =CH stretching vibrations (Cakmak et al, 2012). The effect of analog treatment on saturated lipid content was investigated by

analyzing CH₂ antisymmetric and symmetric stretching bands. Area changes of CH₃ antisymmetric, CH₂ antisymmetric, CH₂ symmetric stretching bands for the control, analog and α -tocopherol treated MCF7 cells are given in Figure 24.

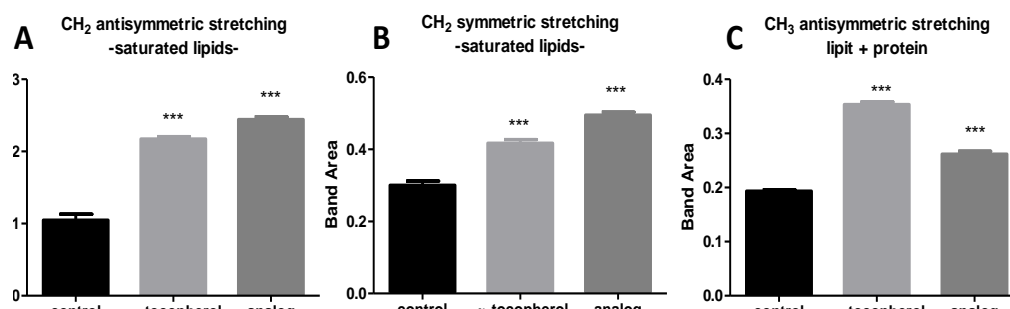


Figure 24. Band area values of (A) CH₂ antisymmetric, (B) CH₂ symmetric and (C) CH₃ antisymmetric bands (Results are represented as mean \pm SEM, * p <0.05, ** p <0.01, *** p <0.001; n =6 for each group).

In absorption spectroscopy, band signal intensity or band area under the curve is directly proportional to the sample amount obeying to the Beer-Lambert law (Cakmak et al, 2012; Garip et al, 2013; Severcan et al, 2010). As it can be seen from Figure 24 the band area increases in the analog and α -tocopherol treated groups as compared to control, significantly. These results indicate the increase in lipid biosynthesis and/or decrease in lipid degradation in response to drug treatment.

3.3.2.2.2. The effect of VE Analog on lipid acyl chain length

Changes in lipid biosynthesis and/or lipid degradation can also be monitored by following ratio changes of the CH₂ antisymmetric / CH₃ antisymmetric band areas. Increase and decrease in the ratio show the increase and decrease in lipid

hydrocarbon chain length respectively (Wang, 2005). This ratio increased with the analog treatment while it was decreasing due to α -tocopherol (Figure 25).

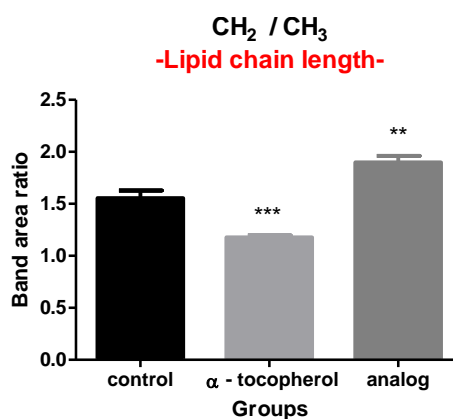


Figure 25. Area ratio of CH₂ antisymmetric / CH₃ antisymmetric bands (Results are represented as mean \pm SEM, * p <0.05, ** p <0.01, *** p <0.001; n =6 for each group).

Increase in the ratio can be related with the decreased lipid degradation in response to the analog treatment. Results are correlated with the lipid peroxidation tests.

Correspondingly, changing of the balance between the short and long fatty acyl chain could trigger other downstream events. It has been known that fatty acids can induce apoptosis (Karaskov et al, 2006; Shimabukuro et al, 1998). Short chain fatty acids are able to inhibit histone deacetylases (Boffa et al, 1992) thus causes the hyperacetylation of histones which in turn associated with the growth inhibition of colon epithelial cells (Matthews et al, 2007). On the other hand, long chain fatty acids can induce ER stress resulting in the activation of JNK and CHOP. JNK upregulates the PUMA (p53 upregulated modulator of apoptosis) while CHOP enhances the expression of Bim and PUMA and mediates the ROS generation and activation of pro-apoptotic protein Bax. Bax causes mitochondrial membrane permeabilization, caspase activation and eventually cell death (Malhi & Gores, 2008). In our case, it is possible to associate increased number of long chained fatty acids with increased apoptotic cell rate in analog treated cells.

3.3.2.2.3. The effect of VE Analog on lipid dynamics

Wavenumber shifts of CH₂ antisymmetric and symmetric stretching bands give information about a structural parameter namely, membrane lipid order (Severcan, 1997; Severcan et al, 2005). Shifts to the lower values in the wavenumber indicate, the acyl chains are more ordered in the system meaning that the trans/gauche ratio increased (Cakmak et al, 2011; Ozek et al, 2010; Severcan, 1997). On the other hand shifts in the higher values as the indicator of increase in the disorderness of acyl chains indicating decreased trans/gauche ratio in the system (Mantsch, 1984). In Figure 26A, the wavenumber values of CH₂ antisymmetric stretching band are given for the experimental groups. The frequency shifted to the higher values in the analog and α -tocopherol treated MCF7 cells indicating that a decrease in the lipid order (Severcan, 1997).

Changes in the bandwidth values of the CH₂ antisymmetric and symmetric stretching bands reflect the changes in the membrane fluidity (Cakmak et al, 2011; Ozek et al, 2010). Increase and decrease in bandwidth show an increase and a decrease in membrane fluidity respectively. As it can be followed from Figure 26B, the bandwidth values decreased in analog and α -tocopherol treated groups which indicate a decrease in membrane fluidity in response to the drug treatment.

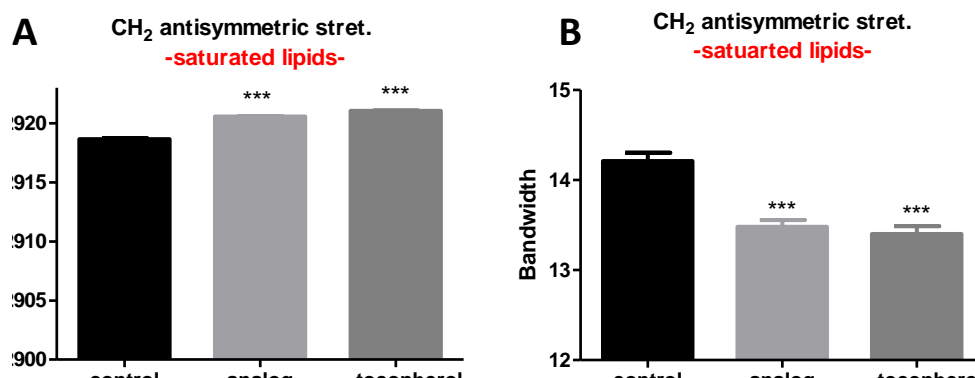


Figure 26. Wavenumber (A) and Bandwidth (B) changes of CH₂ antisymmetric stretching band in experimental groups (Results are represented as mean \pm SEM, * $p < 0.05$, ** $p < 0.01$, *** $p < 0.001$; $n = 6$ for each group).

3.3.2.2.4. The effect of VE Analog on unsaturated lipid amount

The olefinic band located at around 3008 cm^{-1} is a good index for degree of unsaturation (Liu et al, 2002; Severcan et al, 2005). A significant increase in the area of this band ($p < 0.001$) was observed in the analog treated group (Figure 27). Increase in this band area points out an increase in unsaturated acyl chains of lipid molecules. It was previously shown that an increase in the area of olefinic band can be explained by an increase in the synthesis or a decrease in the degradation of unsaturated lipids due to decreased lipid peroxidation. There was no significant change in the α -tocopherol treated groups.

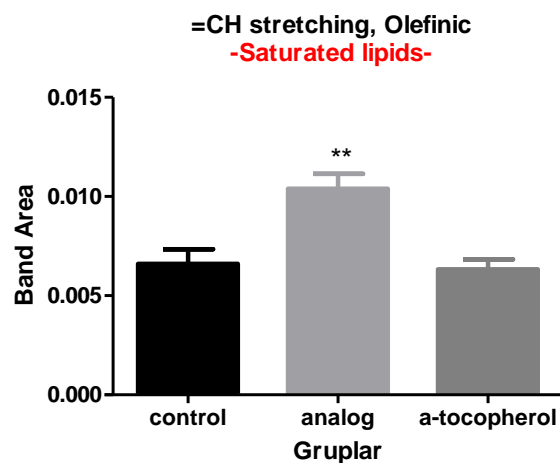


Figure 27. Band area changes of olefinic band (3009 cm^{-1}) in the experimental groups. (Results are represented as mean \pm SEM, * $p < 0.05$, ** $p < 0.01$, *** $p < 0.001$; $n = 6$ for each group).

3.3.2.2.5. The effect of VE Analog on cellular cholesterol amount in MCF7 cells

The $1800\text{-}1500\text{ cm}^{-1}$ region of the spectrum is shaped by the $\text{C}=\text{O}$ stretching vibrations of ester carbonyl groups in lipids and the amide groups of protein backbone. The cholesterol esters and triglycerides were investigated by analyzing the bands located at 1746 cm^{-1} ($\text{C}=\text{O}$ stretching) and 1172 cm^{-1} ($\text{CO}-\text{O}-\text{C}$ asymmetric stretching) (Table 2). Locations of these bands in the spectra are shown in Figure 28 and 29, respectively.

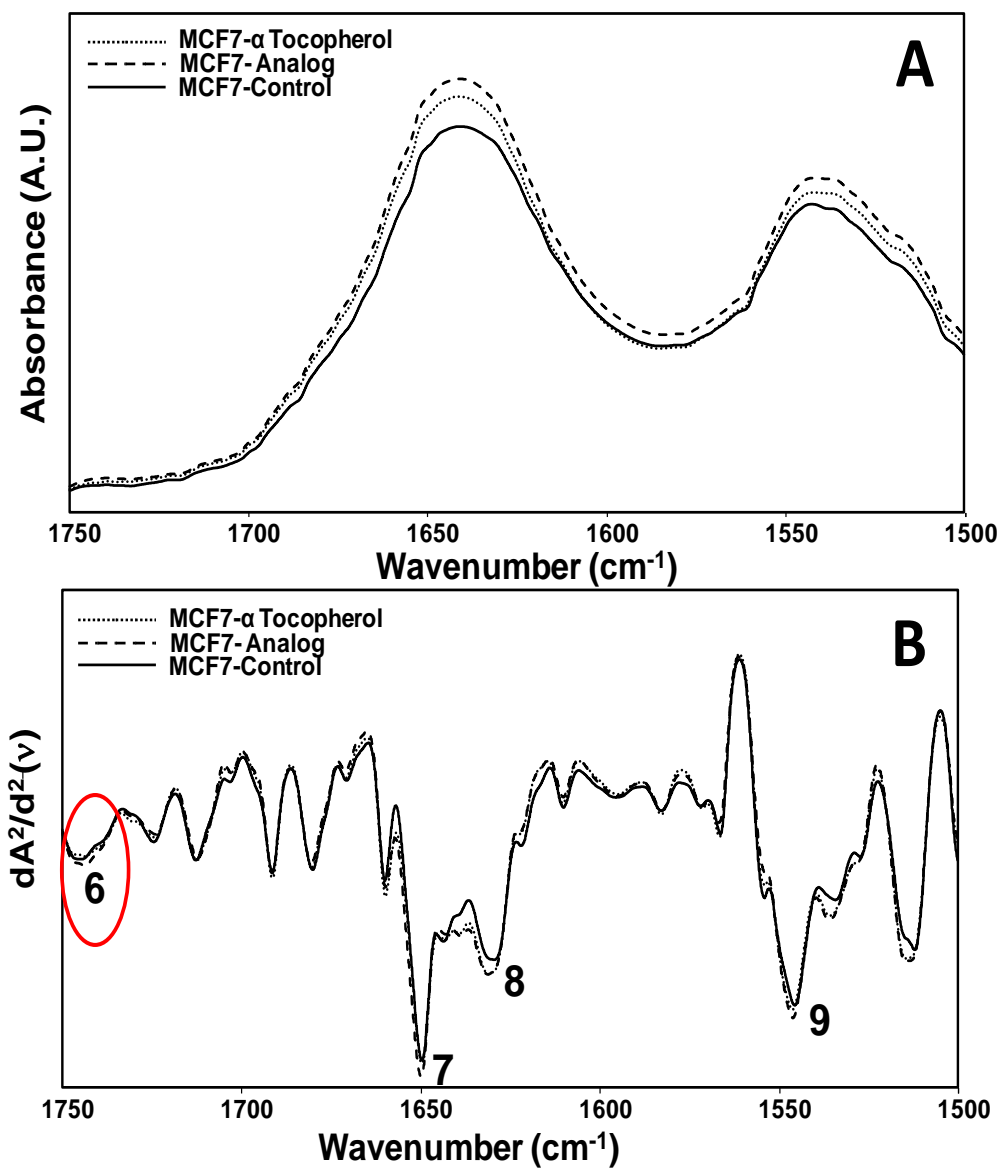


Figure 28. Representative absorbance (A) and second derivative (B) spectra of the experimental groups in the 1750-1500 cm^{-1} region.

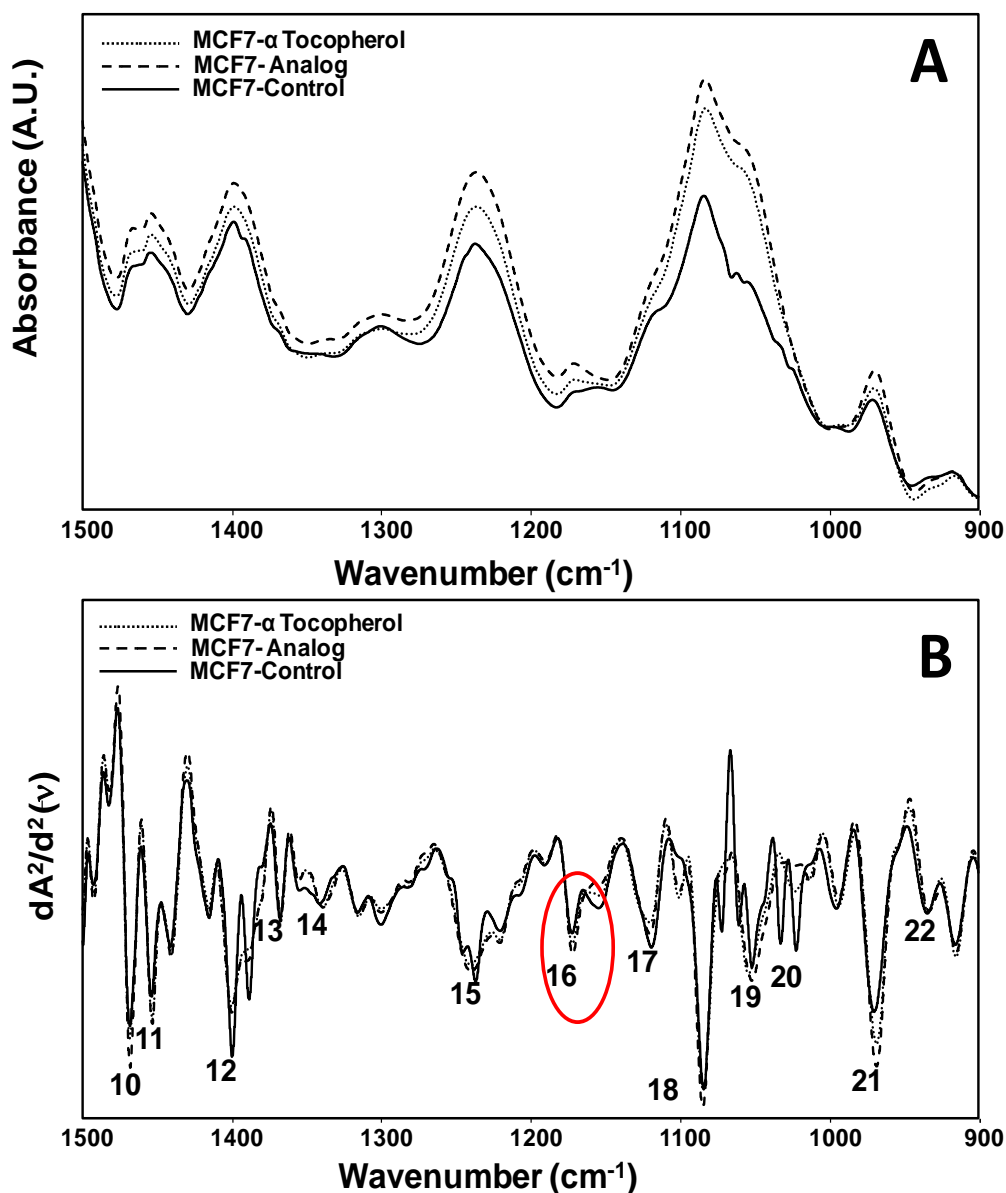


Figure 29. Representative absorbance (A) and second derivative (B) spectra of the experimental groups in the 1500-900 cm^{-1} region.

Area of the C=O stretching band was increased in both analog and α -tocopherol treated groups significantly (Figure 30A). This increase was also confirmed by the increase in the area of the other cholesterol ester band (CO–O–C asymmetric stretching), located at 1172 cm^{-1} (Figure 30B). Increase is more in the analog treated group than the α -tocopherol treated ones.

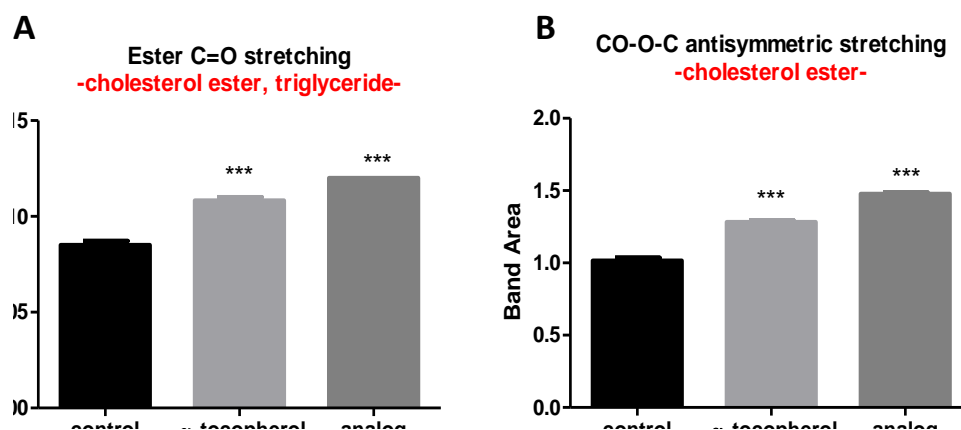


Figure 30. Band Area changes of the C=O stretching (1746 cm⁻¹) (A) and CO-O-C antisymmetric stretching (1172 cm⁻¹) (B) bands in the experimental groups (Results are represented as mean \pm SEM, * p <0.05, ** p <0.01, *** p <0.001; n =6 for each group).

In previous studies it was shown that tocotrienols but not the tocopherols able to suppress HMGCoA reductase that directly inhibits cholesterol biosynthesis due to the presence of 3 double bonds in the isoprenoid chain (Parker et al, 1993; Pearce et al, 1994; Qureshi et al, 1986). In a clinical study it was clearly observed that tocotrienols lowered the serum cholesterol and proposed that the tocopherols may increase cholesterol level by inducing HMGCoA reductase (Qureshi et al, 2002). Our findings for the α -tocopherol are in consistent with these literature findings. VE analog behaves also similar but more effective than α -tocopherol.

Cholesterol, an essential component of plasma membrane, is controlled strictly by balancing the intracellular cholesterol synthesis with the uptake and efflux mechanisms. Cholesterol synthesis is regulated by a series of enzymatic reactions in mevalonate pathway and generally upregulated due to carcinogenesis. A rate limiting primary enzyme is HMG-CoA, responsible for the conversion of hydroxy-methyl-glutaryl-coenzyme A into mevalonate. Abundance of acetyl-CoA (precursor) as a byproduct of glycolysis which also potentiates de novo lipid synthesis or increase in the activity of Sterol regulatory element binding protein (SREBP) or dysregulation in the control of HMG-CoA reductase enzyme can yield increased cholesterol levels in

cell (Cruz et al, 2013). When our case is considered, the expression of HMG-CoA at mRNA level significantly increased (Table 5) in the treated group which could explain the increase cellular cholesterol levels.

Although cholesterol promotes cell proliferation and tumor progression in carcinogenesis, oxidized cholesterol can induce apoptosis. Cholesterol oxidation produces oxysterols that induce modification of pro and anti-apoptotic proteins, alter gene expression and mitochondrial membrane properties. Accumulation of oxysterols strongly stimulates intrinsic apoptotic pathways (Schroepfer, 2000; Sottero et al, 2009). In addition, triglycerides (Kotas et al, 2013) and cholesterol itself is (Schroeder & Hilbi, 2007) able to trigger caspase-1 activation thus induce apoptosis. When all these considered, it is possible to say that, increased cholesterol levels could contribute the cellular apoptosis in the analog treated group.

3.3.2.2. ESR Spectroscopy

To confirm the changes in membrane dynamics, that were pointed out by FTIR spectroscopy findings, ESR data was analyzed. In Figure 31, representative 16-DSA labeled ESR spectrum (A) and changes of the correlation time, τ_c of 16-DSA labeled MCF7 cells (B) are shown.

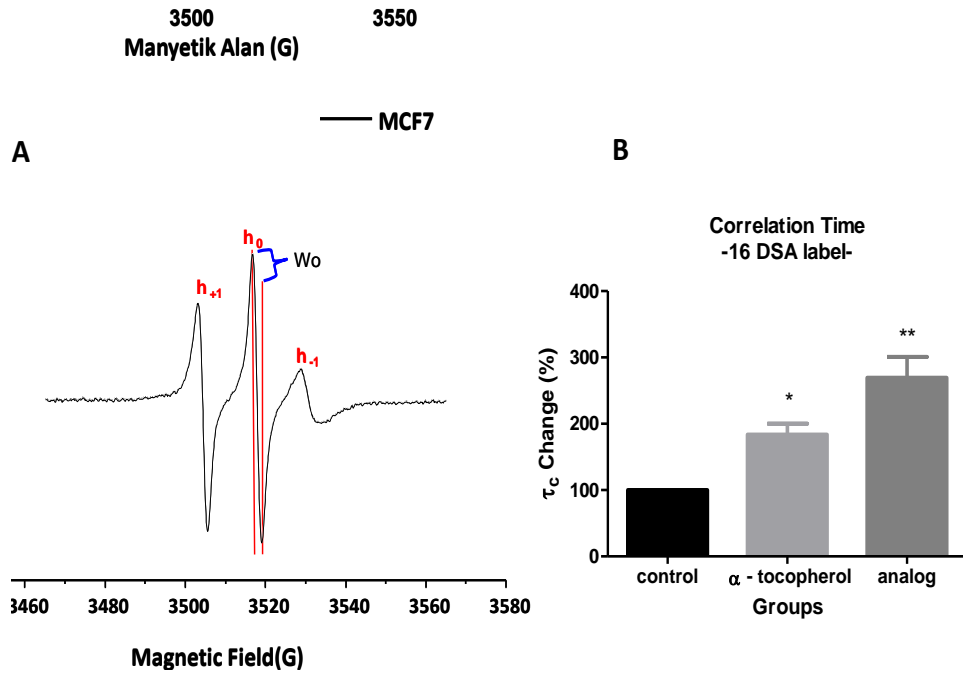


Figure 31. Representative 16-DSA labeled ESR spectra of MCF7 cells (A) and relative correlation time (τ_c) changes in the experimental groups (B) (Results are represented as mean \pm SEM, * $p < 0.05$, ** $p < 0.01$, *** $p < 0.001$; $n = 3$ for each group).

Representative 5-DSA labeled ESR spectrum (A) and Order parameter (S) changes of 5-DSA labeled MCF7 cells (B) are given in Figure 32.

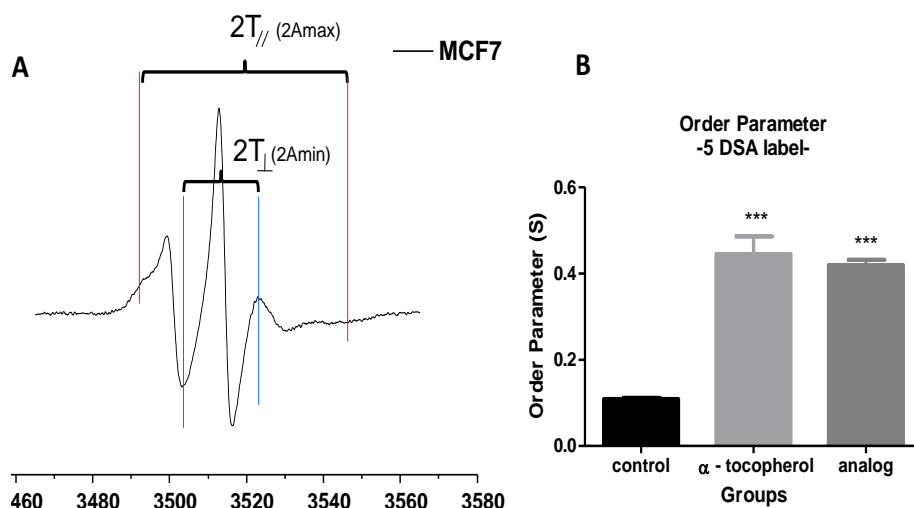


Figure 32. Representative 5DSA labeled ESR spectra of MCF7 cells (A) and relative changes in the order parameter (S) for the experimental groups (B) (Results are represented as mean \pm SEM, * p <0.05, ** p <0.01, *** p <0.001; n =3 for each group).

Reduction in lipid dynamics, indicated with FTIR spectroscopy results, was confirmed by ESR spectroscopy. The correlation time, τ_c , is inversely proportional with lipid fluidity. Higher τ_c indicates that the lipid environment is more viscous so more time is needed for the rotation of spin probe (Severcan & Cannistraro, 1990).

Furthermore, S parameter also increased in treated groups as compared to the control which means that the membrane thickness increases as a result of drug-membrane interaction. When this finding compared with the FTIR spectroscopy results, there is a controversy. Shift to the higher wavenumber values of CH_2 antisymmetric stretching band points out increase in the disorderness of acyl chains meaning that the decreased trans/gauche ratio in the system (Mantsch, 1984) while 5-DSA labeled ESR results denote vice versa. This kind of controversy could be possible if the drugs cause the formation of lipid domains on membrane structure. This kind of distribution within the membrane would cause inhomogeneous lateral phase transition profiles. These empirical observations need to be proved additional thermal measurements.

ESR results show that VE analog and α -tocopherol induced changes resulted in significant decrease in lipid fluidity of the system. Presented results for α -tocopherol

are in consisted with literature. There are number of studies considering the biochemical aspects of α -tocopherol in membranes. It was shown that α -tocopherol cause an increase in order parameter and decrease fluidity of the hydrocarbon chains in steady state (Ohyashiki et al, 1986) and time resolved (Bisby & Birch, 1989) fluorescence anisotropy measurements of probe interpolations into the phospholipid membranes. With ESR spectroscopy it was also reported that α -tocopherol increases the τ_c of high resolution amphiphilic spin probe, perdeutero-di-t- butyl nitroxide (PDDTBN) in the liquid crystalline phase whereas in the gel phase it decreases the τ_c and order in model membranes (Severcan & Cannistraro, 1989; Severcan & Cannistraro, 1990). ^{13}C -NMR (Srivastava et al, 1983) and ^2H -NMR (Wassall et al, 1986) relaxation measurements of α -tocopherol in phospholipids in the fluid phase indicate a restriction in the motional freedom. ESR measurements conducted with 20 mol% α -tocopherol + phosphatidylcholine bilayer dispersions indicated α -tocopherol causes acyl chain motility restriction within the membrane and the magnitude of increase in order is correlated with the degree of unsaturation (Wassall et al, 1991). Considering the results, VE analog acts similarly as α -tocopherol on lipid dynamics. However, the difference in the biological outcomes might be sourced from the stoichiometric differences. VE does not distribute through the membrane rather forms complexes with membrane components with a defined stoichiometry. α -tocopherol preferentially tends to form complexes with phosphatidylethanolamines (PE) rather than PCs and PE+ α -tocopherol complexes tend to form non-lamellar structures (Wang & Quinn, 1999). Additionally, free fatty acids and lysophospholipids which are the byproducts of lipid hydrolysis form 1:1 stoichiometric complexes with VE and thus the overall balance of hydrophobic : hydrophilic affinity within the membrane is restored. In this way, VE is thought to negate the detergent-like properties of the hydrolytic products that would otherwise disrupt membrane stability (Wang & Quinn, 1999). In the light of these findings the distribution of phospholipid species and the level of lipid hydrolysis within the membrane readily effect the final action of VE analog in cell.

3.3.3 The effect of VE Analog on lipid peroxidation

In order to confirm FTIR spectroscopy results which refer to decreased lipid peroxidation levels, two different indirect peroxidation assays were used. Lipid peroxidation in response to drug treatment was measured by MDA and 8-isoprostane assays (Figure 34 and 34). MDA and 8-isoprostane are the end products of peroxidation, simply and commonly can be measured. Standard curves for both assays are shown in Figure 33B and 34B. Calculated MDA and 8-isoprostane amounts showed that their production was significantly decreased due to analog treatment indicating a decrease in lipid peroxidation.

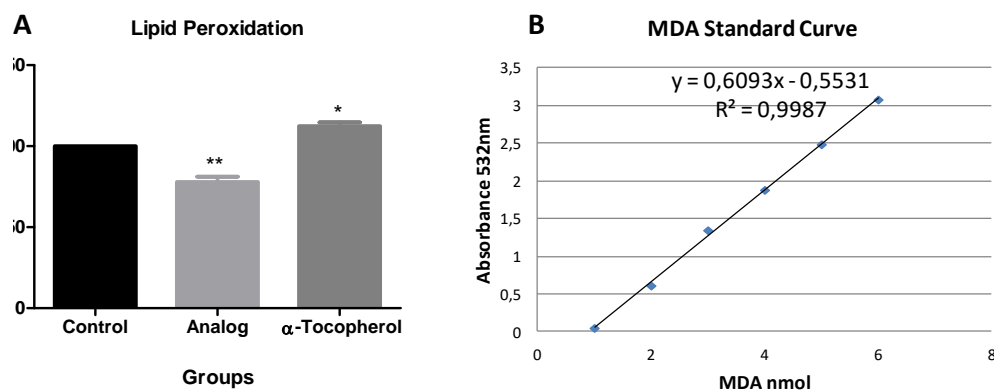


Figure 33. (A) MDA level change in the experimental groups, (B) MDA standard curve. The average of the control group was considered as 100%. (Results are represented as mean \pm SEM, * p <0.05, ** p <0.01, *** p <0.001; n =4 for each group).

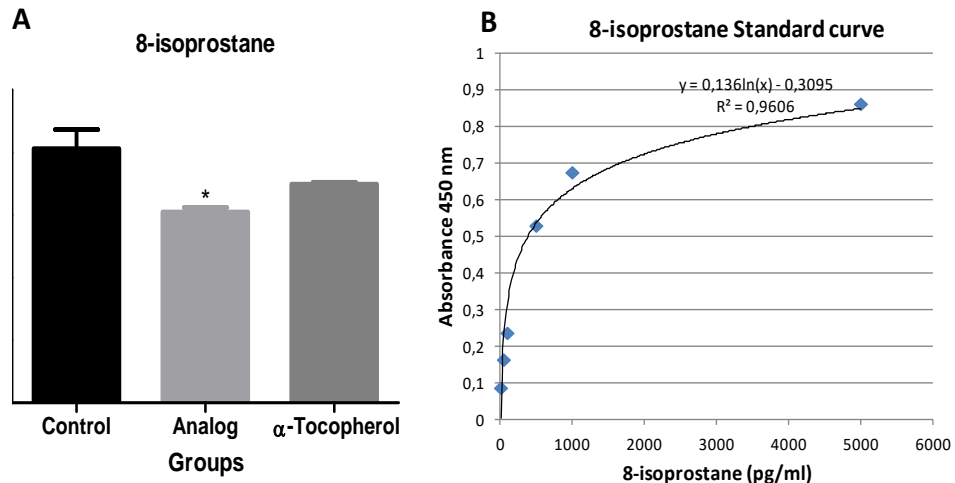


Figure 34. (A) 8-isoprostane level change in the experimental groups, (B) 8-isoprostane standard curve (Results are represented as mean \pm SEM, * $p < 0.05$, ** $p < 0.01$, *** $p < 0.001$; $n = 4$ for each group).

Under normal conditions cells are generally protected from oxidative damage via a balancing the physiological levels of ROS and antioxidant scavengers. Lipid peroxidation is one of the most investigated consequences of ROS actions on membrane. Either the peroxidation will have detrimental or beneficial effects on cell, has been depending on some circumstances. Baseline level of ROS within the cell, the type of cell, proliferation rate etc. can affect the final role of ROS within the cell (Gago-Dominguez et al, 2005). In our observation, the decrease in peroxidation level showed correlation with cell death in response to the analog treatment.

Lipid peroxidation is chain reaction composed of 3 major steps; initiation, propagation and termination. Reactivity of lipid types with peroxy radicals are ordered as PUFA > cholesterol > monounsaturated FAs > saturated FAs. If the radical is reactive enough to continue oxidation after the first action of anti-oxidant, the pro-oxidant action of the anti-oxidant could be triggered. The chain reaction does not stop until the chain carrying peroxy radical meets and combines with another radical to form non-radical products (termination reaction) (Yamauchi, 2007). VE is a lipophilic, hydrophilic peroxy radical scavenging anti-oxidant (Niki, 2014). However, it is now widely accepted that many of the biological actions of VE is independent of its antioxidant potential. Although all the natural forms of VE has an

anti-oxidant potency, they have little or no anti-cancer activity (Kline et al., 2004; Neuzil et al., 2002a; Sylvester and Shah, 2005a; Sylvester et al., 2005). Similarly, the results of the present study also showed that there was no anti-oxidant activity of α -tocopherol. This might be sourced from the pro-oxidant type of action of α -tocopherol.

Studies have showed increased lipid peroxidation in breast cancer patients (Rajneesh et al, 2008). Tamoxifen therapy in postmenopausal women with breast cancer able to reduce the increase in lipid peroxidation (Thangaraju et al, 1994). From the bioenergetic aspect, in addition to glycolytic pathways, survival of cancer cells based on the exogenous fatty acid uptake and consumption through β -oxidation. Fatty acid oxidation (FAO) is also relevant even in cells having high lipogenic activity. FAO yields NADH and FADH₂ which in turn enter the electron transport chain to generate ATP. (Daniels et al, 2014; Kamphorst et al, 2013). However, it has been previously suggested that FAO is not the case for ATP production in certain leukemias, instead, has role in cell survival paths and can influence BAX and BAK dependent mitochondrial transition pore formation. Inhibition of FAO leads to accumulation of lipids and then lipid driven cytotoxicity (Samudio et al, 2010).

The relevance of fatty acid oxidation is generally over-sighted while heavily concentrated on the glycolysis, fatty acid synthesis and glutaminolysis in cancer research. However recent studies have shown the importance and usability of fatty acid oxidation pathways as therapeutic target.

Carnitine palmitoyl transferases CPT1 & CPT2 are the important enzymes responsible for the oxidation of long-chain fatty acids in mitochondria. A CPT1 inhibitor, Perhexiline, has shown anti-tumor effects (Samudio et al, 2010). PCR array results of VE analog treated MCF7 cells showed that there in a significant level of decrease in CPT2 levels (Table 7) which can be associated with decreased lipid peroxidation and increased anti-proliferative effects of analog.

3.3.4. Assessment of Changes in Fatty Acid Metabolism Gene Transcripts via Quantitative RT-PCR Array

qRT-PCR array (Qiagen) designed in 100-wells disc format for the detection of 84 key genes having role in fatty acid metabolism, was used. RT-PCR arrays are accepted as reliable tools for the analysis of the panel of genes for mRNA quantification. The integrity and quality of the isolated RNA samples are shown in Figure 35.

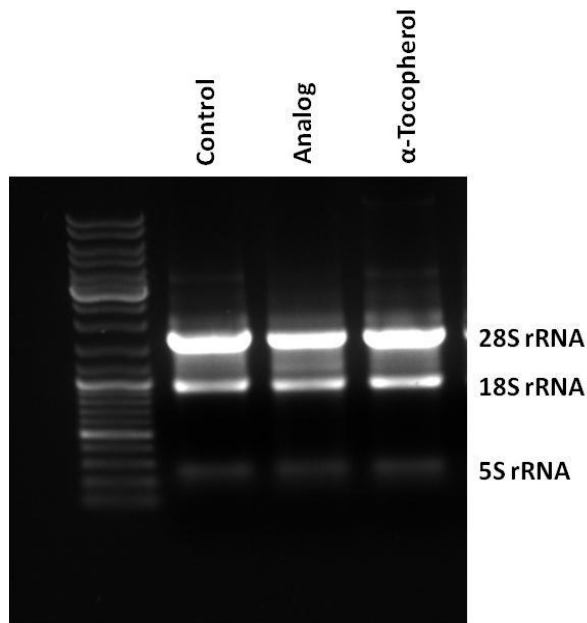


Figure 35. RNA integrity and gDNA contamination test using agarose gel electrophoresis of isolated RNA isolated from the control, analog and α -tocopherol treated MCF cells.

It can be inferred from the figure that highly pure mRNA was isolated as the 28S and 18S ribosomal RNA bands are sharp and intense. Further steps were carried out by using high quality RNA template.

In Figure 36A and B the genes that are upregulated, unchanged and downregulated in Analog vs Control and α -tocopherol vs Control groups are represented respectively. The number of genes having unchanged expression level is higher in the α -tocopherol treated group.

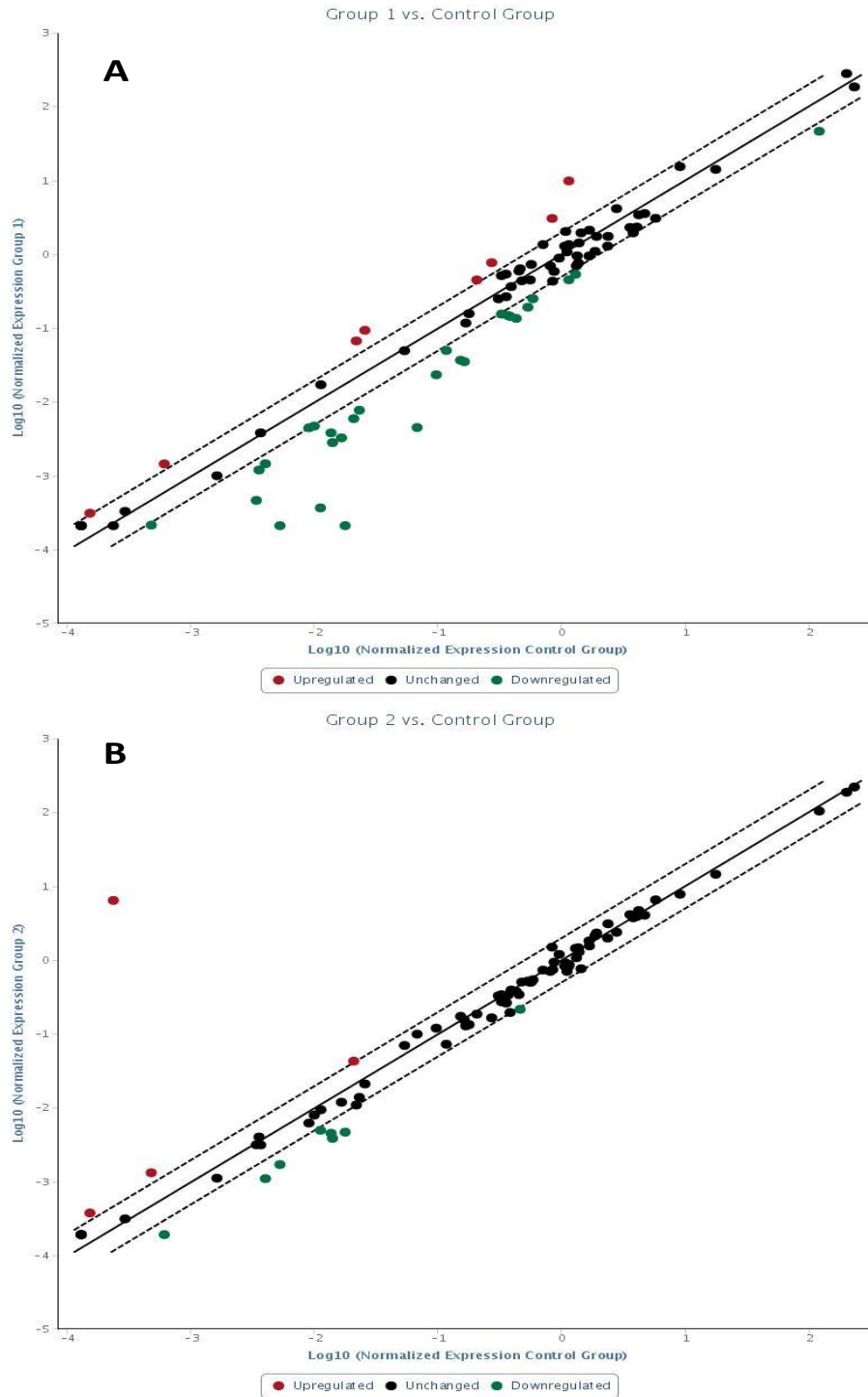


Figure 36. The scatter plot compares the normalized expression of genes on the array between the two selected groups; A: analog vs control, B: α -tocopherol vs control; (n=2). The central line indicates unchanged gene expression. The dotted lines indicate the selected fold regulation threshold. Data points beyond the dotted lines in the upper left and lower right sections meet the selected fold regulation threshold.

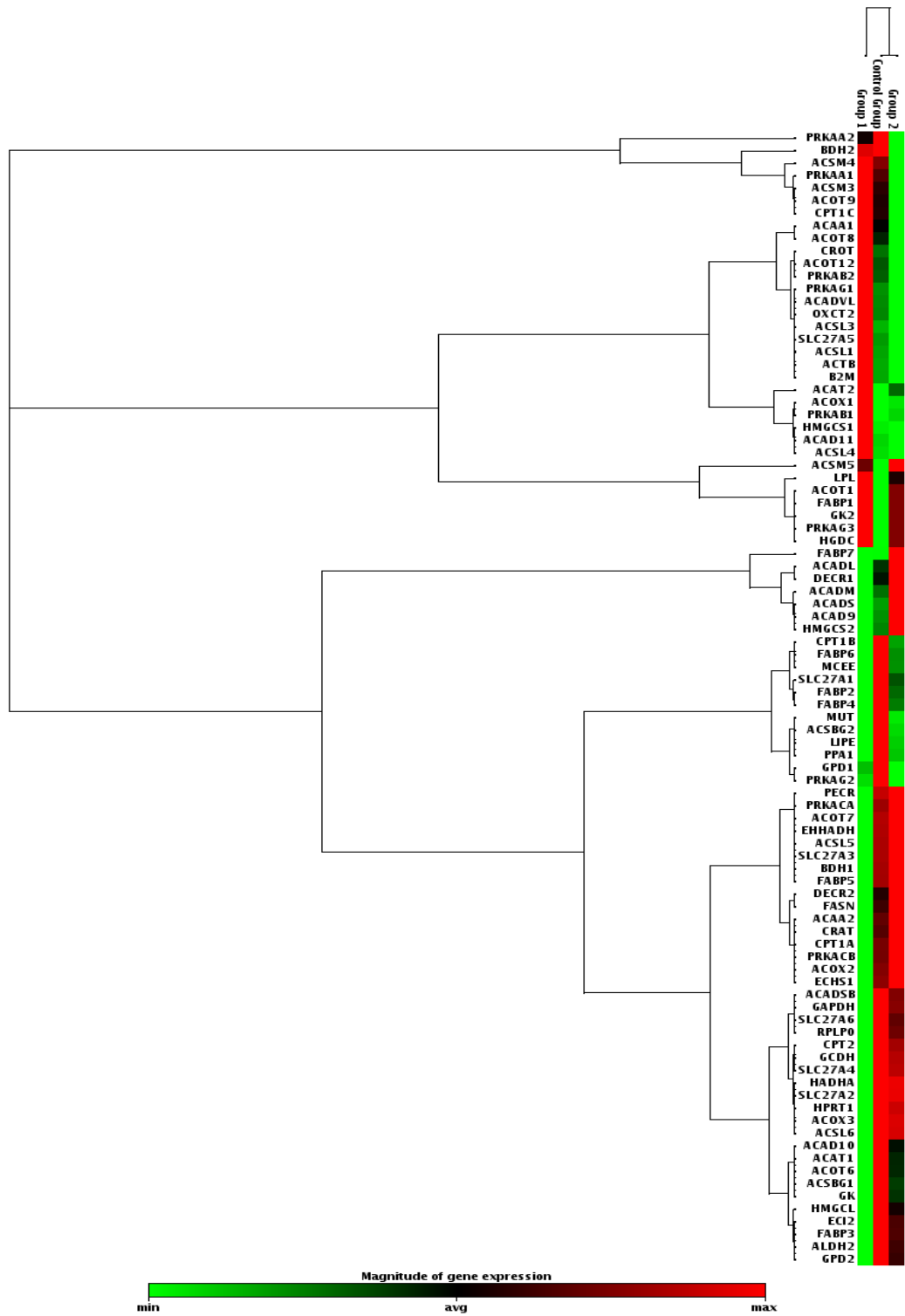


Figure 37. The clustergram shows non-supervised hierarchical clustering of the entire dataset to display a heat map with dendrograms indicating co-regulated genes across groups. Group 1 represents the analog treated group; Group 2 represents the α -tocopherol treated group.

The cluster of experimental groups in terms of gene expression levels is presented in Figure 37.

As can be seen from the clustergram, the genes in α -tocopherol treated cells much more co-regulated with the genes of control cells rather than analog treated cells. This explains the other phenotypic similarities between the control and α -tocopherol treated groups.

The names of the genes which are over and under expressed in response to treatment are given in Table 5 and Table 6, respectively. Threshold value was adjusted to the 2 to show significant fold change.

Table 5. Genes over-expressed in analog treated vs control and tocopherol vs control groups.

Analog versus Control		α -tocopherol versus Control	
Gene Symbol	Fold Regulation	Gene Symbol	Fold Regulation
HMGCS1	8.66	FABP7	27.39
ACSL4	3.68	HMGCS2	2.77
ACAT2	3.66	ACSM5	2.48
SLC27A5	3.09	ACADL	2.07
ACSL1	2.85		
ACOT12	2.39		
ACAD11	2.19		
ACSM5	2.05		

Table 6. Genes under-expressed in analog treated vs control and tocopherol vs control groups

Analog versus Control				α -tocopherol versus Control	
Gene Symbol	Fold Regulation	Gene Symbol	Fold Regulation	Gene Symbol	Fold Regulation
FABP4	-83.37	ACSL5	-2.95	FABP4	-3.78
ACOT6	-30.3	SLC27A2	-2.77	GPD1	-3.64
FABP2	-24.7	GPD1	-2.73	LIPE	-3.63
CRAT	-14.99	MCEE	-2.65	ACOT12	-3.17
ACSL6	-7.24	HMGCL	-2.53	FABP2	-3.07
FABP3	-5.03	GCDH	-2.49	ACSBG2	-3.01
LIPE	-4.95	SLC27A3	-2.41	ACOT6	-2.25
ACOX3	-4.63	SLC27A1	-2.33	ACSM3	-2.14
EHHADH	-4.13	SLC27A4	-2.33		
ACOX2	-4.12	HMGCS2	-2.21		
ACSBG2	-3.55	ALDH2	-2.10		
ACADL	-3.47	SLC27A6	-2.10		
CPT2	-3.16	ACSBG1	-2.00		
GK	-2.96				

Our findings showed increased fatty acid and cholesterol amount in both α -tocopherol & analog treated cells. When the mRNA expression levels are investigated, it was observed that the level of HMG-CoA synthase, a key enzyme in lipid biosynthesis, increases while the enzyme responsible for the conversion of cholesterol ester in the intracellular lipid droplets to free cholesterol, LIPE, decreases significantly in the analog and α -tocopherol treated groups. The VE and VE analog have showed similar effect on lipid synthesis. The increase in lipid content can be associated with the increased lipid synthesis and/or decreased lipid degradation in the experimental groups via HMGCS regulated pathways.

The VE molecules, tocotrienols and mixed isoprenoids with farnesol side chain tend to down regulate HMG-CoA reductase in tumor cells and are able to induce apoptosis (Cruz et al, 2013).

Cholesterols esterified via acyl-CoA cholesterol acyltransferase (ACAT) to cholesterol ester which is then stored as lipid droplet within the cell. Array results revealed an increase in ACAT2 expression which may indicate the high amount of cholesterol ester in analog treated group (Athenstaedt & Daum, 2006). Infrared spectroscopy results also showed that there was a significant increase in cholesterol ester amount in treated cells. It has been thought that accumulated cholesterol would modulate other lipid synthesis pathways in our case.

Carnitine acetyl transferase (CRAT), which resides in the mitochondrial matrix, is responsible for the reconversion of the short and medium chain acyl-CoAs into acylcarnitines using intra-mitochondrial carnitine. There was a decrease in CRAT expression in response to analog treatment. Decreased CRAT activity is associated with the increased levels of acyl-CoA, which leads to inhibition of multiple enzymatic processes involved in oxidative metabolism (Sharma & Black, 2009). This inhibition might yield decreased cellular viability.

Decrease in energy metabolism in response to analog treatment could also be followed by the decrease in the expression of glycerol kinase (GK) which is the key enzyme between fat and carbohydrate metabolism, responsible for the glycerol uptake and has complex network (Rahib et al, 2007). Whereas no change in GK level was detected in α -tocopherol treated group.

The family of fatty acid binding proteins (FABPs) bind fatty acids with high affinity and are able to modulate lipid homeostasis by regulating fatty acid transport throughout inter and intra cellular membranes thus they have significant impact on the establishment of cellular energy homeostasis (Storch & McDermott, 2009). As it can be followed from the Table 6, the expression levels of 3 FABPs are downregulated in response to analog. Previous study conducted with breast tissues have shown that

some forms of FABPs were upregulated in invasive breast carcinoma which interpreted as FABPs were tightly associated with invasive ductal carcinoma development however still the mechanism is unclear (Li et al, 2012). Our study also has proved that there is relationship between the FABPs and cancer cell status that need to be further investigated.

3.4. Effect of VE Analog in Protein Level

3.4.1. Western Blot Analysis

Measurement of mRNA and protein levels is complementary in any experimental setup and both are necessary for the complete understanding of how cell works. Although it has been expected that the mRNA is translated into protein and there should be a correlation between their amounts, it is not always the case. In some cases, there may not be correlation, which, in itself, is also an informative conclusion. Therefore, the protein expression of LIPE and HMGCS1 whose mRNA expressions are remarkably changed and, also have distinct roles in lipid homeostasis, were selected for the correlation check.

Due to the observed significant alterations in cholesterol content, SREBP1 protein level was also checked with western blot.

In Figure 38, Western Blot results for the indicated lipid related proteins are represented.

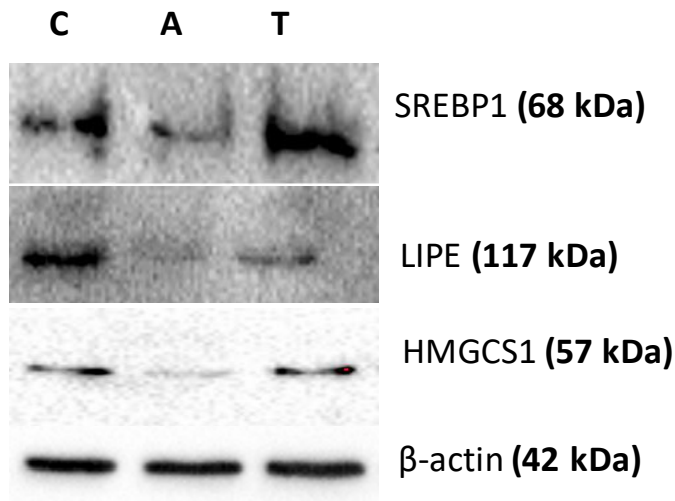


Figure 38. Changes in protein expression levels in Control (C), Analog (A) and α -tocopherol (T) treated groups. Total protein lysates were isolated from both 150 μ M, 48h VE and VE analog treated & untreated control cells and probed with respective antibodies. 50 μ g protein was loaded and β -Actin was used for protein loading control.

SREBP level significantly decreased in VE analog treated group whereas increased due to α -tocopherol. Sterol regulatory element binding proteins (SREBP family) are the master regulators of lipid biogenesis. SREBPs are resided in ER membrane as inactive SREBP-SCAP complex. The decrease in sterol concentration triggers the translocation of SREBP-SCAP complex to the Golgi where SREBP is cleaved into active form (Nohturfft & Zhang, 2009). Also the reduced level of membrane phospholipid (PC) causes the proteolytic cleavage and nuclear transportation of SREBP (Walker et al, 2011). However whether the sterol sensitivity of SREBP is maintained in cancer cells or not is controversial (Krycer et al, 2009).

In a recent surprising study, it was demonstrated that the loss of SREBP activity inhibited the cancer cell growth and viability not by reducing global fatty acid and cholesterol availability but by uncoupling de novo long chain saturated FA biosynthesis from desaturation. The result of uncoupling causes the accumulation of newly synthesized saturated fatty acids and altered ratio of saturated to monounsaturated FAs which yields cellular dysfunction or lipotoxicity (Williams et

al, 2013). In our case the decrease in SREBP1 level could explain the lipotoxicity triggered cell death.

The decrease in LIPE protein expression in both analog and α -tocopherol treated group is correlated with the decrease in LIPE mRNA which can be associated with increased cholesterol ester amount as explain before.

Although we have shown a significant level of increase in mRNA transcripts of HMGCS1, the decrease in protein level was recorded (Figure 39). HMGCS1 is the first level enzyme of mevalonate pathway, catalyzes the condensation of acetylCoA with acetoacetyl-CoA towards 3-hydroxy-3-methylglutaryl (HMG)-CoA. Then, in a subsequent step HMGCR uses HMG-CoA for mevalonate synthesis. In a comprehensive study, it has been shown that accumulation of cholesterol increased the ratio of alternatively spliced to full length transcripts of several genes involved in cholesterol biosynthesis including HMGCS1. They clarify their findings by showing the alternative splicing of 5'UTR of HMGCS1 reduces the half-life of transcript which results in a decrease in HMGCS1 protein levels. Authors suggest that the modulating the ratio of full-length to alternative spliced variants of transcripts is the generalized mechanism for the regulation of gene expression involved in cholesterol metabolism (Medina et al, 2011). In our case the cholesterol level in the analog treated cells significantly increased. It has been thought that this increase would trigger the alternative splicing of HMGCS1 mRNA which in turn results in decreased protein levels. In addition, the cholesterol sensitivity of the HMGCS1 regulation is also proved with these results.

In addition to the expression levels of lipid metabolism associated proteins; ER stress associated protein, p-AKT; cellular proliferation associated protein, p-ERK; apoptosis associated marker, cleaved caspase 3 and metastatic marker, Vimentin protein expression levels are investigated.

In Figure 39, Western Blot results for the indicated proteins are represented.

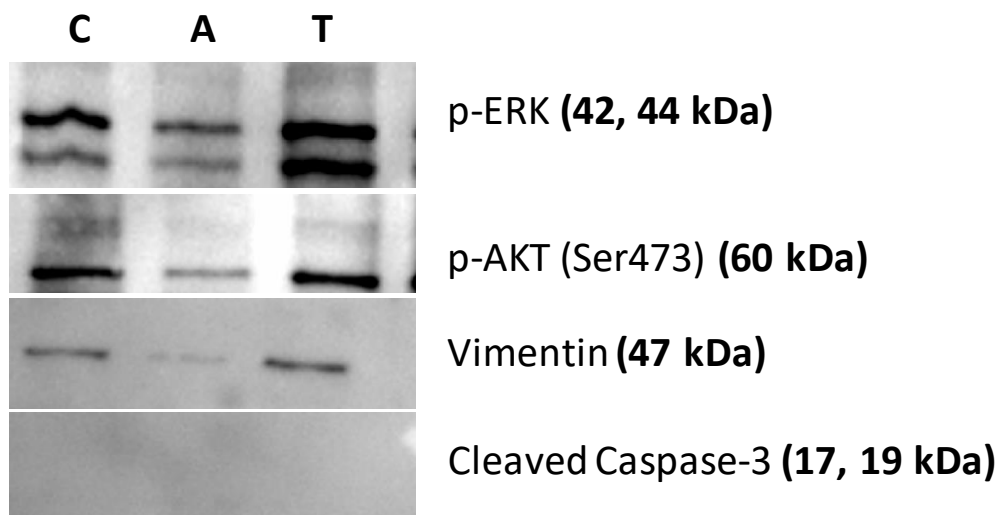


Figure 39. Changes in protein expression levels in Control (C), Analog (A) and α -tocopherol (T) treated groups. Total protein lysates were isolated from both 150 μ M, 48h VE and VE analog treated & untreated control cells and probed with respective antibodies.

p-AKT expression is downregulated in response to analog treatment whereas there is no significant change in α -tocopherol treated group related to the control. AKT, a serine/threonine protein kinase, activity is associated with ER stress. It was reported that ER stress induced phosphorylation of AKT alter substrate recognition profile of AKT in a severity dependent manner and ER stress also reduces both total and phosphorylated AKT without affecting the activity of upstream kinase PDK1 (Yung et al, 2011). Endoplasmic Reticulum (ER) is the center of synthesis, maturation and exportation of secreted and membrane proteins. ER stress associated with the common human diseases like cancer, metabolic syndromes, neurodegenerative diseases etc. Disruption of ER homeostasis by any intrinsic or extrinsic factor can results in the accumulation of unfolded or misfolded proteins which in turn yields ER stress. ER stress triggers unfolded protein response (UPR) to restore ER homeostasis (Rutkowski & Kaufman, 2004). AKT signaling regulates wide range of cellular processes through phosphorylation of different downstream targets like, p21Cip, BAD, FOXO, mTOR, HDM2, MDM3, eNOS etc. Therefore, AKT is a pivotal kinase for ER stress to target. Downregulation of p-AKT can be associated with the

decreased cellular proliferation as a downstream event due to analog treatment induced ER stress.

Figure 39 depicts the expression of phospho-ERK after 48h drug exposure. There was a decrease in p-ERK level in analog treated group. Extracellular signal related kinase (ERK1/2) is a member of mitogen activated protein kinase signal transduction pathway and is key player in the control of proliferation. Phosphorylated form of ERK (p-ERK) represents the effector molecule in the RAS/RAF/MEK cascade in EGFR signaling. Phosphorylation of both threonine (Thr202) and tyrosine (Tyr204) residues are required for full kinase activity (Roskoski Jr, 2012). It was reported that various tumor types have high levels of ERK/MEK activity (Loda et al, 1996; Schmidt et al, 1997). Decreased p-ERK expression could be linked with the decreased proliferation rate in analog treated cells.

Vimentin, a type III intermediate filament protein and overexpressed in many aggressive cancer cell lines, is downregulated in analog treated cells as compared to control (Thiery, 2002). MCF7 is the slightly metastatic cell line therefore Vimentin bands were hardly detected by western blot (Figure 39).

Cleaved caspase 3 protein could not be detected as MCF7 cells do not express caspase 3.

3.4.2. Protein Array

In order to establish an overall perspective of the proteins related to carcinogenesis, an array analysis of multiple oncogenic proteins was performed. Dot blot and 3D expression pattern are shown in Figure 40A and B, respectively. The coordinates of the protein spots are given as Appendix A.

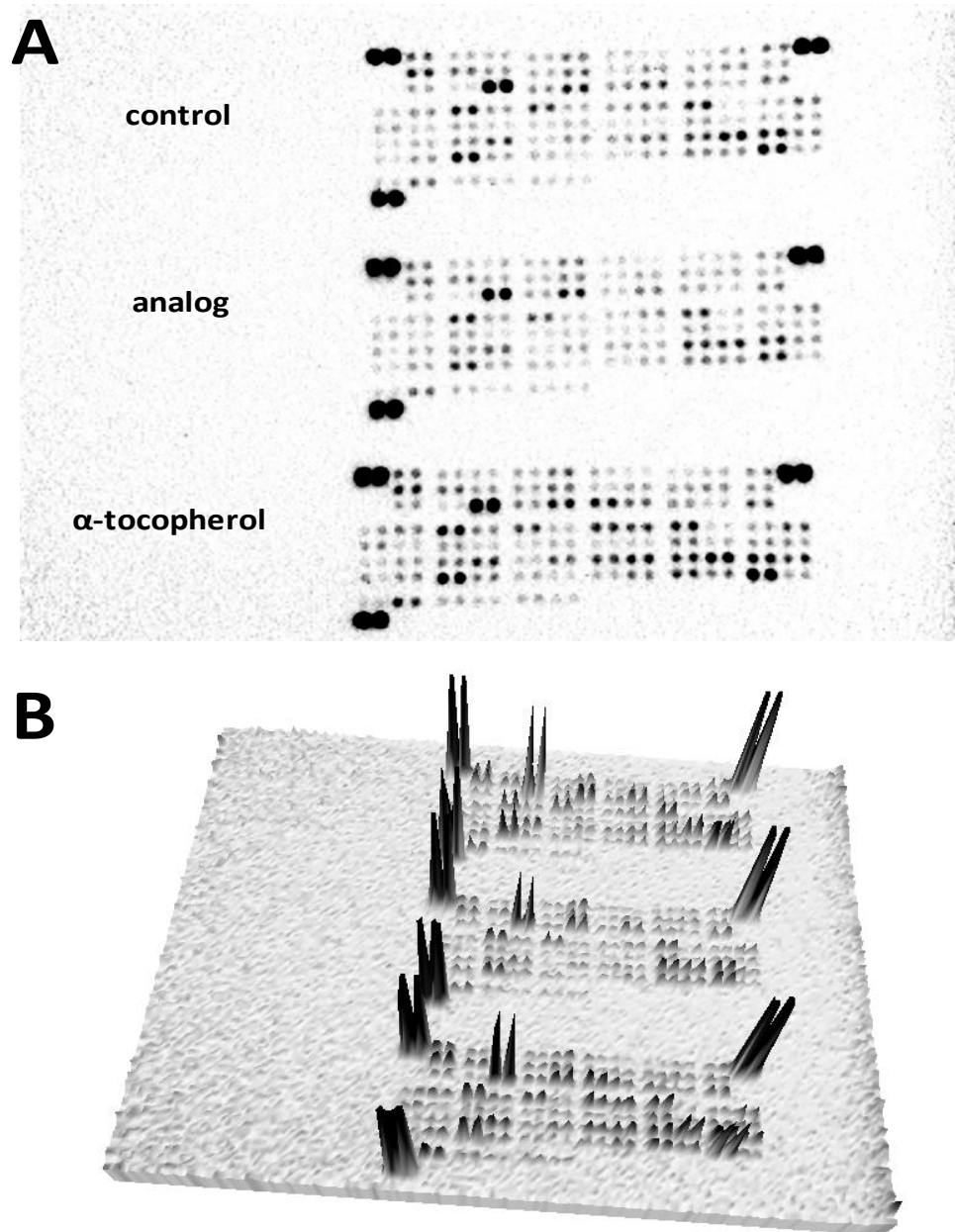


Figure 40. Proteome profiler array expression patterns of experimental groups. (A) Dot blot, (B) 3D representation.

The changes in protein expression levels of selected genes which showed significant alterations, are given in Figure 41. Selected genes are important cancer markers associated with aggressiveness, viability of cancer cell and metastasis in breast cancer.

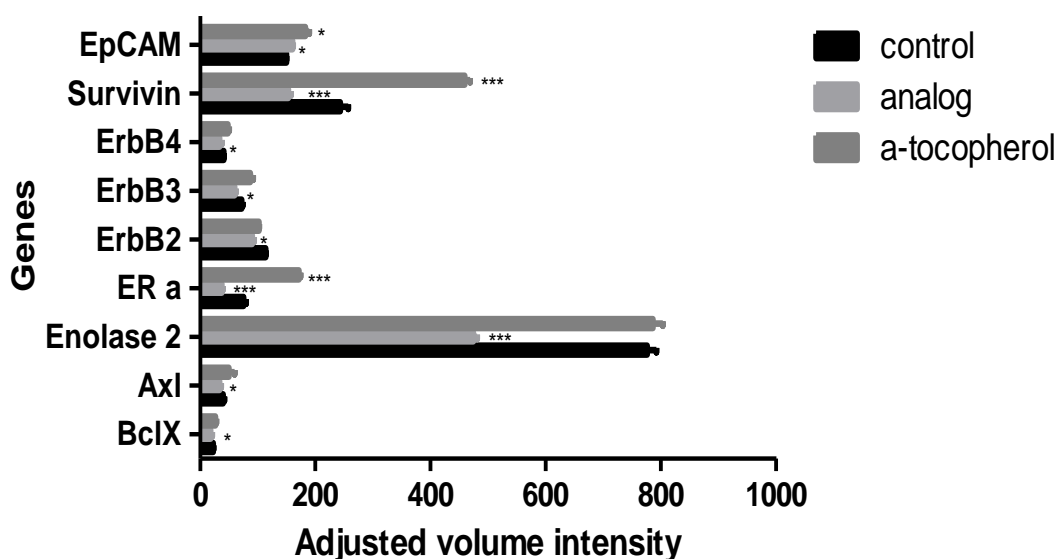


Figure 41. Changes in the protein expression levels of selected genes in the control, analog and α -tocopherol treated groups.

Type 1 growth factor receptor ErbB family consists of 4 members (ErbB1-4). MCF7 cells have high endogenous ErbB3, but low levels of endogenous ErbB2 and ErbB4 (Mooser et. al., 2001). As it can be represented in Figure 41 the expression of all ErbB receptors decreased due to analog treatment whereas there was no significant change in α -tocopherol group.

The receptor tyrosine kinases Her2/neu and EGFR receptors are over expressed in a class of breast tumors. ErbB2 over-expression is associated with the activation of PI3-kinase, Akt and serine/threonine kinase triggered signaling pathways which exerts anti-apoptotic effects and promotes cell survival. ErbB2 (HER2) and other growth factor receptors are associated to lipid rafts and their signaling control is strictly dependent on the cholesterol content of the raft formation. It has been shown that disruption of the lipid rafts due to the altered cholesterol content interfere with the receptor activation and yield cell growth inhibition (Chen & Resh, 2002). In our case, it has been suggested that the increased cholesterol amount would change the lipid raft distribution thus interfered with the ErbB receptors which in turn yield cellular apoptosis.

In a detailed study, it was reported that the over-expression of ErbB2 does not compromise different breast cancer cells towards killing via different VE analogs. It has been meaning that VE analogs cause apoptosis regardless of the ErbB2 status of the cells thereby bypass the pro-survival effects of ErbB2 triggered pathways (Wang et al, 2005) . Together with these findings our data suggest that our VE analog may be useful for the treatment of breast cancers with elevated ErbB2 expression levels.

Estrogen binding to the estrogen receptor (ER) have important role in breast cancer development and researches show that antioxidants like VE possibly mitigate this effect. Analog treated cells show decreased ER- α level which revealed the effect of VE analog on ER signaling pathways. It has been known that VE reduced the response of ER positive cells to the estrogen and the proliferation rate also decreased concurrently (Chamras et al, 2005). From our findings, it can be proposed that VE analog may exert its anti-proliferative activity by decreasing the ER expression which interfere downstream cancer cell survival pathways.

BclX is a pro-survival protein exerts its function by preventing the cytochrome c release from the mitochondria and linked to the multidrug resistant phenotype of cancer cells (Minn et al, 1995). Decrease in BclX level can suggest the caspase activation via cytochrome c release that may yield apoptosis.

The level of Survivin which is the member of inhibitors of apoptosis protein (IAP) family was also investigated. Survivin selectively over-expressed in various cancer cells and have role in cell viability and drug resistance. Survivin expression was down-regulated in analog treated cells. It has been shown that siRNA mediated Survivin inhibition sensitizes cells to the therapy. Similarly a study conducted with VES, Survivin is the possible target for VES (Patacsil et al, 2012).

Another protein which had been decreased was Enolase, is a glycolytic enzyme catalyzes the conversion of 2-phosphoglycerate into phosphoenolpyruvate has three tissue specific isoenzymes. Although the ENO1 is the predominant enolase in normal breast tissue while ENO2 levels are very low, the proportion of ENO2 is being

higher in breast carcinomas than normal tissue. Therefore ENO2 has been employed as a tumor marker for neuroendocrine differentiation of cancer cells (Nesland et al, 1986; Soh et al, 2011). Over-expression of enolase is associated with tumor progression via triggering of aerobic glycolysis (Warburg effect). Decrease in ENO2 levels can be associated with the decreased metabolism of cancer cells due to analog treatment which correlates with the previous findings.

Axl receptor tyrosine kinase, overexpression was reported in breast carcinoma and associated with invasiveness and metastasis (Meric et al, 2002). In Axl inhibition study, knockdown of Axl attenuated the migration of MDA-MB-231 cells and inhibited the lung metastasis in an orthotopic model (Li et al, 2009). Analog treatment also causes the Axl inhibition which in turn might result in reduced cell motility.

Another metastasis marker is the epithelial cell adhesion molecule (EpCAM). Analog and α -tocopherol treatment increase EpCAM level. Depending on the data coming from number of independent researches, EpCAM has controversial biological role in carcinogenesis. In addition to its promoting role in tumor formation, it also described as a tumor suppressive protein. It has been widely reviewed that EpCAM could promote metastasis by abrogating E-Cadherin mediated cell-cell adhesion, on the other hand, could mediate homophilic adhesion interactions which in turn might prevent metastasis. Therefore EpCAM over-expression has been associated with both increased and decreased survival rate of cancer patients (van der Gun et al, 2010). Our observation was also proved the contradictory role of EpCAM. Its expression and apoptotic activity of the cells increased while the metastatic activity decreased due to analog treatment.

CHAPTER IV

CONCLUSION

The last decade has witnessed the search for novel anti-cancer drugs that have the capability in inducing cell death selectively in cancer cells. To date, many well-established treatment strategies show detrimental side effects and often lead to secondary complications and also failed to target and eliminate just cancer cells (Chakraborty & Rahman, 2012). TC6OH, a derivative of α -tocopherol with side chain modification, has been suggested as anti-tumor agent, independent of its anti-oxidant function. The VE derivative has shown anti-tumor activity by decreasing the tumor size, while has no significant effect on normal in-vivo mice models. However, it has not been established that how could it exert its anti-cancer effects on cellular level. The primary question throughout this dissertation is that whether it does its function by changing the lipid homeostasis or not. The goal of this study was to further delineate the mechanism of action of TC6OH as an α -tocopherol based anti-cancer agent, which possesses suitable characteristics for chemotherapeutic use in humans, for the first time.

In order to measure the cellular response to the VE analog treatment, a series of cell response assays were conducted. It was clearly identified that VE analog is toxic for breast cancer cells whereas it does not effective on MCF10A normal breast epithelial cells at the same doses. This finding has showed the tumor cell targeting specificity of the novel VE analog. The results of cell viability assay were confirmed with the cellular proliferation and apoptosis assays. The population of apoptotic and necrotic cells were significantly high in VE analog treated group as compared to α -tocopherol treated and non-treated cells. Notwithstanding our and vast majority of results from the works of others clearly point to mitochondria as very important organelle which involved in the induction of apoptosis in cancer cells by analogs of VE (Prochazka et al, 2010; Wang et al, 2005; Weber et al, 2003; Yan et al, 2015). The JC-1 assay

clearly demonstrated that induction of apoptosis involves mitochondrial pathway.

The mitochondrial membrane potential was severely affected as a result of analog treatment, which strongly suggests that the VE analog might modulate mitochondrial cytochrome c and caspase activity. This hypothesis needs to be further investigated. One of the evidence that projected the role of cytochrome c – caspase regulation is that the decreased protein expression level of BclX due to the analog treatment.

The results of the wound healing and transwell migration assays showed that, metastatic potential of tumor cells was also severely inhibited by analog treatment. In addition, the level of metastatic proteins; Vimentin and Axl have significantly decreased. These proteins could be suggested as the target of VE analog.

Throughout cell response measurements, α -tocopherol treated cells behave similarly as non-treated group as suggested in the literature. Even, in some cases, viability and aggressiveness of α -tocopherol treated cells were increased.

Depending on the extensive literature about α -tocopherol – lipid interactions, the primary goal of the study was to shed light on changes in cellular lipids and membrane systems while analog has been exerting its anti-tumor function. The exploratory chemometric analyses based on the infrared spectroscopic data confirm our hypothesis that, the lipids were the most effected class of molecules in treated cells. The detailed analyses on lipid specific vibrational bands showed that the total lipid and cholesterol amount was increased in both analog and α -tocopherol treated groups, which comes to mind that lipotoxicity driven apoptosis. The qualitative oil red o staining results also confirmed the increase in the number of lipid droplets in cytoplasm. Although the parallel increase in overall lipid content has been observed in analog and α -tocopherol groups, the final outcomes are different. When the ratio of CH₂ symmetric vibrations / CH₃ symmetric vibrations were calculated, it has been noticed that the number of longer fatty acyl chains were differ between these groups. Therefore, it could be suggested that rather than the increase, the imbalance in lipid homeostasis able to undergo system into apoptosis.

The membrane dynamic information was collected by IR and ESR spectroscopy. Results pointed out a decrease in lipid fluidity in analog and α -tocopherol groups. Findings about α -tocopherol are in consisted with the literature. On the other hand,

while the IR data has showing a decrease in lipid order, ESR data indicated an increase. These controversial results suggested that, there must be a domain formation on cellular membrane. Similar results are documented in literature about several drugs which form domains. Taking these results together, it has been thought that, VE analog binds to membrane lipids through its hydrophobicity and makes it more rigid and thicker. These changes in cellular membrane directly and indirectly affect the function of lipids and lipid anchored membrane proteins which have the potential to modulate downstream signaling events.

In order to reveal genetic background in lipid metabolism changes, the fatty acid (FA) metabolism gene expression profile at mRNA level, was examined. For the confirmation, the expression changes of selected 3 important genes at protein level were checked. When the overall scenario was taken into consideration, it can be interpreted that, the increased cellular FA level was sourced from the decreased FA degradation rather than increased FA synthesis. Newly synthesized fatty acids accumulated via LIPE and SREBP down-regulation.

It has been thought that the increase in cholesterol amount was also triggered by ACAT2 over-expression. In addition, the inconsistency between the mRNA and protein levels of HMGCS1 indicates that the accumulated cholesterol could triggered the alternative splicing of HMGCS1 mRNA and broke down sterol sensitivity of cells. On the other hand, the lipid transport pathways were altered by down-regulation of some FABPs. Decreased metabolism in analog treated group firstly proposed by depending on IR data. Genetic data also showed that the metabolic status of cells was also altered by down-regulation of GK and CRAT transcription, in addition to decreased Enolase protein level which all directly affect energy uptake, in response to analog treatment whereas no significant change was observed in α -tocopherol group. When all the FA metabolism gene expression profile was considered, the pattern of change is much more similar in α -tocopherol treated ones with control whereas analog induced changes were considerably different.

When the expression level of specific oncoproteins, which have great importance in breast carcinogenesis, were measured, the data reported here showed that the down-regulation in Survivin, ErbB family proteins and Estrogen Receptor might play major roles in the anti-tumor activity of VE analog. In addition, the downregulation of p-

AKT can be associated with the ER stress driven UPR and decreased cell proliferation. Decreased expression level of p-ERK also inconsistent with the decreased cell viability.

Data documented in this study pointed out the corner stones of analog induced changes and would help us to identify possible targets of new VE analog. This study also highlighted the importance of lipid biology for the development of possible novel cancer treatment strategies. The findings would guide us for the further in-vivo studies which have a potential to offer VE analog as a chemotherapeutic or adjuvant agent for cancer therapy in near future.

REFERENCES

Ackerman D, Simon MC (2014) Hypoxia, lipids, and cancer: surviving the harsh tumor microenvironment. *Trends in cell biology* **24**: 472-478

Alleva R, Tomasetti M, Andera L, Gellert N, Borghi B, Weber C, Murphy MP, Neuzil J (2001) Coenzyme Q blocks biochemical but not receptor-mediated apoptosis by increasing mitochondrial antioxidant protection. *FEBS letters* **503**: 46-50

Anderson K, Lawson KA, Simmons-Menchaca M, Sun L, Sanders BG, Kline K (2004a) Alpha-TEA plus cisplatin reduces human cisplatin-resistant ovarian cancer cell tumor burden and metastasis. *Experimental biology and medicine* (Maywood, NJ) **229**: 1169-1176

Anderson K, Simmons-Menchaca M, Lawson KA, Atkinson J, Sanders BG, Kline K (2004b) Differential response of human ovarian cancer cells to induction of apoptosis by vitamin E Succinate and vitamin E analogue, alpha-TEA. *Cancer research* **64**: 4263-4269

Arya P, Alibhai N, Qin H, Burton GW, Batist G, You SX, Alaoui-Jamali MA (1998) Design and synthesis of analogs of vitamin E: antiproliferative activity against human breast adenocarcinoma cells. *Bioorganic & medicinal chemistry letters* **8**: 2433-2438

Athenstaedt K, Daum G (2006) The life cycle of neutral lipids: synthesis, storage and degradation. *Cellular and molecular life sciences* : CMLS **63**: 1355-1369

Baenke F, Peck B, Miess H, Schulze A (2013) Hooked on fat: the role of lipid synthesis in cancer metabolism and tumour development. *Disease models & mechanisms* **6**: 1353-1363

Barnard AN (2014) 1, 25-dihydroxyvitamin D alters lipid metabolism and epithelial-to-mesenchymal transition in metastatic epithelial breast cancer cells. PURDUE UNIVERSITY,

Baselga J, Norton L (2002) Focus on breast cancer. *Cancer Cell* **1**: 319-322

Birringer M, EyTina JH, Salvatore BA, Neuzil J (2003) Vitamin E analogues as inducers of apoptosis: structure-function relation. *British journal of cancer* **88**: 1948-1955

Bisby RH, Birch DJS (1989) A time-resolved fluorescence anisotropy study of bilayer membranes containing α -tocopherol. *Biochemical and Biophysical Research Communications* **158**: 386-391

Blancato J, Singh B, Liu A, Liao DJ, Dickson RB (2004) Correlation of amplification and overexpression of the c-myc oncogene in high-grade breast cancer: FISH, in situ hybridisation and immunohistochemical analyses. *British journal of cancer* **90**: 1612-1619

Boffa LC, Lupton JR, Mariani MR, Ceppi M, Newmark HL, Scalmati A, Lipkin M (1992) Modulation of colonic epithelial cell proliferation, histone acetylation, and luminal short chain fatty acids by variation of dietary fiber (wheat bran) in rats. *Cancer research* **52**: 5906-5912

Bougnoux P, Hajjaji N, Maheo K, Couet C, Chevalier S (2010) Fatty acids and breast cancer: Sensitization to treatments and prevention of metastatic re-growth. *Progress in lipid research* **49**: 76-86

Bozkurt O, Severcan M, Severcan F (2010) Diabetes induces compositional, structural and functional alterations on rat skeletal soleus muscle revealed by FTIR spectroscopy: a comparative study with EDL muscle. *The Analyst* **135**: 3110-3119

Cakmak G, Miller LM, Zorlu F, Severcan F (2012) Amifostine, a radioprotectant agent, protects rat brain tissue lipids against ionizing radiation induced damage: An FTIR microspectroscopic imaging study. *Arch Biochem Biophys* **520**: 67-73

Cakmak G, Zorlu F, Severcan M, Severcan F (2011) Screening of protective effect of amifostine on radiation-induced structural and functional variations in rat liver microsomal membranes by FT-IR spectroscopy. *Analytical chemistry* **83**: 2438-2444

Campbell ID, Dwek RA (1984) *Biological spectroscopy*: Benjamin/Cummings Pub. Co.

Cary LA, Cooper JA (2000) Molecular switches in lipid rafts. *Nature* **404**: 945, 947

Chakraborty S, Rahman T (2012) The difficulties in cancer treatment. *ecancermedicalsecience* **6**: ed16

Chamras H, Barsky SH, Ardashian A, Navasartian D, Heber D, Glaspy JA (2005) Novel interactions of vitamin E and estrogen in breast cancer. *Nutr Cancer* **52**: 43-48

Chen X, Resh MD (2002) Cholesterol depletion from the plasma membrane triggers ligand-independent activation of the epidermal growth factor receptor. *The Journal of biological chemistry* **277**: 49631-49637

Cruz PM, Mo H, McConathy WJ, Sabnis N, Lacko AG (2013) The role of cholesterol metabolism and cholesterol transport in carcinogenesis: a review of scientific findings, relevant to future cancer therapeutics. *Frontiers in pharmacology* **4**: 119

Daniels VW, Smans K, Royaux I, Chypre M, Swinnen JV, Zaidi N (2014) Cancer cells differentially activate and thrive on de novo lipid synthesis pathways in a low-lipid environment. *PloS one* **9**: e106913

Deo N, Somasundaran P (2002) Electron spin resonance study of phosphatidyl choline vesicles using 5-doxyl stearic acid. *Colloids and Surfaces B: Biointerfaces* **25**: 225-232

Derenne A, Claessens T, Conus C, Goormaghtigh E (2013) Infrared Spectroscopy of Membrane Lipids. In *Encyclopedia of Biophysics*, Roberts GCK (ed), pp 1074-1081. Berlin, Heidelberg: Springer Berlin Heidelberg

Fabian CJ (2007) The what, why and how of aromatase inhibitors: hormonal agents for treatment and prevention of breast cancer. *International Journal of Clinical Practice* **61**: 2051-2063

Fahy E, Cotter D, Sud M, Subramaniam S (2011) Lipid classification, structures and tools. *Biochimica et Biophysica Acta (BBA) - Molecular and Cell Biology of Lipids* **1811**: 637-647

Gago-Dominguez M, Castelao JE, Pike MC, Sevanian A, Haile RW (2005) Role of lipid peroxidation in the epidemiology and prevention of breast cancer. *Cancer*

epidemiology, biomarkers & prevention : a publication of the American Association for Cancer Research, cosponsored by the American Society of Preventive Oncology **14**: 2829-2839

Galli F, Stabile AM, Betti M, Conte C, Pistilli A, Rende M, Floridi A, Azzi A (2004) The effect of alpha- and gamma-tocopherol and their carboxyethyl hydroxychroman metabolites on prostate cancer cell proliferation. *Arch Biochem Biophys* **423**: 97-102

Garip S, Sahin D, Severcan F (2013) Epileptic seizure-induced structural and functional changes in rat femur and tibia bone tissues: a Fourier transform infrared imaging study. *J Biomed Opt* **18**: 111409

Gasper R, Dewelle J, Kiss R, Mijatovic T, Goormaghtigh E (2009) IR spectroscopy as a new tool for evidencing antitumor drug signatures. *Biochimica et Biophysica Acta (BBA)-Biomembranes* **1788**: 1263-1270

Germain E, Chajes V, Cognault S, Lhuillery C, Bounoux P (1998) Enhancement of doxorubicin cytotoxicity by polyunsaturated fatty acids in the human breast tumor cell line MDA-MB-231: relationship to lipid peroxidation. *International journal of cancer* **75**: 578-583

Gerweck LE, Kozin SV, Stocks SJ (1999) The pH partition theory predicts the accumulation and toxicity of doxorubicin in normal and low-pH-adapted cells. *British journal of cancer* **79**: 838-842

Gok S, Aydin OZ, Sural YS, Zorlu F, Bayol U, Severcan F (2016) Bladder cancer diagnosis from bladder wash by Fourier transform infrared spectroscopy as a novel test for tumor recurrence. *Journal of biophotonics*

Gok S, Severcan M, Goormaghtigh E, Kandemir I, Severcan F (2015) Differentiation of Anatolian honey samples from different botanical origins by ATR-FTIR spectroscopy using multivariate analysis. *Food Chemistry* **170**: 234-240

Guthrie N, Gapor A, Chambers AF, Carroll KK (1997) Inhibition of proliferation of estrogen receptor-negative MDA-MB-435 and -positive MCF-7 human breast cancer cells by palm oil tocotrienols and tamoxifen, alone and in combination. *The Journal of nutrition* **127**: 544s-548s

Gysin R, Azzi A, Visarius T (2002) Gamma-tocopherol inhibits human cancer cell cycle progression and cell proliferation by down-regulation of cyclins. *FASEB*

journal : official publication of the Federation of American Societies for Experimental Biology **16**: 1952-1954

Holliday DL, Speirs V (2011) Choosing the right cell line for breast cancer research. Breast cancer research : BCR **13**: 215

Huang C, Freter C (2015) Lipid metabolism, apoptosis and cancer therapy. International journal of molecular sciences **16**: 924-949

Inan Genc A, Gok S, Banerjee S, Severcan F (2016) Valdecoxib Recovers the Lipid Composition, Order and Dynamics in Colon Cancer Cell Lines Independent of COX-2 Expression: An ATR-FTIR Spectroscopy Study. Applied spectroscopy

Jemal A, Bray F, Center MM, Ferlay J, Ward E, Forman D (2011) Global cancer statistics. CA: a cancer journal for clinicians **61**: 69-90

Kamphorst JJ, Cross JR, Fan J, de Stanchina E, Mathew R, White EP, Thompson CB, Rabinowitz JD (2013) Hypoxic and Ras-transformed cells support growth by scavenging unsaturated fatty acids from lysophospholipids. Proceedings of the National Academy of Sciences of the United States of America **110**: 8882-8887

Karaskov E, Scott C, Zhang L, Teodoro T, Ravazzola M, Volchuk A (2006) Chronic palmitate but not oleate exposure induces endoplasmic reticulum stress, which may contribute to INS-1 pancreatic beta-cell apoptosis. Endocrinology **147**: 3398-3407

Kline K, Yu W, Sanders BG (2004) Vitamin E and breast cancer. The Journal of nutrition **134**: 3458s-3462s

Kocherginsky N. SHM (1995) Nitroxide Spin Labels. Reactions in Biology and Chemistry, Boca Raton, FL: CRC Press.

Kogure K, Morita M, Nakashima S, Hama S, Tokumura A, Fukuzawa K (2001) Superoxide is responsible for apoptosis in rat vascular smooth muscle cells induced by alpha-tocopheryl hemisuccinate. Biochimica et biophysica acta **1528**: 25-30

Kotas ME, Jurczak MJ, Annicelli C, Gillum MP, Cline GW, Shulman GI, Medzhitov R (2013) Role of caspase-1 in regulation of triglyceride metabolism. Proceedings of the National Academy of Sciences of the United States of America **110**: 4810-4815

Kourtidis A, Srinivasaiah R, Carkner RD, Brosnan MJ, Conklin DS (2009) Peroxisome proliferator-activated receptor-gamma protects ERBB2-positive breast cancer cells from palmitate toxicity. *Breast cancer research : BCR* **11**: R16

Kozin SV, Shkarin P, Gerweck LE (2001) The cell transmembrane pH gradient in tumors enhances cytotoxicity of specific weak acid chemotherapeutics. *Cancer research* **61**: 4740-4743

Krycer JR, Kristiana I, Brown AJ (2009) Cholesterol homeostasis in two commonly used human prostate cancer cell-lines, LNCaP and PC-3. *PloS one* **4**: e8496

Lawson KA, Anderson K, Menchaca M, Atkinson J, Sun L, Knight V, Gilbert BE, Conti C, Sanders BG, Kline K (2003) Novel vitamin E analogue decreases syngeneic mouse mammary tumor burden and reduces lung metastasis. *Molecular cancer therapeutics* **2**: 437-444

Lee PE, Tierney MC, Wu W, Pritchard KI, Rochon PA (2016) Endocrine treatment-associated cognitive impairment in breast cancer survivors: evidence from published studies. *Breast cancer research and treatment*: 1-14

Li H, Li J, Lv Q, Wang X, Yang H (2012) The study of fatty acid binding protein expression in human breast cancer tissue and its significance. *The Journal of Bioscience and Medicine* **2**

Li Y, Ye X, Tan C, Hongo JA, Zha J, Liu J, Kallop D, Ludlam MJC, Pei L (2009) Axl as a potential therapeutic target in cancer: role of Axl in tumor growth, metastasis and angiogenesis. *Oncogene* **28**: 3442-3455

Liu K-Z, Bose R, Mantsch HH (2002) Infrared spectroscopic study of diabetic platelets. *Vibrational Spectroscopy* **28**: 131-136

Loda M, Capodieci P, Mishra R, Yao H, Corless C, Grigioni W, Wang Y, Magi-Galluzzi C, Stork PJ (1996) Expression of mitogen-activated protein kinase phosphatase-1 in the early phases of human epithelial carcinogenesis. *The American journal of pathology* **149**: 1553-1564

Malhi H, Gores GJ (2008) Molecular mechanisms of lipotoxicity in nonalcoholic fatty liver disease. *Seminars in liver disease* **28**: 360-369

Malhotra V, Perry MC (2003) Classical chemotherapy: mechanisms, toxicities and the therapeutic window. *Cancer biology & therapy* **2**: 1-3

Mamede AC, Tavares SD, Abrantes AM, Trindade J, Maia JM, Botelho MF (2011) The role of vitamins in cancer: a review. *Nutr Cancer* **63**: 479-494

Mantsch HH (1984) Biological applications of fourier transform infrared spectroscopy: a study of phase transitions in biomembranes. *Journal of Molecular Structure* **113**: 201-212

Mardones P, Rigotti A (2004) Cellular mechanisms of vitamin E uptake: relevance in α -tocopherol metabolism and potential implications for disease. *The Journal of Nutritional Biochemistry* **15**: 252-260

Matthews GM, Howarth GS, Butler RN (2007) Short-chain fatty acid modulation of apoptosis in the Kato III human gastric carcinoma cell line. *Cancer biology & therapy* **6**: 1051-1057

McIntyre BS, Briski KP, Gapor A, Sylvester PW (2000a) Antiproliferative and apoptotic effects of tocopherols and tocotrienols on preneoplastic and neoplastic mouse mammary epithelial cells. *Proceedings of the Society for Experimental Biology and Medicine Society for Experimental Biology and Medicine (New York, NY)* **224**: 292-301

McIntyre BS, Briski KP, Tirmenstein MA, Fariss MW, Gapor A, Sylvester PW (2000b) Antiproliferative and apoptotic effects of tocopherols and tocotrienols on normal mouse mammary epithelial cells. *Lipids* **35**: 171-180

Medina MW, Gao F, Naidoo D, Rudel LL, Temel RE, McDaniel AL, Marshall SM, Krauss RM (2011) Coordinately Regulated Alternative Splicing of Genes Involved in Cholesterol Biosynthesis and Uptake. *PloS one* **6**: e19420

Menendez JA, Lupu R (2007) Fatty acid synthase and the lipogenic phenotype in cancer pathogenesis. *Nature reviews Cancer* **7**: 763-777

Meric F, Lee WP, Sahin A, Zhang H, Kung HJ, Hung MC (2002) Expression profile of tyrosine kinases in breast cancer. *Clinical cancer research : an official journal of the American Association for Cancer Research* **8**: 361-367

Minn A, Rudin C, Boise L, Thompson C (1995) Expression of bcl-xL can confer a multidrug resistance phenotype. *Blood* **86**: 1903-1910

Mollinedo F, Gajate C (2015) Lipid rafts as major platforms for signaling regulation in cancer. *Advances in biological regulation* **57**: 130-146

Mustacich DJ, Bruno RS, Traber MG (2007) Vitamin E. In *Vitamins & Hormones*, Gerald L (ed), Vol. Volume 76, pp 1-21. Academic Press

Nabi IR, Le PU (2003) Caveolae/raft-dependent endocytosis. *The Journal of cell biology* **161**: 673-677

Neophytou CM, Constantinou AI (2015) Drug Delivery Innovations for Enhancing the Anticancer Potential of Vitamin E Isoforms and Their Derivatives. *BioMed Research International* **2015**: 584862

Nesland JM, Holm R, Johannessen JV, Gould VE (1986) Neurone specific enolase immunostaining in the diagnosis of breast carcinomas with neuroendocrine differentiation. Its usefulness and limitations. *The Journal of pathology* **148**: 35-43

Neuzil J, Zhao M, Ostermann G, Sticha M, Gellert N, Weber C, Eaton JW, Brunk UT. (2002a) Alpha-tocopheryl succinate, an agent with in vivo anti-tumour activity, induces apoptosis by causing lysosomal instability. *The Biochemical journal* **362(Pt 3)**:709-715.

Neuzil J, Kagedal K, Andera L, Weber C, Brunk UT (2002b) Vitamin E analogs: a new class of multiple action agents with anti-neoplastic and anti-atherogenic activity. *Apoptosis : an international journal on programmed cell death* **7(2)**:179-187.

Neuzil J, Weber T, Schroder A, Lu M, Ostermann G, Gellert N, Mayne GC, Olejnicka B, Negre-Salvayre A, Sticha M, Coffey RJ, Weber C (2001a) Induction of cancer cell apoptosis by alpha-tocopheryl succinate: molecular pathways and structural requirements. *FASEB journal : official publication of the Federation of American Societies for Experimental Biology* **15**: 403-415

Neuzil J, Weber T, Terman A, Weber C, Brunk UT (2001b) Vitamin E analogues as inducers of apoptosis: implications for their potential antineoplastic role. *Redox report : communications in free radical research* **6**: 143-151

Niki E (2014) Role of vitamin E as a lipid-soluble peroxy radical scavenger: in vitro and in vivo evidence. *Free radical biology & medicine* **66**: 3-12

Nohturfft A, Zhang SC (2009) Coordination of Lipid Metabolism in Membrane Biogenesis. *Annual Review of Cell and Developmental Biology* **25**: 539-566

Ohyashiki T, Ushiro H, Mohri T (1986) Effects of α -tocopherol on the lipid peroxidation and fluidity of porcine intestinal brush-border membranes. *Biochimica et Biophysica Acta (BBA) - Biomembranes* **858**: 294-300

Ozek NS, Tuna S, Erson-Bensan AE, Severcan F (2010) Characterization of microRNA-125b expression in MCF7 breast cancer cells by ATR-FTIR spectroscopy. *The Analyst* **135**: 3094-3102

Parker RA, Pearce BC, Clark RW, Gordon DA, Wright JJ (1993) Tocotrienols regulate cholesterol production in mammalian cells by post-transcriptional suppression of 3-hydroxy-3-methylglutaryl-coenzyme A reductase. *The Journal of biological chemistry* **268**: 11230-11238

Patacsil D, Osayi S, Tran AT, Saenz F, Yimer L, Shajahan AN, Gokhale PC, Verma M, Clarke R, Chauhan SC, Kumar D (2012) Vitamin E succinate inhibits survivin and induces apoptosis in pancreatic cancer cells. *Genes & Nutrition* **7**: 83-89

Pearce BC, Parker RA, Deason ME, Dischino DD, Gillespie E, Qureshi AA, Volk K, Wright JJ (1994) Inhibitors of cholesterol biosynthesis. 2. Hypocholesterolemic and antioxidant activities of benzopyran and tetrahydronaphthalene analogues of the tocotrienols. *Journal of medicinal chemistry* **37**: 526-541

Pike LJ (2003) Lipid rafts: bringing order to chaos. *Journal of lipid research* **44**: 655-667

Prochazka L, Dong LF, Valis K, Freeman R, Ralph SJ, Turanek J, Neuzil J (2010) α -Tocopheryl succinate causes mitochondrial permeabilization by preferential formation of Bak channels. *Apoptosis : an international journal on programmed cell death* **15**: 782-794

Qureshi AA, Burger WC, Peterson DM, Elson CE (1986) The structure of an inhibitor of cholesterol biosynthesis isolated from barley. *The Journal of biological chemistry* **261**: 10544-10550

Qureshi AA, Sami SA, Salser WA, Khan FA (2002) Dose-dependent suppression of serum cholesterol by tocotrienol-rich fraction (TRF25) of rice bran in hypercholesterolemic humans. *Atherosclerosis* **161**: 199-207

Rahib L, MacLennan NK, Horvath S, Liao JC, Dipple KM (2007) Glycerol kinase deficiency alters expression of genes involved in lipid metabolism, carbohydrate metabolism, and insulin signaling. *Eur J Hum Genet* **15**: 646-657

Rajneesh CP, Manimaran A, Sasikala KR, Adaikappan P (2008) Lipid peroxidation and antioxidant status in patients with breast cancer. *Singapore medical journal* **49**: 640-643

Rao X, Di Leva G, Li M, Fang F, Devlin C, Hartman-Frey C, Burow ME, Ivan M, Croce CM, Nephew KP (2011) MicroRNA-221/222 confers breast cancer fulvestrant resistance by regulating multiple signaling pathways. *Oncogene* **30**: 1082-1097

Roskoski Jr R (2012) ERK1/2 MAP kinases: Structure, function, and regulation. *Pharmacological Research* **66**: 105-143

Rutkowski DT, Kaufman RJ (2004) A trip to the ER: coping with stress. *Trends in cell biology* **14**: 20-28

Sade A, Tuncay S, Cimen I, Severcan F, Banerjee S (2012) Celecoxib reduces fluidity and decreases metastatic potential of colon cancer cell lines irrespective of COX-2 expression. *Bioscience reports* **32**: 35-44

Samudio I, Harmancey R, Fiegl M, Kantarjian H, Konopleva M, Korchin B, Kaluarachchi K, Bornmann W, Duvvuri S, Taegtmeier H, Andreeff M (2010) Pharmacologic inhibition of fatty acid oxidation sensitizes human leukemia cells to apoptosis induction. *The Journal of clinical investigation* **120**: 142-156

Schmidt CM, McKillop IH, Cahill PA, Sitzmann JV (1997) Increased MAPK expression and activity in primary human hepatocellular carcinoma. *Biochem Biophys Res Commun* **236**: 54-58

Schroeder GN, Hilbi H (2007) Cholesterol is required to trigger caspase-1 activation and macrophage apoptosis after phagosomal escape of *Shigella*. *Cellular microbiology* **9**: 265-278

Schroepfer GJ, Jr. (2000) Oxysterols: modulators of cholesterol metabolism and other processes. *Physiological reviews* **80**: 361-554

Severcan F (1997) Vitamin E decreases the order of the phospholipid model membranes in the gel phase: an FTIR study. *Bioscience reports* **17**: 231-235

Severcan F, Bozkurt O, Gurbanov R, Gorgulu G (2010) FT-IR spectroscopy in diagnosis of diabetes in rat animal model. *Journal of biophotonics* **3**: 621-631

Severcan F, Cannistraro S (1988) Direct electron spin resonance evidence for alpha-tocopherol-induced phase separation in model membranes. *Chem Phys Lipids* **47**: 129-133

Severcan F, Cannistraro S (1989) Model membrane partition ESR study in the presence of alpha-tocopherol by a new spin probe. *Bioscience reports* **9**: 489-495

Severcan F, Cannistraro S (1990) A spin label ESR and saturation transfer ESR study of alpha-tocopherol containing model membranes. *Chem Phys Lipids* **53**: 17-26

Severcan F, Gorgulu G, Gorgulu ST, Guray T (2005) Rapid monitoring of diabetes-induced lipid peroxidation by Fourier transform infrared spectroscopy: evidence from rat liver microsomal membranes. *Analytical biochemistry* **339**: 36-40

Severcan F, Haris PI (2012) *Vibrational Spectroscopy in Diagnosis and Screening-Advances in Biomedical Spectroscopy*. Severcan F, Haris PI (eds), 1st edn, pp 386–418. Amsterdam, The Netherlands: IOS Press

Sharma S, Black SM (2009) CARNITINE HOMEOSTASIS, MITOCHONDRIAL FUNCTION, AND CARDIOVASCULAR DISEASE. *Drug discovery today Disease mechanisms* **6**: e31-39

Shiau CW, Huang JW, Wang DS, Weng JR, Yang CC, Lin CH, Li C, Chen CS (2006) alpha-Tocopheryl succinate induces apoptosis in prostate cancer cells in part through inhibition of Bcl-xL/Bcl-2 function. *The Journal of biological chemistry* **281**: 11819-11825

Shimabukuro M, Zhou YT, Levi M, Unger RH (1998) Fatty acid-induced beta cell apoptosis: a link between obesity and diabetes. *Proceedings of the National Academy of Sciences of the United States of America* **95**: 2498-2502

Sigounas G, Anagnostou A, Steiner M (1997) dl-alpha-tocopherol induces apoptosis in erythroleukemia, prostate, and breast cancer cells. *Nutr Cancer* **28**: 30-35

Soh MA, Garrett SH, Somji S, Dunlevy JR, Zhou XD, Sens MA, Bathula CS, Allen C, Sens DA (2011) Arsenic, cadmium and neuron specific enolase (ENO2, gamma-enolase) expression in breast cancer. *Cancer cell international* **11**: 41

Son J, Lyssiotis CA, Ying H, Wang X, Hua S, Ligorio M, Perera RM, Ferrone CR, Mullarky E, Shyh-Chang N, Kang Y, Fleming JB, Bardeesy N, Asara JM, Haigis MC, DePinho RA, Cantley LC, Kimmelman AC (2013) Glutamine supports pancreatic cancer growth through a KRAS-regulated metabolic pathway. *Nature* **496**: 101-105

Sottero B, Gamba P, Gargiulo S, Leonarduzzi G, Poli G (2009) Cholesterol oxidation products and disease: an emerging topic of interest in medicinal chemistry. *Current medicinal chemistry* **16**: 685-705

Srivastava S, Phadke RS, Govil G, Rao CNR (1983) Fluidity, permeability and antioxidant behaviour of model membranes incorporated with α -tocopherol and vitamin E acetate. *Biochimica et Biophysica Acta (BBA) - Biomembranes* **734**: 353-362

Storch J, McDermott L (2009) Structural and functional analysis of fatty acid-binding proteins. *Journal of lipid research* **50**: S126-S131

Sylvester PW, Shah S (2005) Intracellular mechanisms mediating tocotrienol-induced apoptosis in neoplastic mammary epithelial cells. *Asia Pacific journal of clinical nutrition* **14(4)**:366-373.

Sylvester PW, Shah SJ (2005) Mechanisms mediating the antiproliferative and apoptotic effects of vitamin E in mammary cancer cells. *Frontiers in bioscience : a journal and virtual library* **10**:699-709.

Sylvester PW, Shah SJ, Samant GV (2005) Intracellular signaling mechanisms mediating the antiproliferative and apoptotic effects of gamma-tocotrienol in neoplastic mammary epithelial cells. *Journal of plant physiology* **162(7)**:803-810.

Thangaraju M, Vijayalakshmi T, Sachdanandam P (1994) Effect of tamoxifen on lipid peroxide and antioxidative system in postmenopausal women with breast cancer. *Cancer* **74**: 78-82

Thiery JP (2002) Epithelial-mesenchymal transitions in tumour progression. *Nature reviews Cancer* **2**: 442-454

Thomas C, Gustafsson JA (2011) The different roles of ER subtypes in cancer biology and therapy. *Nature reviews Cancer* **11**: 597-608

Thompson TA, Wilding G (2003) Androgen antagonist activity by the antioxidant moiety of vitamin E, 2,2,5,7,8-pentamethyl-6-chromanol in human prostate carcinoma cells. *Molecular cancer therapeutics* **2**: 797-803

Tomic-Vatic A, Eytina J, Chapman J, Mahdavian E, Neuzil J, Salvatore BA (2005) Vitamin E amides, a new class of vitamin E analogues with enhanced proapoptotic activity. *International journal of cancer* **117**: 188-193

van der Gun BTF, Melchers LJ, Ruiters MHJ, de Leij LFMH, McLaughlin PMJ, Rots MG (2010) EpCAM in carcinogenesis: the good, the bad or the ugly. *Carcinogenesis* **31**: 1913-1921

Vishnyakova EA, Ruuge AE, Golovina EA, Hoekstra FA, Tikhonov AN (2000) Spin-labeling study of membranes in wheat embryo axes. 1. Partitioning of doxyl stearates into the lipid domains. *Biochimica et Biophysica Acta (BBA) - Biomembranes* **1467**: 380-394

Walker AK, Jacobs RL, Watts JL, Rottiers V, Jiang K, Finnegan DM, Shioda T, Hansen M, Yang F, Niebergall LJ, Vance DE, Tzoneva M, Hart AC, Naar AM (2011) A conserved SREBP-1/phosphatidylcholine feedback circuit regulates lipogenesis in metazoans. *Cell* **147**: 840-852

Wang L, Mizaikoff B (2008) Application of multivariate data-analysis techniques to biomedical diagnostics based on mid-infrared spectroscopy. *Analytical and bioanalytical chemistry* **391**: 1641-1654

Wang X-F, Witting PK, Salvatore BA, Neuzil J (2005) Vitamin E analogs trigger apoptosis in HER2/erbB2-overexpressing breast cancer cells by signaling via the

mitochondrial pathway. *Biochemical and Biophysical Research Communications* **326**: 282-289

Wang X, Quinn PJ (1999) Vitamin E and its function in membranes. *Progress in lipid research* **38**: 309-336

Warburg O (1956) On the origin of cancer cells. *Science (New York, NY)* **123**: 309-314

Wassall SR, Thewalt JL, Wong L, Gorrissen H, Cushley RJ (1986) Deuterium NMR study of the interaction of alpha-tocopherol with a phospholipid model membrane. *Biochemistry* **25**: 319-326

Wassall SR, Wang L, Yang McCabe RC, Ehringer WD, Stillwell W (1991) Electron spin resonance study of the interaction of alpha-tocopherol with phospholipid model membranes. *Chemistry and Physics of Lipids* **60**: 29-37

Weber T, Dalen H, Andera L, Negre-Salvayre A, Auge N, Sticha M, Lloret A, Terman A, Witting PK, Higuchi M, Plasilova M, Zivny J, Gellert N, Weber C, Neuzil J (2003) Mitochondria play a central role in apoptosis induced by alpha-tocopheryl succinate, an agent with antineoplastic activity: comparison with receptor-mediated pro-apoptotic signaling. *Biochemistry* **42**: 4277-4291

Weber T, Lu M, Andera L, Lahm H, Gellert N, Fariss MW, Korinek V, Sattler W, Ucker DS, Terman A, Schroder A, Erl W, Brunk UT, Coffey RJ, Weber C, Neuzil J (2002) Vitamin E succinate is a potent novel antineoplastic agent with high selectivity and cooperativity with tumor necrosis factor-related apoptosis-inducing ligand (Apo2 ligand) in vivo. *Clinical cancer research : an official journal of the American Association for Cancer Research* **8**: 863-869

Williams KJ, Argus JP, Zhu Y, Wilks MQ, Marbois BN, York AG, Kidani Y, Pourzia AL, Akhavan D, Lisiero DN, Komisopoulou E, Henkin AH, Soto H, Chamberlain BT, Vergnes L, Jung ME, Torres JZ, Liao LM, Christofk HR, Prins RM, Mischel PS, Reue K, Graeber TG, Bensinger SJ (2013) An essential requirement for the SCAP/SREBP signaling axis to protect cancer cells from lipotoxicity. *Cancer research* **73**: 2850-2862

Yamauchi R (2007) Addition Products of α -Tocopherol with Lipid-Derived Free Radicals. In *Vitamins & Hormones*, Gerald L (ed), Vol. Volume 76, pp 309-327. Academic Press

Yan B, Stantic M, Zobalova R, Bezawork-Geleta A, Stapelberg M, Stursa J, Prokopova K, Dong L, Neuzil J (2015) Mitochondrially targeted vitamin E succinate efficiently kills breast tumour-initiating cells in a complex II-dependent manner. *BMC cancer* **15**: 401

Yang CS, Suh N, Kong AN (2012) Does vitamin E prevent or promote cancer? *Cancer prevention research (Philadelphia, Pa)* **5**: 701-705

Yaqoob P (2009) The nutritional significance of lipid rafts. *Annual review of nutrition* **29**: 257-282

Ying H, Kimmelman AC, Lyssiotis CA, Hua S, Chu GC, Fletcher-Sananikone E, Locasale JW, Son J, Zhang H, Coloff JL, Yan H, Wang W, Chen S, Viale A, Zheng H, Paik JH, Lim C, Guimaraes AR, Martin ES, Chang J, Hezel AF, Perry SR, Hu J, Gan B, Xiao Y, Asara JM, Weissleder R, Wang YA, Chin L, Cantley LC, DePinho RA (2012) Oncogenic Kras maintains pancreatic tumors through regulation of anabolic glucose metabolism. *Cell* **149**: 656-670

You H, Yu W, Sanders BG, Kline K (2001) RRR-alpha-tocopheryl succinate induces MDA-MB-435 and MCF-7 human breast cancer cells to undergo differentiation. *Cell growth & differentiation : the molecular biology journal of the American Association for Cancer Research* **12**: 471-480

Yung HW, Charnock-Jones DS, Burton GJ (2011) Regulation of AKT phosphorylation at Ser473 and Thr308 by endoplasmic reticulum stress modulates substrate specificity in a severity dependent manner. *PloS one* **6**: e17894

Zhang S, Lawson KA, Simmons-Menchaca M, Sun L, Sanders BG, Kline K (2004) Vitamin E analog alpha-TEA and celecoxib alone and together reduce human MDA-MB-435-FL-GFP breast cancer burden and metastasis in nude mice. *Breast cancer research and treatment* **87**: 111-121

Zu K, Ip C (2003) Synergy between selenium and vitamin E in apoptosis induction is associated with activation of distinctive initiator caspases in human prostate cancer cells. *Cancer research* **63**: 6988-6995

APPENDICES

APPENDIX A

Table 1. Coordinates of protein spots on array membrane

Coordinate	Analyte / Control
A1-A2	Reference Spot
A3-A4	a-fetoprotein
A5-A6	Amphiregulin
A7-A8	Angiopoietin-1
A9-A10	Angiopoietin-like4
A11-A12	ENPP-2
A13-A14	Axl
A15-A16	BCL-x
A17-A18	CA125/MUC16
A19-A20	E-Cadherin
A21-A22	VE-Cadherin
A23-A24	Reference Spot
B3-B4	CapG
B5-B6	Carbonic anhydrase IX
B7-B8	Cathepsin B
B9-B10	Cathepsin D
B11-B12	Cathepsin S
B13-B14	CEACAM-5
B15-B16	Decorin
B17-B18	Dkk-1
B19-B20	DLL1
B21-B22	EGF R/ErbB1
C3-C4	Endoglin/CD105
C5-C6	Endostatin
C7-C8	enolase 2
C9-C10	eNOS
C11-C12	EpCAM
C13-C14	Era
C15-C16	ErbB2
C17-C18	ErbB3/Her3
C19-C20	ErbB4
C21-C22	FGF basic
D1-D2	FoxC2
D3-D4	Fox01
D5-D6	Galectin-3
D7-D8	GM-CSF
D9-D10	CG a/b
D11-D12	HGF R /c-Met
D13-D14	HIF-1a
D15-D16	HNF-3b
D17-D18	H0-1/HMOX1 (HSP32)
D19-D20	ICAM-1
D21-D22	IL-2 Ra

D23-D24	IL-6
E1-E2	CXCL8
E3-E4	IL18BP
E5-E6	Kallikrein 3
E7-E8	Kallikrein 5
E9-E10	Kallikrein 6
E11-E12	Leptin
E13-E14	Lumican
E15-E16	CCL2
E17-E18	CCL8
E19-E20	CCL7
E21-E22	M-CSF
E23-E24	Mesothelin
F1-F2	CCL3
F3-F4	CCL20
F5-F6	MMP-2
F7-F8	MMP-3
F9-F10	MMP-9
F11-F12	MSP
F13-F14	MUC-1
F15-F16	Nectin-4
F17-F18	Osteopontin
F19-F20	p27
F21-F22	p53
F23-F24	PDGF-AA
G1-G2	CD31
G3-G4	Progesterone
G5-G6	Progranulin
G7-G8	Prolactin
G9-G10	Prostasin
G11-G12	E-Selectin
G13-G14	Serpin B5
G15-G16	Serpin E1
G17-G18	Snail
G19-G20	SPARC
G21-G22	Survivin
G23-G24	Tenascin C
H1-H2	Thrombospondin-1
H3-H4	Tie-2
H5-H6	u-plasminogen activator
H7-H8	VCAM
H9-H10	VEGF
H11-H12	Vimentin
I1-I2	Reference Spot
I23-I24	Negative Control

APPENDIX B

Table 1. Gene table: RT² Profiler PCR Array

Position	UniGene	GenBank	Symbol	Description
A01	Hs.70675	NM_001607	ACAA1	Acetyl-CoA acyltransferase 1
A02	Hs.20013	NM_006111	ACAA2	Acetyl-CoA acyltransferase 2
A03	Hs.33114	NM_025247	ACAD10	Acyl-CoA dehydrogenase family, member 10
A04	Hs.44137	NM_032169	ACAD11	Acyl-CoA dehydrogenase family, member 11
A05	Hs.56748	NM_014049	ACAD9	Acyl-CoA dehydrogenase family, member 9
A06	Hs.47127	NM_001608	ACADL	Acyl-CoA dehydrogenase, long chain
A07	Hs.44504	NM_000016	ACADM	Acyl-CoA dehydrogenase, C-4 to C-12 straight chain
A08	Hs.50707	NM_000017	ACADS	Acyl-CoA dehydrogenase, C-2 to C-3 short chain
A09	Hs.81934	NM_001609	ACADSB	Acyl-CoA dehydrogenase, short/branched chain
A10	Hs.43717	NM_000018	ACADVL	Acyl-CoA dehydrogenase, very long chain
A11	Hs.23237	NM_000019	ACAT1	Acetyl-CoA acetyltransferase 1
A12	Hs.57103	NM_005891	ACAT2	Acetyl-CoA acetyltransferase 2
B01	Hs.56804	NM_00103716	ACOT1	Acyl-CoA thioesterase 1
B02	Hs.59175	NM_130767	ACOT12	Acyl-CoA thioesterase 12
B03	Hs.12203	NM_00103716	ACOT6	Acyl-CoA thioesterase 6
B04	Hs.12613	NM_181866	ACOT7	Acyl-CoA thioesterase 7
B05	Hs.44477	NM_005469	ACOT8	Acyl-CoA thioesterase 8
B06	Hs.29888	NM_00103358	ACOT9	Acyl-CoA thioesterase 9
B07	Hs.46413	NM_004035	ACOX1	Acyl-CoA oxidase 1, palmitoyl
B08	Hs.44495	NM_003500	ACOX2	Acyl-CoA oxidase 2, branched chain
B09	Hs.47912	NM_003501	ACOX3	Acyl-CoA oxidase 3, pristanoyl
B10	Hs.65576	NM_015162	ACSBG1	Acyl-CoA synthetase bubblegum family member 1
B11	Hs.46572	NM_030924	ACSBG2	Acyl-CoA synthetase bubblegum family member 2
B12	Hs.40667	NM_001995	ACSL1	Acyl-CoA synthetase long-chain family member 1
C01	Hs.65577	NM_004457	ACSL3	Acyl-CoA synthetase long-chain family member 3
C02	Hs.26878	NM_004458	ACSL4	Acyl-CoA synthetase long-chain family member 4
C03	Hs.11638	NM_016234	ACSL5	Acyl-CoA synthetase long-chain family member 5
C04	Hs.14945	NM_00100918	ACSL6	Acyl-CoA synthetase long-chain family member 6
C05	Hs.70675	NM_005622	ACSM3	Acyl-CoA synthetase medium-chain family member 3
C06	Hs.45080	NM_00108045	ACSM4	Acyl-CoA synthetase medium-chain family member 4
C07	Hs.65960	NM_017888	ACSM5	Acyl-CoA synthetase medium-chain family member 5
C08	Hs.63273	NM_000690	ALDH2	Aldehyde dehydrogenase 2 family (mitochondrial)
C09	Hs.27453	NM_004051	BDH1	3-hydroxybutyrate dehydrogenase, type 1
C10	Hs.12469	NM_020139	BDH2	3-hydroxybutyrate dehydrogenase, type 2
C11	Hs.50304	NM_001876	CPT1A	Carnitine palmitoyltransferase 1A (liver)
C12	Hs.43977	NM_004377	CPT1B	Carnitine palmitoyltransferase 1B (muscle)
D01	Hs.11219	NM_152359	CPT1C	Carnitine palmitoyltransferase 1C
D02	Hs.70537	NM_000098	CPT2	Carnitine palmitoyltransferase 2
D03	Hs.12068	NM_000755	CRAT	Carnitine O-acetyltransferase
D04	Hs.12503	NM_021151	CROT	Carnitine O-octanoyltransferase
D05	Hs.49221	NM_001359	DECR1	2,4-dienoyl CoA reductase 1, mitochondrial
D06	Hs.62883	NM_020664	DECR2	2,4-dienoyl CoA reductase 2, peroxisomal
D07	Hs.76394	NM_004092	ECHS1	Enoyl CoA hydratase, short chain, 1, mitochondrial
D08	Hs.15250	NM_006117	ECI2	Enoyl-CoA delta isomerase 2
D09	Hs.42987	NM_001966	EHHADH	Enoyl-CoA, hydratase/3-hydroxyacyl CoA dehydrogenase
D10	Hs.38013	NM_001443	FABP1	Fatty acid binding protein 1, liver
D11	Hs.28226	NM_000134	FABP2	Fatty acid binding protein 2, intestinal
D12	Hs.65724	NM_004102	FABP3	Fatty acid binding protein 3, muscle and heart (mammary-derived growth inhibitor)
E01	Hs.39156	NM_001442	FABP4	Fatty acid binding protein 4, adipocyte
E02	Hs.40806	NM_001444	FABP5	Fatty acid binding protein 5 (psoriasis-associated)
E03	Hs.51971	NM_001445	FABP6	Fatty acid binding protein 6, ileal
E04	Hs.26770	NM_001446	FABP7	Fatty acid binding protein 7, brain
E05	Hs.83190	NM_004104	FASN	Fatty acid synthase
E06	Hs.53269	NM_000159	GCDH	Glutaryl-CoA dehydrogenase
E07	Hs.1466	NM_000167	GK	Glycerol kinase
E08	Hs.98008	NM_033214	GK2	Glycerol kinase 2
E09	Hs.52441	NM_005276	GPD1	Glycerol-3-phosphate dehydrogenase 1 (soluble)
E10	Hs.51238	NM_000408	GPD2	Glycerol-3-phosphate dehydrogenase 2 (mitochondrial)
E11	Hs.51603	NM_000182	HADHA	Hydroxyacyl-CoA dehydrogenase/3-ketoacyl-CoA
E12	Hs.53344	NM_000191	HMGCL	3-hydroxymethyl-3-methylglutaryl-CoA lyase
F01	Hs.39772	NM_002130	HMGCS1	3-hydroxy-3-methylglutaryl-CoA synthase 1 (soluble)

F02	Hs.59889	NM_005518	HMGCS2	3-hydroxy-3-methylglutaryl-CoA synthase 2
F03	Hs.65698	NM_005357	LIPE	Lipase, hormone-sensitive
F04	Hs.18087	NM_000237	LPL	Lipoprotein lipase
F05	Hs.94949	NM_032601	MCEE	Methylmalonyl CoA epimerase
F06	Hs.48552	NM_000255	MUT	Methylmalonyl CoA mutase
F07	Hs.47249	NM_022120	OXCT2	3-oxoacid CoA transferase 2
F08	Hs.28168	NM_018441	PECR	Peroxisomal trans-2-enoyl-CoA reductase
F09	Hs.43740	NM_021129	PPA1	Pyrophosphatase (inorganic) 1
F10	Hs.43322	NM_006251	PRKAA1	Protein kinase, AMP-activated, alpha 1 catalytic subunit
F11	Hs.43703	NM_006252	PRKAA2	Protein kinase, AMP-activated, alpha 2 catalytic subunit
F12	Hs.71551	NM_006253	PRKAB1	Protein kinase, AMP-activated, beta 1 non-catalytic
G01	Hs.50732	NM_005399	PRKAB2	Protein kinase, AMP-activated, beta 2 non-catalytic
G02	Hs.63163	NM_002730	PRKACA	Protein kinase, cAMP-dependent, catalytic, alpha
G03	Hs.48732	NM_182948	PRKACB	Protein kinase, cAMP-dependent, catalytic, beta
G04	Hs.53086	NM_002733	PRKAG1	Protein kinase, AMP-activated, gamma 1 non-catalytic
G05	Hs.64707	NM_016203	PRKAG2	Protein kinase, AMP-activated, gamma 2 non-catalytic
G06	Hs.59163	NM_017431	PRKAG3	Protein kinase, AMP-activated, gamma 3 non-catalytic
G07	Hs.36313	NM_198580	SLC27A1	Solute carrier family 27 (fatty acid transporter),
G08	Hs.11729	NM_003645	SLC27A2	Solute carrier family 27 (fatty acid transporter),
G09	Hs.43872	NM_024330	SLC27A3	Solute carrier family 27 (fatty acid transporter),
G10	Hs.65669	NM_005094	SLC27A4	Solute carrier family 27 (fatty acid transporter),
G11	Hs.29217	NM_012254	SLC27A5	Solute carrier family 27 (fatty acid transporter),
G12	Hs.49765	NM_014031	SLC27A6	Solute carrier family 27 (fatty acid transporter),
H01	Hs.52064	NM_001101	ACTB	Actin, beta
H02	Hs.53425	NM_004048	B2M	Beta-2-microglobulin
H03	Hs.59235	NM_002046	GAPDH	Glyceraldehyde-3-phosphate dehydrogenase
H04	Hs.41270	NM_000194	HPRT1	Hypoxanthine phosphoribosyltransferase 1
H05	Hs.54628	NM_001002	RPLP0	Ribosomal protein, large, P0
H06	N/A	SA_00105	HGDC	Human Genomic DNA Contamination
H07	N/A	SA_00104	RTC	Reverse Transcription Control
H08	N/A	SA_00104	RTC	Reverse Transcription Control
H09	N/A	SA_00104	RTC	Reverse Transcription Control
H10	N/A	SA_00103	PPC	Positive PCR Control
H11	N/A	SA_00103	PPC	Positive PCR Control
H12	N/A	SA_00103	PPC	Positive PCR Control

CURRICULUM VITAE

PERSONAL INFORMATION

Surname, Name: Gök, Seher

Nationality: Turkish (TC)

Date and Place of Birth: 21.01.1987 / Manisa

Phone: +90 536 705 26 25

e.mail: shrgok@gmail.com

EDUCATION

2013 / 2017

Ph.D. Middle East Technical University, Department of Biological Sciences (Major in Biophysics & Minor in Molecular Genetics)

2011 / 2013

M.Sc. Middle East Technical University, Department of Biological Sciences (GPA: 4.00 / 4.00)

2010 / 2011

M.Sc. Istanbul Technical University, Molecular Biology & Genetics and Biotechnology

2006 / 2010

B.Sc. Izmir Institute of Technology, Molecular Biology and Genetics (GPA : 3.42 / 4.00)

2007 / 2011

B.A. Anadolu University, Public Administration, (GPA: 67.64/100)

2002 / 2005

Turgutlu Anatolian High School, Branch of Science (GPA: 5.00 / 5.00)

ACADEMIC EXPERIENCE

2016 – 2017: Research & Teaching Assistant, Bilecik S.E. University, Department of Molecular Biology & Genetics

2010 - 2016 : Research & Teaching Assistant, Middle East Technical University, Department of Biological Sciences

PUBLICATIONS

SCI Papers:

- **Gok S**, Aydin OZ, Sural YS, Zorlu F, Bayol U, Severcan F. Bladder cancer diagnosis from bladder wash by Fourier transform infrared spectroscopy as a novel test for tumor recurrence. Journal of biophotonics 2016. doi: 10.1002/jbio.201500322.
- Inan Genc A, **Gok S**, Banerjee S, Severcan F. Valdecoxib Recovers the Lipid Composition, Order and Dynamics in Colon Cancer Cell Lines Independent of COX-2 Expression: An ATR-FTIR Spectroscopy Study. Applied spectroscopy 2016. doi: 10.1177/0003702816654164.
- **Gok S**, Severcan M, Goormaghtigh E, Kandemir I, Severcan F. Differentiation of Anatolian honey samples from different botanical origins by ATR-FTIR spectroscopy using multivariate analysis. Food Chemistry 2015;170:234-40. doi: 10.1016/j.foodchem.2014.08.040.
- Ozer Z, **Gok S**, Altan H, Severcan F. Concentration-based measurement studies of L-tryptophan using terahertz time-domain spectroscopy (THz-TDS). Applied spectroscopy 2014;68:95-100. doi: 10.1366/13-07165.
- Altan H, Simsek Ozek N, **Gok S**, Ozyurt I, Severcan F. Monitoring of tryptophan as a biomarker for cancerous cells in Terahertz (THz) sensing. Proceedings of SPIE 2016; 9703: 97030X-1-8. doi: 10.1117/12.2218032

doi: 10.1117/12.2218032.

- **Gok S**, Kuzmenko O, Severcan F. Novel Vitamin E analog TC6OH induce apoptosis by modulating the cellular lipids and membrane dynamics in human breast cancer cells. *Free Radical Biology & Medicine*. Manuscript in preparation
- **Gok S**, Kuzmenko O, Severcan F. FTIR spectral signatures of the effect of Novel Vitamin E derivative with anti-tumoral properties on human breast cancer cell line. *Analyst*. Manuscript in preparation
- Ergen N, **Gok S**, Kuzmenko O, Severcan F. The novel Vitamin E analogue prevents prostate cancer progression by altering lipid metabolism. Manuscript in preparation

Abstracts Published in International Conferences:

- Nuri Ergen, **Seher Gok**, Oleksandr Kuzmenko, Feride Severcan, A novel alphacopherol analog induces apoptosis by causing lipid driven cytotoxicity in prostate cancer cells, 15th Euro Fed Lipids congress, Uppsala, SWEDEN, 27-30 August 2017.
- Nuri Ergen, **Seher Gok**, Oleksandr Kuzmenko, Feride Severcan, Lipid related signatures of the effect of novel vitamin E analog with antitumorol properties on a prostate cancer cell line, 15th Euro Fed Lipids congress, Uppsala, SWEDEN, 27-30 August 2017.
- Hakan Altan, Yıldız Mentеше, **Seher Gok**, Ipek Ozyurt, Feride Severcan, Characterization of liquid sweeteners in the terahertz (THz) frequency region. 4th annual conference of COST action MP1204 & SMMO2016 Conference, Lisbon, PORTUGAL, 21-24 March 2016.

- Severcan F, Simsek Ozek N, **Gok S**. Fourier Transform Infrared Spectroscopy and Imaging in Cancer Diagnosis and Characterization. *Biophysical Journal* 2015;108:479a-80a. 59th Annual Meeting of the Biophysical-Society, Baltimore, USA, 7-11 February 2015.
doi: <http://dx.doi.org/10.1016/j.bpj.2014.11.2619>.
- **Seher Gok**, Ozge Z. Aydin, Yavuz S. Sural, Ferruh Zorlu, Feride Severcan, A new test for bladder tumor recurrence from bladder wash sample: Fourier Transform Infrared Spectroscopy. ITNANO, 2nd International translational nanomedicine conference, Boston MA, 25-27 July 2014.
- **S. Gok**, N.S. Ozek, F. Severcan, Analysis of histone deacetylase inhibitor treatment- induced alterations in cancer cells by FTIR spectroscopic and microspectroscopic techniques. SPEC 2014 “shedding new light on diseases”, Krakow, POLAND. 17-22 August 2014
- Nihal Simsek Ozek, Basak Oztan, **Seher Gok**, Bülent Yener, Sreeparna Banerjee, Feride Severcan, Quantitative analysis of sodium butyrate induced differentiation of colon cancer cells by FTIR microspectroscopic and computational methods. FT-IR Meeting in Berlin: "FT-IR Spectroscopy in Microbiological and Medical Diagnostics", Robert Koch-Institute, Berlin, GERMANY, 24 – 25 October 2013.
- **Seher Gok**, Fatma Arvas, Oğün Adabali, Feride Severcan, Mete Severcan, Molecular Classification of Honey Samples from Different Botanical Origins via ATR-FTIR Spectroscopy, 57th Biophysical Society Meeting, Philadelphia, USA, 2-6 February, 2013.
- Ozek NS, **Gok S**, Banerjee S, Severcan F. FTIR microspectroscopic analysis of sodium butyrate induced differentiation in colon cancer cells in a time-dependent manner. *Faseb J* 2013;27:1, Experimental Biology Annual Meeting, Boston, MA, USA, 20-24 April 2013. wos:000319860501396

- Zeynep Özer, **Seher Gok**, Hakan Altan, Feride Severcan, Concentration Based Measurement Studies of L-Tryptophan using THz-Time Domain Spectroscopy, International Turkish Congress on Molecular Spectroscopy, Istanbul/TURKEY, Abstract Book, September 15-20, 2013.
- **Seher Gok**, Ozge Dural. Evaluation of the concept of Molecular Information in Accordance with the Methodological Naturalism. 9th International Turkish World Social Sciences Congress, Baku, Azerbaijan, 15-16 June, 2011.
- Durcan C, **Gok S**, Bassoy EY, Can G, Baran Y. Combination Of Fludarabine and Imatinib-Induced Apoptosis Through Loss Of Mitochondrial Membrane Potential and Caspase-3 Enzyme Activity In Human K562 Chronic Myeloid Leukemia Cells. 32nd World Congress of International Society of Hematology, Bangkok, Thailand, 19-23 October 2008.

Abstracts published in National Conferances:

1. **Seher Gök**, Nihal Şimşek Özek, Sreeparna Banerjee, Feride Severcan, Time-Lapse FTIR Microspectroscopic Imaging of Sodium Butyrate Induced Differentiation in Human Colon Cancer Cell Lines, XIII. National Spectroscopy Congress, Burdur, TÜRKİYE, May 15-18, 2013.

BOOK CHAPTERS

1. **Gok. S.**, Severcan F., “Sahte bal ve farklı botanik kökenden gelme Türk ballarının kızıl ötesi spektroskopisi ile süratli ve hassas olarak teşhisi”, Marka bal olma yolunda Samsun Sempozyumu, (Eds: T. Bakır, H. Duran, D. Altan), Dizgi ve Baskı Renk Vizyon Matbaacılık, Yayıncılık A.Ş., 151-162, **2015**.

PROJECT WORKS

- Synthesis and the investigation of possible anti-cancer effects of novel Vitamin E analog with biochemical, biophysical and molecular biological methods on breast and prostate cancer cell lines.

TÜBİTAK-NASU bilateral project (Project No: 114Z424), Budget 270.000TL, 15.01.2015 - 15.01.2017, Project Fellow

- Investigation of the concentration dependent sodium butyrate induced differentiation in human colon adenocarcinoma cells by Raman, FTIR and Terahertz spectroscopy methods.

METU Interdiscipliner project, Budget: 20.500 TL, 01.01.2013 – 01.01.2015, Researcher

- The Investigation of the Therapeutic Effects of Histone Deacetylase Inhibitors on Colon Cancer Cells by Micro-nanotechnological Methods

METU Interdiscipliner project, Budget: 23.000 TL, 01.02.2015-30.12.2015 Researcher

- Evaluation of Attenuated Total Reflectance Fourier Transform Infrared (ATR-FTIR) Spectroscopy as a Diagnostic Method for the Diagnosis of Malignant Pleural Mesothelioma From Body Fluids.

TUBITAK – SBAG (Project No: 113S294), Budget: 297.650 TL, 5.10.2013-15.10.2015, Researcher

- “Identification of Mitochondrial Electron Transport Chain Mutations that Affect Aging

TUBA project, 2008-2009, Intern at IZTECH molecular genetics lab.

COURSES & TRAININGS

- COST Action BM1401, Raman4Clinics summer school, Leibniz Institute of Photonics Technology, Jena, Germany, 29.05.2016 – 03.06.2016

- State University of Newyork at Albany, Department of Chemistry, Raman imaging practical training, Albany, NY, USA, 24.01.2013 – 08.02.2013.
- Joint COST Training School and King's College London on Introduction to R, R-QTL and GeneNetwork London, UK, 9-13 September, 2013.
- Differential Scanning Calorimetry (DSC) theoretical training, TA Instruments Roadshow seminars, Ankara, 26.04.2016.
- McGill University, Faculty of Medicine, Continuing medical education activity; “International certificate program on predictive and personalized medicine in daily modern medicine and pharmacy” 22 credits accredited course, Eskişehir, 13-16 September 2012.
- Intern, Epigenetic analysis Techniques, İstanbul University, Oncology Institute, İstanbul, 2009.
- Intern, Ege University, Science and Technology research center (EBİLTEM), İzmir, 2008.

RESEARCH INTERESTS

Cancer Molecular Biology, Drug-Cell interactions, Membrane Biophysics, Medical Diagnostics, Molecular Biophysics, Spectroscopy Applications in Biological Sciences